Title

Development of Performance-Based Specifications for Asphalt Rubber Binder: Phase 2g Testing of Plant-Sampled Binders and RHMA-G Mixes

Authors

Jones, David
Rizvi, Hasham
Brotschi, Julian

Publication Date

2023

DOI

10.7922/G29Z937J

January 2023
Research Report: UCPRC-RR-2020-09

Development of Performance-Based Specifications for Asphalt Rubber Binder: Phase 2g Testing of Plant-Sampled Binders and RHMA-G Mixes

Authors:
David Jones, Hashim Rizvi, and Julian Brotschi

Partnered Pavement Research Center (PPRC) Contract Strategic Plan Elements 4.63 (DRISI Task 3186)
Performance-Related Specifications for Asphalt Rubber Binder

PREPARED FOR:

California Department of Transportation
Division of Research, Innovation and System Information
Office of Materials and Infrastructure Roadway Research

PREPARED BY:

University of California
Pavement Research Center
UC Davis and UC Berkeley

TECHNICAL REPORT DOCUMENTATION PAGE

1. REPORT NUMBER UCPRC-RR-2020-09	2. GOVERNMENT ASSOCIATION NUMBER	3. RECIPIENT'S CATALOG NUMBER
4. TITLE AND SUBTITLE Development of Performance-Based Specifications for Asphalt Rubber Binder: Phase 2g Testing of Plant-Sampled Binders and RHMA-G Mixes		5. REPORT PUBLICATION DATE January 2023 6. PERFORMING ORGANIZATION CODE
7. AUTHOR(S) David Jones (ORCID 0000-0002-2938-076X) Hashim Rizvi (ORCID 0000-0002-2529-0724) Julian Brotschi (ORCID 0000-0002-1752-2898)		8. PERFORMING ORGANIZATION REPORT NO. UCPRC-RR-2020-09 UCD-ITS-RR-20-114
9. PERFORMING ORGANIZATION NAME AND ADDRESS University of California Pavement Research Center Department of Civil and Environmental Engineering, UC Davis 1 Shields Avenue Davis, CA 95616		10. WORK UNIT NUMBER 11. CONTRACT OR GRANT NUMBER 65A0628
12. SPONSORING AGENCY AND ADDRESS California Department of Transportation Division of Research, Innovation, and System Information P.O. Box 942873 Sacramento, CA 94273-0001		13. TYPE OF REPORT AND PERIOD COVERED Research Report 14. SPONSORING AGENCY CODE
15. SUPPLEMENTAL NOTES doi:10.7922/G29Z937J		

16. ABSTRACT

The work discussed in this interim report is part of a larger study, funded by the California Department of Transportation. The study objective focuses on developing and recommending testing procedures and criteria for performance-based specifications of asphalt rubber binders used in gap-graded and open-graded mixes using current Superpave performance grade (PG) equipment. Work in this phase covered the testing of 19 plant-produced binders and the base binders used to produce them. Plant-produced gap-graded rubberized hot mix asphalt mixes from five of the projects were also tested. The following important observations from the binder rheology tests were made:

- Although the low-temperature performance grades appeared to be reasonable, the high-temperature grades appeared to be unrealistically high, while the intermediate-temperature grades appeared to be potentially lower than anticipated, when compared to the base binders. Fourteen of the binders tested with concentric cylinder geometry and 13 tested with parallel plate geometry had PGs higher than the maximum grade of 82°C listed in the AASHTO M 320 standard. Grades higher than 82 are considered to be unrealistically high and probably not a true indication of likely high-temperature performance (i.e., rut resistance under heavy loads on hot days).
- A comparison of the concentric cylinder and parallel plate (3 mm gap) geometries indicated that the results between the two geometries are different and are likely to be higher than the precision and bias of the individual procedures. Precision and bias statements for these procedures had not been developed at the time of preparing this report. These results indicate that the two geometries cannot be used interchangeably.
- No consistent trends in results were observed between any of the parameters tested.
- Observations from previous testing and during this phase of the study indicated that incompletely digested rubber particles—which have different sensitivities to temperature, aging, and applied stress and strain than the base asphalt binder—appeared to have a dominant influence on results and caused variability between results, regardless of the testing geometry used. Considering these incompletely digested particles as part of a homogenous binder may therefore not be appropriate when determining performance grades. Work is continuing in Phase 3 of this study to adjust testing procedures to account for the influence that these incompletely digested particles have on results.

The proposed modifications to short- and long-term aging procedures (i.e., rolling thin-film oven and pressure aging vessel) and to the bending beam rheometer specimen preparation procedures developed in Phase 2 are considered to be more aligned with the original intent of the tests and will likely reduce the variability between replicate specimens during testing.

Preliminary test results indicate that Fourier transformed infrared spectroscopy is a potentially valid method for quantifying rubber content in rubber-modified binders.

17. KEYWORDS asphalt rubber binder, AR binder, performance grade	18. DISTRIBUTION STATEMENT No restrictions. This document is available to the public through the National Technical Information Service, Springfield, VA 22161	
19. SECURITY CLASSIFICATION (of this report) Unclassified	20. NUMBER OF PAGES 115	21. PRICE None

UCPRC ADDITIONAL INFORMATION

1. DRAFT STAGE Final	2. VERSION NUMBER 1
3. PARTNERED PAVEMENT RESEARCH CENTER STRATEGIC PLAN ELEMENT NUMBER 4.63	4. DRISI TASK NUMBER 3186
5. CALTRANS TECHNICAL LEAD AND REVIEWER(S) Kee Foo (Technical Lead) Cathrina Barros Guadalupe Magana	6. FHWA NUMBER CA243186A

7. PROPOSALS FOR IMPLEMENTATION
None

8. RELATED DOCUMENTS

Hung, S.S., Farshidi, F., Jones, D., Alavi, M.Z., Harvey J.T., and Sadraie, H. 2014. *Investigation of Wet-Process Asphalt Rubber Binder Testing with Modified Dynamic Shear Rheometer: Interim Report on Screening Tests* (Technical Memorandum: UCPRC-TM-2014-02). Davis and Berkeley, CA: University of California Pavement Research Center.

Jones, D., Rizvi, H., Liang, Y., Hung, S., Buscheck, J., Alavi, Z., and Hofko, B. 2017. *Development of Performance-Based Specifications for Asphalt Rubber Binder: Interim Report on Phase 1 and Phase 2 Testing* (Research Report: UCPRC-RR-2017-01). Davis and Berkeley, CA: University of California Pavement Research Center.

Jones, D., Rizvi, H., and Brotschi, J. 2023. *Development of Performance-Based Specifications for Asphalt Rubber Binder: Phase 2g Additional Testing of Five Plant-Sampled Binders and RHMA G Mixes* (Research Report: UCPRC-RR-2020-08). Davis and Berkeley, CA: University of California Pavement Research Center.

9. VERSION UPDATES
None

10. LABORATORY ACCREDITATION
The UCPRC laboratory is accredited by AASHTO resource and CCRL for the laboratory testing discussed in this report.

11. SIGNATURES

D. Jones **FIRST AUTHOR**	J.T. Harvey **TECHNICAL REVIEW**	C. Fink **EDITOR**	J.T. Harvey **PRINCIPAL INVESTIGATOR**	K. Foo **CALTRANS TECH. LEAD**	T.J. Holland **CALTRANS CONTRACT MANAGER**

DISCLAIMER STATEMENT

This document is disseminated in the interest of information exchange. The contents of this report reflect the views of the authors who are responsible for the facts and accuracy of the data presented herein. The contents do not necessarily reflect the official views or policies of the State of California or the Federal Highway Administration. This publication does not constitute a standard, specification, or regulation. This report does not constitute an endorsement by the Department of any product described herein.

ACKNOWLEDGMENTS

The University of California Pavement Research Center acknowledges the following individuals and organizations who contributed to the project:

- The California Department of Transportation
- Nathanial Gauff and William Heung from the California Department of Resources, Recycling and Recovery
- The UCPRC laboratory operations team

PROJECT OBJECTIVES

The objective of this study is to recommend appropriate contract acceptance criteria for wet-process asphalt rubber binders used in gap- and open-graded mixes using current Superpave PG equipment with testing procedures that have been modified where appropriate. This objective will be met by completing the following tasks in a series of phases. Tasks completed in Phase 1 and Phase 2 are noted.

Task 1: Review relevant literature on the topic. Contact dynamic shear rheometer (DSR) equipment manufacturers and discuss test requirements and alternative geometries.

Task 2: Collect samples of asphalt binder, crumb rubber particles, and extender oil for laboratory preparation of asphalt rubber binders. On completion of initial screening tests, identify completed and current projects where asphalt rubber binder samples can be collected for additional testing. Prepare laboratory-conditioned samples for testing with a DSR.

Task 3: Evaluate the use and ability of the alternative concentric cylinder DSR geometry to provide realistic and repeatable results for unmodified, polymer-modified, and tire rubber-modified binders that are comparable to results from the same tests using conventional parallel plate geometries. The performance of these binders is routinely measured with parallel plate geometry in terms of the Superpave performance grading system.

Task 4: Compare the abilities of the parallel plate and concentric cylinder geometries for testing asphalt rubber binder containing crumb rubber particles of various sizes, and evaluate the effects of different crumb rubber particles and asphalt rubber binder properties on test results.

Task 5: Evaluate and refine short- and long-term aging procedures for asphalt rubber binders.

Task 6: Evaluate and refine specimen preparation procedures for low-temperature testing of asphalt rubber binders in a bending beam rheometer.

Task 7: Evaluate whether the concentric cylinder geometry is appropriate for intermediate-temperature and multiple stress creep recovery testing.

Task 8: Evaluate the high-, intermediate-, and low-temperature rheological properties of field-sampled asphalt rubber binders using the refined procedures developed in Tasks 1 through 7, and interpret the test results in conjunction with results from tests on field-sampled gap-graded mixes prepared with the same binders.

Task 9: Evaluate the influence of incompletely digested rubber particles on testing procedures and results.

Task 10: Prepare provisional procedures for conducting the recommended tests and interpreting the test results.

Task 11: Suggest provisional performance grading criteria, provisional contract acceptance criteria for wet-process asphalt rubber binders, and a provisional California performance grade (PG) map for asphalt rubber binders.

Task 12: Prepare reports documenting this research effort, with recommendations for specification language and, if required, recommendations for further research to validate the provisional performance grading and contract acceptance criteria.

This report provides an update on work completed in Phase 2g covering Task 8.

EXECUTIVE SUMMARY

Introduction

The work discussed in this interim report is part of a larger study, funded by the California Department of Transportation (Caltrans). The study objective focuses on developing and recommending testing procedures and criteria for performance-based specifications of asphalt rubber binders used in gap-graded and open-graded mixes using current Superpave performance grade (PG) equipment. Work in this phase covered the testing of 19 plant-produced binders and five of the gap-graded rubberized hot mix asphalt mixes produced with them.

Testing Summary

Rheology Testing

Rheology testing to determine the high-, intermediate-, and low-temperature performance grades and multiple stress creep recovery (MSCR) of 19 plant-produced asphalt rubber binders, using the testing procedures developed in Phase 2 of the study, was undertaken to test the procedures. The following important observations from the tests were made:

- Testing in this phase of the study provided results that were consistent with those obtained during preliminary testing in Phase 2e of the larger study.
- Although the low-temperature performance grades appeared to be reasonable, the high-temperature grades appeared to be unrealistically high, while the intermediate-temperature grades appeared to be potentially lower than anticipated, when compared to the base binders. Fourteen of the binders tested with concentric cylinder geometry and 13 tested with parallel plate geometry had PGs higher than the maximum grade of 82°C listed in the AASHTO M 320 standard. Grades higher than 82 are considered to be unrealistically high and probably not a true indication of likely high-temperature performance (i.e., rut resistance under heavy loads on hot days).
- A comparison of the concentric cylinder and parallel plate (3 mm gap) geometries indicated that the results between the two geometries are different, with differences likely to be higher than the precision and bias of the individual procedures. Precision and bias statements for these procedures had not been developed at the time of preparing this report. These results indicate that the two geometries cannot be used interchangeably.
- No consistent trends in results were observed between any of the parameters tested.
- Observations in Phase 2e and during this phase of the study indicated that incompletely digested rubber particles appeared to have a dominant influence on results and caused

variability between results, regardless of the testing geometry used. Considering these incompletely digested particles as part of a homogenous binder may therefore not be appropriate when determining performance grades. This observation has prompted further study (Phase 3) to investigate the extent to which these incompletely digested particles might affect performance grading results along with testing procedures to overcome the problems. The study focuses on removal of larger incompletely digested particles from the binder by sieving or centrifuging and then testing the binders following standard performance grading procedures using parallel plate geometry with either 1 mm or 2 mm gaps. Results after removal of incompletely digested rubber particles larger than 250, 500, and 850 µm will be compared with unprocessed binders. The 19 asphalt rubber binders tested in this phase of the study are being retested in Phase 3 to assess the removal of larger incompletely digested rubber particles on performance grades.

Mix Testing

Mix testing was undertaken to assess rutting and cracking performance in relation to binder performance grading to determine whether the rheology testing approaches provide properties that are representative of likely field performance. A comparison of binder and mix test results did not show any consistent trends. However, the following trends between some results were observed:

- Rutting test result rankings (flow number and cycles to 5% permanent axial strain) were consistent with the binder high-temperature PG result rankings.
- Flexibility index rankings (highest to lowest) were consistent with Delta T_C (lowest to highest) and non-recoverable creep compliance (highest to lowest). Flexibility index results (highest to lowest) also corresponded with mix rutting results (lowest to highest) as expected (i.e., cracking and rutting results are opposite).
- Beam fatigue rankings did not match any binder testing rankings. However, excluding the binder and mix results from one "outlier," the mix fatigue life and binder m-value rankings were the same for the other four binders/mixes.

Rubber Content Determination

Limited exploratory testing was conducted to assess the use of Fourier-transform infrared (FTIR) spectroscopy to determine rubber content in rubber-modified binders. One base binder with eight different crumb rubber modifier (CRM) contents, ranging from 2.5% to 35% by weight of the base binder, were tested in unaged and PAV-aged condition. Extender oil alone and base binder modified with extender oil only were also tested to determine the potential influence of

extender oil on the results. A known styrene-butadiene rubber (SBR, 75% butadiene and 25% styrene) signature was used to identify the presence of CRM.

In both aging conditions, the SBR signature values increased with increasing rubber dosage. Values for the PAV-aged binders were notably higher than those for the unaged binders, indicating that aging will influence values over time. The results indicate that FTIR is a potentially valid method for quantifying rubber content in rubber-modified binders.

Conclusions

Incompletely digested rubber particles—which have different sensitivities to temperature, aging, and applied stress and strain than the base asphalt binder—appear to dominate the binder rheology test results, leading to what appears to be unrealistic performance grades. Work is continuing in Phase 3 of this study to adjust testing procedures to account for the influence that these incompletely digested particles have on results.

The proposed modifications to short- and long-term aging procedures (i.e., rolling thin-film oven and pressure aging vessel) and to the bending beam rheometer specimen preparation procedures developed in Phase 2 are considered to be more aligned with the original intent of the tests and will likely reduce the variability between replicate specimens during testing.

Recommendations

No recommendations for implementation are warranted at this stage of the study.

TABLE OF CONTENTS

LIST OF TABLES

LIST OF FIGURES

LIST OF ABBREVIATIONS

AASHTO	American Association of State Highway and Transportation Officials
AMPT	Asphalt mix performance tester
AR	Asphalt rubber
ASTM	American Society for Testing and Materials
BBR	Bending beam rheometer
CalRecycle	California Department of Resources Recycling and Recovery
Caltrans	California Department of Transportation
CC	Concentric cylinder
CG	Continuous grade
CRM	Crumb rubber modifier
CT	Caltrans test
DGAC	Dense-graded asphalt concrete
DSR	Dynamic shear rheometer
E^*	Dynamic modulus
FI	Flexibility index
FTIR	Fourier Transformed Infrared Spectroscopy
G^*	Complex shear modulus
G_f	Fracture energy
Gmb	Bulk specific gravity
GTR	Ground tire rubber
HMA	Hot mix asphalt
J_{nr}	Non-recoverable creep compliance
LVDT	Linear variable displacement transducer
MSCR	Multiple stress creep recovery
PAV	Pressurized aging vessel
PG	Performance grade
PM	Polymer modified
PP	Parallel plate
RAC	Rubberized asphalt concrete
RAP	Recycled asphalt pavement
RHMA-G	Gap-graded rubberized hot mix asphalt
RHMA-O	Open-graded rubberized hot mix asphalt
RTFO	Rolling thin-film oven
SCB	Semicircular bend
SBR	Styrene-butadiene rubber
TR	Tire rubber modified
UCPRC	University of California Pavement Research Center
δ	Phase angle

TEST METHODS CITED IN THE TEXT

AASHTO

M 320 Standard Specification for Performance-Graded Asphalt Binder
M 332 Standard Specification for Performance-Graded Asphalt Binder Using Multiple Stress Creep Recovery (MSCR) Test
R 28 Standard Practice for Accelerated Aging of Asphalt Binder Using a Pressurized Aging Vessel (PAV)
T 166 Standard Method of Test for Bulk Specific Gravity (Gmb) of Compacted Hot Mix Asphalt (HMA) Using Saturated Surface-Dry Specimens
T 240 Standard Method of Test for Effect of Heat and Air on a Moving Film of Asphalt (Rolling Thin-Film Oven Test)
T 269 Standard Method of Test for Percent Air Voids in Compacted Dense and Open Asphalt Mixtures
T 313 Standard Method of Test for Determining the Flexural Creep Stiffness of Asphalt Binder Using the Bending Beam Rheometer
T 315 Standard Method of Test for Determining the Rheological Properties of Asphalt Binder Using a Dynamic Shear Rheometer
T 321 Standard Method of Test for Determining the Fatigue Life of Compacted Asphalt Mixtures Subjected to Repeated Flexural Bending
T 331 Bulk Specific Gravity (Gmb) and Density of Compacted Hot Mix Asphalt (HMA) Using Automatic Vacuum Sealing Method
T 378 Standard Method of Test for Determining the Dynamic Modulus and Flow Number for Asphalt Mixtures Using the Asphalt Mixture Performance Tester (AMPT)
T 393 Standard Method of Test for Determining the Fracture Potential of Asphalt Mixtures Using Illinois Flexibility Index Test (I-FIT)

ASTM

D8 Standard Terminology Relating to Materials for Roads and Pavements
D36 Standard Test Method for Softening Point of Bitumen (Ring-and-Ball Apparatus)
D92 Standard Test Method for Flash and Fire Points by Cleveland Open Cup Tester
D217 Standard Test Methods for Cone Penetration of Lubricating Grease
D297 Standard Test Methods for Rubber Products—Chemical Analysis
D445 Standard Test Method for Kinematic Viscosity of Transparent and Opaque Liquids (and Calculation of Dynamic Viscosity)
D2007 Standard Test Method for Characteristic Groups in Rubber Extender and Processing Oils and Other Petroleum-Derived Oils by the Clay-Gel Absorption Chromatographic Method
D5329 Standard Test Methods for Sealants and Fillers, Hot-Applied, for Joints and Cracks in Asphalt Pavements and Portland Cement Concrete Pavements
D7741 Standard Test Method for Measurement of Apparent Viscosity of Asphalt-Rubber or Other Asphalt Binders by Using a Rotational Handheld Viscometer
D7405 Standard Test Method for Multiple Stress Creep and Recovery (MSCR) of Asphalt Binder Using a Dynamic Shear Rheometer

D7643 Standard Practice for Determining the Continuous Grading Temperatures and Continuous Grades for PG Graded Asphalt Binders

D8225 Standard Test Method for Determination of Cracking Tolerance Index of Asphalt Mixture Using the Indirect Tensile Cracking Test at Intermediate Temperature

Caltrans CT

208 Method of Test for Apparent Specific Gravity of Fine Aggregates

385 Method of Test for Sampling and Testing Crumb Rubber Modifier

388 Method of Test for Sampling and Reheating Asphalt Rubber Binder Field Samples Prior to Viscosity Testing in Accordance to ASTM D7741

SI* (MODERN METRIC) CONVERSION FACTORS

APPROXIMATE CONVERSIONS TO SI UNITS

Symbol	When You Know	Multiply By	To Find	Symbol
		LENGTH		
in.	inches	25.40	millimeters	mm
ft.	feet	0.3048	meters	m
yd.	yards	0.9144	meters	m
mi.	miles	1.609	kilometers	km
		AREA		
in^2	square inches	645.2	square millimeters	mm^2
ft^2	square feet	0.09290	square meters	m^2
yd^2	square yards	0.8361	square meters	m^2
ac.	acres	0.4047	hectares	ha
mi^2	square miles	2.590	square kilometers	km^2
		VOLUME		
fl. oz.	fluid ounces	29.57	milliliters	mL
gal.	gallons	3.785	liters	L
ft^3	cubic feet	0.02832	cubic meters	m^3
yd^3	cubic yards	0.7646	cubic meters	m^3
		MASS		
oz.	ounces	28.35	grams	g
lb.	pounds	0.4536	kilograms	kg
T	short tons (2000 pounds)	0.9072	metric tons	t
		TEMPERATURE (exact degrees)		
°F	Fahrenheit	(F-32)/1.8	Celsius	°C
		FORCE and PRESSURE or STRESS		
lbf	pound-force	4.448	newtons	N
lbf/in^2	pound-force per square inch	6.895	kilopascals	kPa

APPROXIMATE CONVERSIONS FROM SI UNITS

Symbol	When You Know	Multiply By	To Find	Symbol
		LENGTH		
mm	millimeters	0.03937	inches	in.
m	meters	3.281	feet	ft.
m	meters	1.094	yards	yd.
km	kilometers	0.6214	miles	mi.
		AREA		
mm^2	square millimeters	0.001550	square inches	in^2
m^2	square meters	10.76	square feet	ft^2
m^2	square meters	1.196	square yards	yd^2
ha	hectares	2.471	acres	ac.
km^2	square kilometers	0.3861	square miles	mi^2
		VOLUME		
mL	milliliters	0.03381	fluid ounces	fl. oz.
L	liters	0.2642	gallons	gal.
m^3	cubic meters	35.31	cubic feet	ft^3
m^3	cubic meters	1.308	cubic yards	yd^3
		MASS		
g	grams	0.03527	ounces	oz.
kg	kilograms	2.205	pounds	lb.
t	metric tons	1.102	short tons (2000 pounds)	T
		TEMPERATURE (exact degrees)		
°C	Celsius	1.8C + 32	Fahrenheit	°F
		FORCE and PRESSURE or STRESS		
N	newtons	0.2248	pound-force	lbf
kPa	kilopascals	0.1450	pound-force per square inch	lbf/in^2

* SI is the abbreviation for the International System of Units. Appropriate rounding should be made to comply with Section 4 of ASTM E380. (Revised March 2021)

1. INTRODUCTION

1.1 Background

1.1.1 Use of Rubberized Asphalt Concrete

Each year the United States generates nearly 300 million scrap tires, the approximate equivalent of one passenger car tire per person per year *(1)*. Most of these tires end up in landfills, with the consequent environmental impacts. One tire disposal solution involved grinding the tires into crumbs that are incorporated into asphalt binders used to produce rubberized asphalt concrete (RAC), which includes gap- and open-graded rubberized hot mix asphalt (RHMA-G and RHMA-O, respectively). RAC is commonly used in California, Arizona, Texas, Florida, and New Jersey. Successful, documented use of this material has created growing interest in many other states *(2,3)*.

The maximum allowable crumb rubber particle size in asphalt rubber binders differs among the states (e.g., California and Arizona specify rubber particles passing the #8 [2.36 mm] sieve, while Florida limits the maximum size to that passing the #30 [0.6 mm] sieve). Crumb rubber particle size in asphalt rubber chip seal applications is typically limited to that passing the #18 (1 mm) sieve to prevent clogging of binder spray nozzles.

In addition to recognizing the environmental benefits of recycling tires into asphalt concrete, research has also shown that RAC, when used in overlays, has better resistance to the fatigue and reflective cracking caused by traffic and exposure to temperature extremes than conventional dense-graded asphalt concrete (DGAC). Studies have also shown that half-thickness RAC used in overlays on cracked pavement can typically provide the same reflective cracking life as full thickness DGAC overlays *(4-6)*.

1.1.2 Production of Rubber-Modified Binders

In California, crumb rubber from scrap tires is generally added to asphalt binder in a so-called wet process. Wet-process rubber-modified binder can be produced at an asphalt plant, at a nearby distribution center (field blending), or at a supplier's terminal or a refinery (terminal blending). Two forms of modified binder are currently produced: *asphalt rubber binder* and *tire rubber-modified binder*:

- Asphalt rubber (AR) binders, by ASTM definition, must contain 15% or more rubber by weight of the binder. California Department of Transportation (Caltrans) specifications require 18% to 22%. The rubber particles have a coarse gradation (between 250 µm and 2.36 mm), and extender oils are often used to promote digestion. Larger particles are typically not fully digested into the binder.
- Tire rubber-modified (TR) binders typically contain less than 10% rubber, and the rubber particles are usually smaller than 250 µm. These binders have characteristics similar to those of polymer-modified binders and can be characterized accordingly using existing Superpave performance grading (PG) procedures (AASHTO M 320 and ASTM D7643). In California, these binders must meet Caltrans PG-M modified binder specifications.

The significant differences in the constituents and production procedures of asphalt rubber binders result in a product very different from unmodified asphalt binders and therefore different approaches are required to test and characterize them.

The Superpave PG procedures (AASHTO M 320 and ASTM D7643) were developed for asphalt binders that contain no additives or particles and are therefore mostly inappropriate for testing asphalt rubber binders. Consequently, current quality control testing of asphalt rubber binders is limited to rotational viscosity (Haake) and cone penetration. For this reason, it is generally agreed that alternative binder grading procedures consistent with Superpave PG procedures are needed to characterize asphalt rubber binders. The research discussed in this report contributes to the development of these performance grading procedures for wet-process asphalt rubber binders.

1.1.3 Crumb Rubber Modifier Production

Crumb rubber modifier (CRM) (also known as ground tire rubber [GTR]) is produced by grinding waste tires. The two main methods used are ambient grinding and cryogenic fracturing. In the ambient grinding process, the scrap tires are cut into small pieces and then shredded and ground at ambient temperature into small crumbs. The ambient grinding method results in irregular-shaped rubber particles with rough surfaces. In cryogenic fracturing, the cut scrap tire pieces are frozen with liquid nitrogen and then fractured into small crumbs. Cryogenic fracturing usually results in cubical-shaped rubber particles with smooth surfaces. The CRM used to produce asphalt rubber binders in California is primarily derived from ambient grinding.

1.1.4 Current Caltrans Asphalt Rubber Binder Specifications

Current Caltrans specifications for the constituents of asphalt rubber binder, the asphalt rubber binder reaction design profile, and the criteria for quality control and acceptance are summarized in Table 1.1, Table 1.2, and Table 1.3, respectively. Asphalt rubber binder quality is characterized based on rotational viscosity (Haake), cone penetration, resilient properties, and softening properties. The asphalt rubber binder must meet the specified limits in Table 1.3 after at least 45 minutes of reaction time between the asphalt binder and the crumb rubber.

Table 1.1: Caltrans Specifications for Asphalt Rubber Binder Constituents

Component	Characteristic	Test Method	Value
Base asphalt binder	Viscosity, m^2/s ($\times 10^{-6}$) at 100°C	ASTM D445	X ± 3[a]
	Flash point, Cleveland Open Cup (°C)	ASTM D92	>207
	Asphaltenes (% by mass)	ASTM D2007	<0.1
	Aromatics (% by mass)	ASTM D2007	>55
Crumb rubber modifier[b]	Scrap tire crumb rubber gradation (% passing #8 sieve)	CT 385	100
	High natural rubber gradation (% passing #10 sieve)	CT 385	100
	Wire in CRM (% max.)	CT 385	0.01
	Fabric in CRM (% max.)	CT 385	0.05
	CRM particle length (in. max.)[c]	—	3/16
	CRM specific gravity[c]	CT 208	1.1–1.2
	Natural rubber content in high natural rubber (%)[c]	ASTM D297	40.0–48.0

[a] The symbol "X" is the proposed extender oil viscosity. "X" must be from 19 to 36. A change in "X" requires a new asphalt rubber binder design.

[b] CRM must be ground and granulated at ambient temperature. If the steel and fiber are cryogenically separated, this must occur before grinding and granulating. If cryogenically produced, CRM particles must be large enough to be ground or granulated and must not pass through the grinder or granulator.

[c] Test at mix design and for certificate of compliance.

Table 1.2: Asphalt Rubber Binder Reaction Design Profile

Characteristic	Test Method	Minutes of Reaction[a]							Value
		45	60	90	120	240	360	1440	
Cone penetration @77°F (0.10 mm)	ASTM D217	X				X		X	25–70
Resilience @ 77°F (% rebound)	ASTM D5329	X				X		X	>18
Field softening point (°F)	ASTM D36	X				X		X	125–165
Viscosity @ 375°F, (centipoise)	ASTM D7741[b]	X	X	X	X	X	X	X	1,500–4,000

[a] Six hours (360 minutes) after CRM addition, the oven temperature is reduced to 275°F for 16 hours. After the 16-hour (1,320-minute) cool down after CRM addition, the binder is reheated to the reaction temperature expected during production for sampling and testing at 24 hours (1,440 minutes). "X" denotes required testing.

[b] Sample prepared according to CT 388.

Table 1.3: Caltrans Specifications for Asphalt Rubber Binder Quality Control and Acceptance

Characteristic	Test Purpose	Test Method	Value	
			Minimum	Maximum
Cone penetration @77°F (0.10 mm)	Acceptance	ASTM D217	25	70
Resilience @ 77°F (% rebound)	Acceptance	ASTM D5329	18	—
Field softening point (°F)	Acceptance	ASTM D36	125	165
Viscosity @ 375°F (centipoise)	Quality control	ASTM D7741[a]	1,500	4,000

[a] Sample prepared according to CT 388.

According to the ASTM D8 test method, a minimum of 15% CRM by weight of the asphalt binder is required to meet the definition of asphalt rubber binder. However, Caltrans specifications require a CRM content between 18% and 22% by weight of the base binder, of which 25% must be natural rubber. An extender oil must be added at a rate of 2% to 6% by weight of the base asphalt binder to facilitate the reaction between the asphalt binder and rubber particles.

Current Caltrans specifications also require crumb rubber particles finer than 2.36 mm (100% passing the #8 sieve). Cryogenic grinding is only permitted as a first step for the separation of metals and fibers, after which larger rubber particles are ground at ambient temperatures to meet the required sizes.

For each Caltrans project, asphalt rubber binder producers must propose a design and profile for the binder that will be used. The proposed design must specify the materials to be used, including base binder, extender oil, and crumb rubber. The asphalt rubber binder profile serves as a production quality indicator and is not used as a performance specification. The profile illustrates the characteristics of the binder over a 24-hour (1,440-minute) reaction period.

1.2 Problem Statements

A number of limitations to the current asphalt rubber binder specification have been identified through a review of the literature and discussions with stakeholders *(3)*. These include the following:

- The current Caltrans specification for wet-process asphalt rubber binders focuses mainly on measuring viscosity at the plant using a handheld rotational viscometer. Temperature control requirements during testing are limited, which can influence results, given that asphalt binder properties are highly influenced by temperature. While viscosity is an important parameter for the pumpability and workability of the binder and ultimately of the mix, it does not directly relate to the in-service performance of the binder within a rubberized asphalt concrete mix or a rubberized asphalt surface treatment. Additionally, due to the particulate phase of these binders, viscosity measurements alone lack sufficient accuracy to completely describe their complex behavioral and performance properties.
- Although cone penetration grading and resilience properties do provide a means to evaluate the stiffness and resilience of asphalt rubber binders, the Superpave performance grading testing procedure moved away from these tests because they have several limitations, including the following:

  - They are empirical tests that measure a binder's viscous and elastic properties, but the tests do not necessarily correlate with field performance.
  - The tests only measure a binder's properties at a single intermediate temperature and thereby fail to provide an accurate indication of its properties at typical high and low service temperatures, or of its temperature susceptibility (change of stiffness with change of temperature).
  - The tests do not address the effects of short-term aging (during mixing and compaction) and long-term aging (during service life) on binder properties.
- Softening point generally indicates the phase change temperature of binders and may not be sufficient for comprehensive performance/rheological characterization.
- Rheological testing using a dynamic shear rheometer (DSR) and a bending beam rheometer (BBR) is now considered standard practice for evaluating performance-related characteristics of unmodified, polymer-modified, and tire rubber-modified asphalt binders. However, the standard parallel plate geometry used in a DSR test is potentially inappropriate for measuring the properties of asphalt rubber binders produced per Caltrans specifications. When an asphalt rubber binder is tested in a DSR using parallel plate geometry with a 1 mm or 2 mm gap, incompletely digested rubber particles can contact both the top and bottom plates and interfere with the torque and strain measurements. This interference results in the rheology of the rubber particles dominating the measurement and potentially providing misleading information about the rheology of the blended asphalt rubber binder as a whole. A potential consequence of this misleading information can be the choice/use of an inappropriate binder for a given climatic region. According to AASHTO T 315 (Standard Method of Test for Determining the Rheological Properties of Asphalt Binder Using a Dynamic Shear Rheometer), the gap size between the plates should be at least four times the maximum particle size to provide reliable results (i.e., an 8 mm gap, with correspondingly adjusted plate diameter, would be required to test binders with crumb rubber particles up to 2.0 mm [#10]). However, the maximum gap size recommended by rheologists is about 5 mm to ensure a satisfactory linear shear rate through the asphalt binder sample sandwiched between the plates. Although increasing the gap size is a potential solution for dealing with the larger rubber particle sizes, this increase can introduce other problems, such as difficultly in trimming the specimen, uncontrollable edge effects, unacceptable temperature gradients, poor repeatability, and potentially misleading results. When testing with parallel plate geometry, the modulus of the asphalt binder is proportional to the sample radius to the power of four. Consequently, a 2% reduction in radius due to incorrect trimming implies a potential 16% reduction in the measured modulus.
- Other limitations of the current performance grading testing procedures when testing asphalt rubber binders include the following:

    - Rubber particles do not age in the same way or to the same extent as asphalt binders.
    - Short-term aging in a rolling thin-film oven (RTFO) does not uniformly coat the bottle with the specified sample size (i.e., asphalt content is between 18% and 22% less because of the rubber) and at the current testing temperature because the asphalt rubber binder is more viscous, and it is difficult to remove the aged binder from the bottle.
    - Long-term aging of asphalt rubber binder in a pressurized aging vessel (PAV) does not uniformly coat the pan with the specified sample size.
    - Low-temperature testing of asphalt rubber specimens in the BBR using current specimen preparation procedures is questionable, since the viscous, particulate-rich binders are difficult to pour into the specimen preparation mold. The test method and interpretation of its results also need to be studied in greater detail to confirm their appropriateness for testing asphalt rubber binder.
- The actual grading limits developed for unmodified and polymer-modified asphalt binders may not be appropriate asphalt rubber binder performance indicators as they may not reflect the contribution of the binder rheology in terms of the rutting, fatigue, and low-temperature cracking performance of RAC mixes.

To resolve these issues, there is a need for alternative testing configurations and procedures that can better evaluate the performance characteristics of field-blended wet-process asphalt rubber binders using the same or similar Superpave PG parameters used for unmodified, polymer-modified and tire rubber-modified asphalt binders. These alternate methods can then be used to establish performance-based contract acceptance criteria for the production of asphalt rubber binders, which will in turn lead to more reliable performance in the field.

1.3 Project Objectives

The work discussed in this report is part of a larger study, funded by Caltrans, with the objective of developing and recommending testing procedures and criteria for performance-based specifications of asphalt rubber binders used in gap- and open-graded mixes using current Superpave PG equipment. This objective will be met by completing the following tasks in a series of phases (Figure 1.1). Work that had been completed at the time of preparing this report is noted.

1. Review relevant literature on the topic. Contact DSR equipment manufacturers and discuss test requirements and alternative geometries. (Completed in Phase 1 *[3]*.)

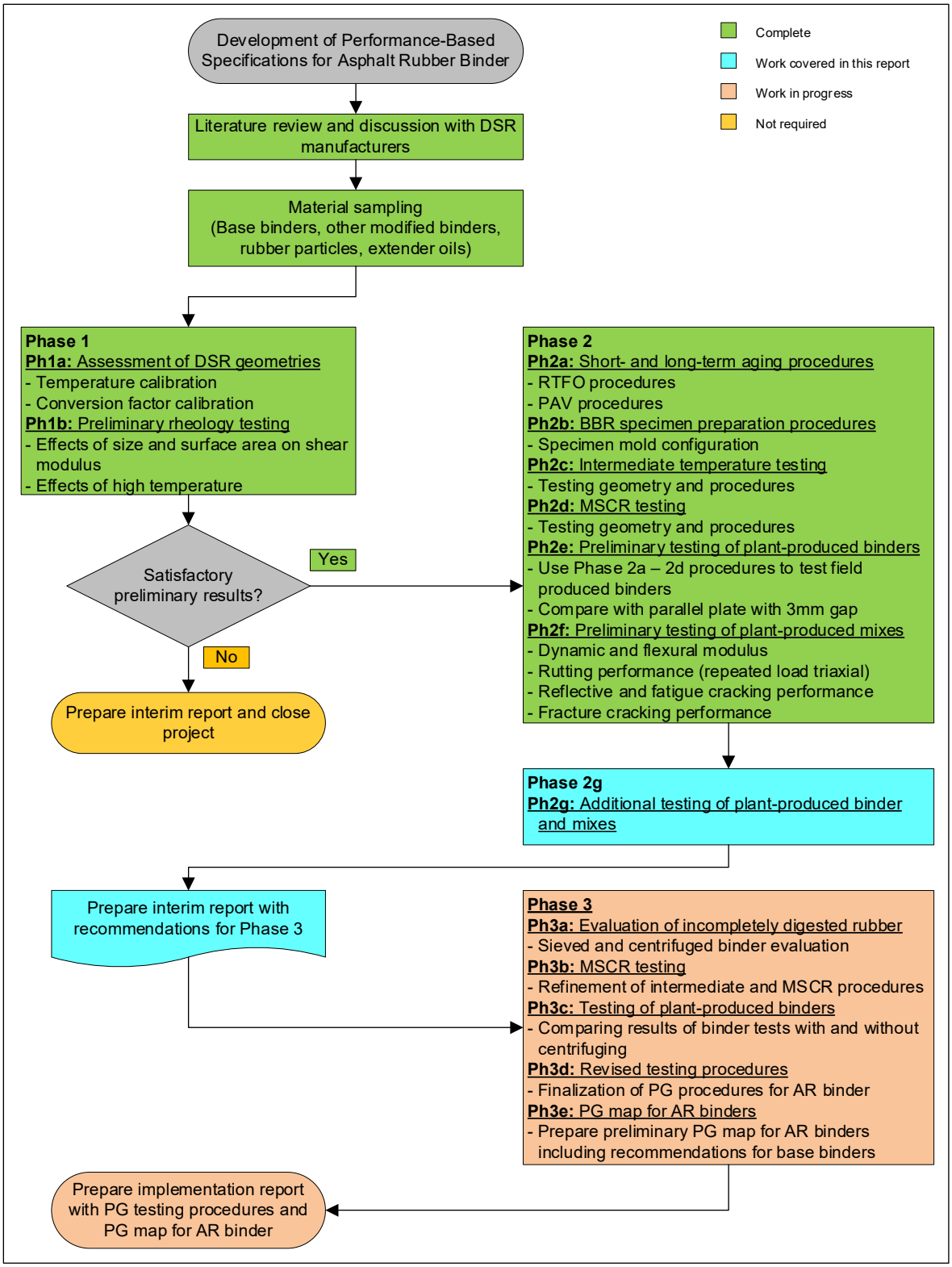

Figure 1.1: Flowchart of project phases and tasks.

2. Collect samples of asphalt binder, crumb rubber particles, and extender oil for laboratory preparation of asphalt rubber binders. On completion of initial screening tests, identify

completed and current projects where asphalt rubber binder samples can be collected for additional testing. Prepare laboratory-conditioned samples for testing with a DSR. (Completed in Phase 1 *[3]*.)

3. Evaluate the use and ability of the alternative concentric cylinder DSR geometry to provide realistic and repeatable results for unmodified, polymer-modified (PM), and tire rubber-modified (TR) binders that are comparable to results from the same tests using conventional parallel plate geometries. The performance of these binders is routinely measured with parallel plate geometry in terms of the Superpave performance grading system. (Completed in Phase 1a *[3]*.)
4. Compare the abilities of the parallel plate and concentric cylinder geometries for testing asphalt rubber binder containing crumb rubber particles of various sizes, and evaluate the effects of different crumb rubber particles and asphalt rubber binder properties on test results. (Completed in Phase 1b *[3]*.)
5. Evaluate and refine short- and long-term aging procedures for asphalt rubber binders. (Completed in Phase 2a *[3]*.)
6. Evaluate and refine specimen preparation procedures for low-temperature testing of asphalt rubber binders in a BBR. (Completed in Phase 2b *[3]*.)
7. Evaluate whether the concentric cylinder geometry is appropriate for intermediate-temperature and multiple stress creep recovery (MSCR) testing. (Preliminary testing on this task was completed in Phase 2c and Phase 2d *[3]* and updates to the procedure were completed in Phase 2e)
8. Evaluate the high-, intermediate-, and low-temperature rheological properties of field-sampled asphalt rubber binders using the refined procedures developed in Tasks 1 through 7, and interpret the test results in conjunction with results from tests on field-sampled gap-graded mixes prepared with the same binders. (Preliminary testing was completed in Phase 2e for the plant-produced binders and in Phase 2f for the gap-graded mixes *[3]*. Additional testing of 19 binders and five mixes is discussed in this report.)
9. Evaluate the influence of incompletely digested rubber particles on testing procedures and results. (Scheduled for Phase 3.)
10. Suggest provisional performance grading criteria and provisional contract acceptance criteria for wet-process asphalt rubber binders. (Scheduled for Phase 3.)
11. Prepare provisional procedures for conducting the recommended tests and interpreting the test results. (Documented in the Phase 2 report *[3]*. Interpretation of results and development of a California PG map for asphalt rubber binders will be documented in a later report.)
12. Prepare reports documenting this research effort, with recommendations for specification language and, if required, recommendations for pilot studies and multi-laboratory round

robin testing to validate the provisional performance grading procedure and contract acceptance criteria, and to develop precision and bias statements.

This interim report covers Task 8 and provides the results of testing 19 plant-produced asphalt rubber binders and five gap-graded rubberized hot mix asphalt mixes produced with them on five of the projects.

Although this study focuses on testing asphalt rubber binders used in gap- and open-graded mixes, the results are relevant for asphalt rubber binders used in chip seals and other surface treatments. However, to prevent clogging of spray nozzles, the maximum rubber particle size used in these applications is typically limited to that passing the #18 (1 mm) sieve, which is considerably smaller than the #8 (2.36 mm) maximum size specified for binders used in gap- and open-graded mixes.

1.4 Measurement Units

Although Caltrans has returned to the use of US standard measurement units, metric units have always been used by the UCPRC in the design and layout of test tracks and for the laboratory, accelerated wheel load testing, field measurements, and data storage. The Superpave performance grading system is a metric standard and uses metric units. In this report, both English and metric units (provided in parentheses after the English units) are provided in the general discussion. Metric units are used in the reporting of performance grading and mix test results. A conversion table is provided on page xvii.

2. SUMMARY OF PHASE 2 RESEARCH

2.1 Introduction

The first two phases of a three-phase study to investigate test methods for measuring the performance properties of asphalt rubber binders produced according to Caltrans specifications were completed in 2017 *(3)*. The current method of rotational viscosity testing (Haake) used by Caltrans is deemed to be an insufficient measure for assessing the expected performance for asphalt rubber binders compared to the more rigorous testing requirements for unmodified, polymer-modified, and tire rubber-modified binders. The first phase of the study consisted of preliminary testing to compare two different dynamic shear rheometer (DSR) geometries, with a goal to make recommendations about whether to adopt similar testing procedures for asphalt rubber binders to supplement those currently used for unmodified and other modified binders. The second phase of the study investigated short- and long-term aging procedures, developed revised specimen preparation procedures for bending beam rheometer (BBR) testing, and conducted preliminary investigations into the use of the two DSR geometries for intermediate-temperature testing and multiple stress creep recovery (MSCR) testing. Three asphalt rubber binders, and loose mixtures produced with them, were sampled from three different field projects to assess the binder testing procedures developed and to relate the tested properties to expected field performance. This report covers Phase 2g, which entailed the testing of 19 additional asphalt rubber binders and the gap-graded rubberized asphalt (RHMA-G) mixes produced with them.

2.2 Phase 1: DSR Testing Geometries

The high-temperature properties of unmodified and other modified asphalt binders are typically measured in tests that use a DSR with parallel plate geometry, with the gap size between the plates dependent on the size of any particulates in the binder. A 2.0 mm gap size is considered to be the maximum appropriate gap for testing asphalt binders to limit variability in results due to specimen trimming and binder flow at higher temperatures, provided that no particulates in the binder exceed the AASHTO/ASTM-recommended maximum particle size of 0.25 mm (or 250 µm [#60]). In addition, DSR manufacturers recommend that the gap between the plates

should be at least four times the maximum particle size to provide reliable results. However, Caltrans specifications allow crumb rubber particles up to 2.36 mm (passing the #8 sieve), which exceeds this maximum recommended size for parallel plate testing (i.e., an 8 mm gap, with correspondingly adjusted plate diameter, would be required for 2.0 mm [#10] particle sizes). Consequently, the appropriateness of the parallel plate geometry for testing asphalt rubber binders is questionable because the rheology of the large incompletely digested rubber particles may dominate the DSR results and give misleading performance parameters for the binder properties. Phase 1 of the study therefore assessed the concentric cylinder, an alternative geometry that can accommodate larger particles in the asphalt rubber binder. The two geometries were compared using unmodified, polymer-modified, tire rubber-modified (i.e., binders with no particulates), and wet-process asphalt rubber binders (binder containing incompletely digested rubber particles). Binders with no particles were tested with a 1 mm gap, while the asphalt rubber binders were tested with a 3 mm parallel plate gap (to better accommodate the incompletely digested rubber particles). Key findings from the work completed to date include the following:

- The results obtained from testing the same unmodified, polymer-modified, and tire rubber-modified binders with concentric cylinder and parallel plate geometries in a DSR showed that the two geometries produced results for the same binder that were statistically similar at a 95% confidence interval.
- The results obtained from testing asphalt rubber binders with three different crumb rubber particle size ranges (180 µm to 250 µm, 250 µm to 425 µm, and 425 µm to 850 µm [#40 to #20, #60 to #40, and #80 to #60, respectively]) showed strong correlations between the two testing geometries for finer particle size ranges, but the correlations became weaker with increasing particle size. These weaker correlations in the larger size ranges were attributed in part to the increasing influence of the larger incompletely digested rubber particles in proximity of the plates. Strong correlations between the two geometries were also noted in the test results from assessments of the effects of extender oils and from tire-crushing methods (crushing at ambient versus cryogenic temperatures).

2.3 Phase 2a: Short- and Long-Term Aging Procedures

Phase 2a of the study investigated modifications to the AASHTO T 240 rolling thin-film oven (RTFO) and AASHTO R 28 pressurized aging vessel (PAV) tests to make them more representative of the short- and long-term aging that asphalt rubber binders are subjected to during mix

production and during service life. Suggested modifications to the test procedures include the following:

- RTFO testing
  - Preheating the bottles at 190°C (374°C) for 10 minutes to improve the uniformity of the coating.
  - Increasing the sample size from 35 g to 45 g to account for the rubber particles, to ensure that the specified amount of the base asphalt binder is tested, and to ensure that sufficient binder is available for rheology testing.
  - Increasing the RTFO test temperature from 163°C to 190°C (325°F to 374°F) to better represent rubberized asphalt concrete mix production temperatures.
- PAV sample preparation
  - Preheating the pans at 190°C for 10 minutes prior to pouring to facilitate more even spread of the binder to the required thickness.
  - Increasing the sample size from 50 g to 63 g to account for the rubber particles, to ensure that the specified amount of the base asphalt binder is tested, and to ensure that sufficient binder from a single PAV test is available for rheology testing.
  - Increasing the sample preparation temperature from 163°C to 190°C to be consistent with the temperature of the RTFO-aged binder.
  - Altering the pouring procedure and agitating the pan during pouring to facilitate even spread of the binder to the required thickness.

Test results revealed the following:

- RTFO testing
  - Complete coating of the bottle was achieved with the larger sample at the higher temperature. Although coating was satisfactory using the smaller sample at the higher temperature, insufficient material was produced for the desired rheology testing. Film thickness on the bottle was relatively even but marginally thicker than that measured during aging of conventional unmodified binders, with these results primarily attributed to the presence of incompletely digested rubber particles.
  - Aging at 190°C increased the shear modulus of the asphalt rubber binder and reduced the phase angle, as expected. The true high-temperature performance grade (PG) typically increased by about 6°C, which equates to a one-grade bump. Sample size and extender oil had limited effect on these parameters.
  - Rubber particle size had a notable effect on all tests, which is consistent with findings from the literature.
  - The measured carbonyl and sulfoxide indices for unaged and RTFO-aged binders showed clear trends with respect to the effect of aging temperature and sample size, as

expected. Ongoing testing in Phase 3 will include a more detailed comparison of laboratory- and plant-produced binders to determine whether the proposed revised aging procedure is representative of aging conditions during plant production, storage, transport to the project, and placement.

  - The butadiene index appears to increase with increasing rubber content and could be a useful potential indicator of the level of modification in asphalt rubber binders. This index also changed with increasing RTFO-aging temperature and the larger sample size, which implies that some rubber modification may have continued during aging.

- PAV preparation procedures
  - Complete coating of the pan was achieved with the 63 g sample, and the average film thickness after pouring and after PAV aging met the requirements listed in AASHTO R 28.
  - Following this method provides an additional 130 g of aged binder per PAV test compared to following the standard method (i.e., 10 pans of 63 g versus 10 pans of 50 g), which provides sufficient binder for both intermediate-temperature testing (using the concentric cylinder geometry) and low-temperature testing. This is considered to be an important advantage given that one PAV test takes 20 hours, excluding preparation time.
- Preliminary intermediate-temperature testing of PAV-aged binder
  - No clear trends were observed from the preliminary intermediate-temperature test results on three binders for the different preparation procedures. Only two of the three binders could be tested due to torque limitations of the DSR. The results from one of the binders were consistent with expectations. PAV preparation procedures did not appear to have a significant effect on the test results of the second binder.
- Preliminary BBR testing
  - No clear trends were observed from the stiffness testing results, with little variation observed between the different PAV preparation methods across the three binders tested when variation between replicates within each method were considered.
  - The m-value did not appear to be significantly affected by PAV sample preparation method.

Although only limited DSR and BBR testing was conducted in this phase of the research, the modifications proposed above are considered to be appropriate in reflecting the original intent and mechanisms of the tests. Unfortunately, there is no documented procedure to verify the appropriateness of the procedures given that asphalt rubber binders cannot be effectively extracted and recovered from loose mix or core samples removed from highways.

2.4 Phase 2b: Bending Beam Rheometer Specimen Preparation Procedures

Phase 2b investigated modifications to the mold used to prepare BBR specimens. Pouring asphalt rubber binder into a standard BBR mold is very difficult given the mold's small opening and the viscosity and consistency of the binder. Modified molds that allow binder to be poured through a 12.5 mm opening (i.e., the width of the mold) instead of the standard 6.25 mm opening (i.e., the thickness of the specimen) improved the quality of the specimens in terms of dimension uniformity and absence of air bubbles. However, the specimen's wider surface area made trimming more challenging, and the specimen's rougher surface after trimming could influence the dimensions of the beam. Ongoing refinements to the trimming process are being investigated, along with the determination of new variance limits, to accommodate these inconsistencies.

BBR testing indicated that the mold configuration used to prepare beam specimens can affect the measured rheological properties of the binder and that the low-temperature performance grade could change if the modified configuration is used instead of the standard configuration. Results from the modified configuration appeared to be more consistent than those produced with the standard configuration.

2.5 Phase 2c: Intermediate-Temperature Testing

Preliminary intermediate-temperature test results indicated that the concentric cylinder geometry is potentially suitable for testing of asphalt rubber binders at intermediate temperatures. However, all testing in this phase of the study was conducted at 25°C and the test setup will require more testing with a representative set of asphalt rubber binders to determine whether it is appropriate for determining actual intermediate temperatures, and whether maximum torque ranges of the DSR are likely to be exceeded. Refinements to the testing geometry (e.g., different bob sizes) and testing procedures (e.g., different bob immersion depths) will also be investigated during planned additional testing in Phase 3.

2.6 Phase 2d: Multiple Stress Creep Recovery Testing

Preliminary multiple stress creep recovery (MSCR) test results indicated that the concentric cylinder geometry is also potentially suitable for testing this property of asphalt rubber binders.

However, given that only limited testing was undertaken and that the results were somewhat inconsistent, additional testing is required before any conclusions on the appropriateness of using the concentric cylinder geometry for MSCR testing can be drawn. This evaluation will continue in the next phase when field binders are tested.

2.7 Phase 2e: Rheology Testing on Plant-Produced Binders

Preliminary rheology testing to determine the high-, intermediate-, and low-temperature performance grades of three plant-produced asphalt rubber binders using the proposed testing procedures was undertaken to test the procedures. The following observations from the high-temperature tests were made:

- Concentric cylinder
  - An increase of four grades over the base binder was recorded for two of the asphalt rubber binders and an increase of five grades was recorded for the third.
  - Mean continuous grade results showed that all three binders were relatively close and fell in a range between 91°C and 95°C.
  - Variation in results of the three replicates in each test was small.
  - The incompletely digested rubber particles clearly had a significant influence on the results when compared to the base binder.
  - All results were higher than the maximum grade of 82°C listed in the AASHTO M 320 standard.
- Parallel plates with 3 mm gap
  - The same grade increases recorded for the tests with the concentric cylinder were observed for the tests with the parallel plate.
  - Mean continuous grade results showed that all three binders were relatively close and fell in a range between 92°C and 105°C, a range approximately 7°C higher than the concentric cylinder measurements.
  - Variation in results of the three replicates for each binder was notably larger than the variation recorded when testing with the concentric cylinder.
- Difference between concentric cylinder and parallel plate
  - For the unaged binders, G*/sin(δ) values measured with the parallel plate geometry were consistently higher than those determined from concentric cylinder measurements. Similar trends between the different binders were also apparent.
  - For the RTFO-aged binders, G*/sin(δ) values determined with the parallel plate geometry were again considerably higher than those determined with the concentric cylinder for two of the three binders tested.

- Binder grade
  + Testing with both geometries provided the same high-temperature grade despite the noted variations in test results discussed above.

The following observations from the low-temperature tests were made:

- Stiffness values were well below the AASHTO M 320 criteria for determining the low-temperature grade (S ≤ 300) and, consequently, grades were dictated by the m-value (≥ 0.30). The presence of incompletely digested rubber particles and potential phase separation between these particles and the asphalt binder probably contributed to the low stiffness values.
- Although the acceptable ranges between two test results for the same unmodified binder as listed in AASHTO T 313 (7.2% for stiffness and 2.9% for m-value) were exceeded in most instances, the low-temperature grade of each tested binder remained the same. These larger differences between results were attributed in part to the rougher beam surfaces after trimming and to variation in the number, size, and degree of digestion of the rubber particles in each beam. Revised acceptance ranges for asphalt rubber binders will be suggested, if appropriate, after completion of further testing on additional plant-produced binders in Phase 3.
- The AASHTO M 320 procedure contains no recommendations for asphalt rubber binders. The minimum low-temperature grade in the standard table for conventional binders with a high-temperature grade equal to or greater than 76°C is -22°C, which was achieved for two of the tested binders. The low-temperature grade of the third binder did not differ from that of the base binder.
- Questions regarding other factors that may influence results, and specifically the variability between results, and that may require further investigation, include:
  + Whether changes in the properties of the incompletely digested rubber particles occur at very low temperatures (i.e., in the range of glass transition).
  + Whether different rubber particles (e.g., synthetic versus natural rubber) have different coefficients of thermal expansion.
  + Whether the properties of the rubber particles are in any way effected by the type of temperature control medium used in the BBR (i.e., ethanol for the testing discussed in this report).

A small study was conducted to determine the extent to which incompletely digested particles might affect performance grading test results. This was achieved by comparing the results from the three plant-produced asphalt rubber binders with the results produced using the same binder but with all particles larger than 300 µm (> #50 sieve) removed. Preliminary testing was limited

to the high-temperature grading only. Sieved binders were tested using a 25 mm parallel plate geometry with 2 mm gap according to the standard AASHTO T 315 method. The following observations were made:

- The high-temperature performance grades of the sieved binders were consistently two grades lower than those determined for the unsieved binders, indicating that the incompletely digested particles had a significant influence on the test results.
- The percent decrease in G*/sin(δ) when comparing the sieved with the unsieved binders was significant.
- The correlation between the true performance grades of the two types of binders was strong, indicating that testing sieved binders in a standard parallel plate geometry may be an appropriate alternative to testing unsieved binders in the concentric cylinder geometry.

Given that the variability of incompletely digested rubber particles in asphalt rubber binder samples leads to considerable variability in high-, intermediate-, and low-temperature test results, testing sieved binders may be a more appropriate approach to performance grade testing of these binders, or at least for developing a relationship between test results from unsieved and sieved binders as a means to determine a representative PG grading for asphalt rubber binders. Sieved/centrifuged binders will therefore be included as part of the scheduled Phase 3 testing of additional plant-produced binders.

2.8 Phase 2f: Preliminary Performance Testing on Plant-Produced Mixes

Preliminary mix testing was undertaken to assess rutting and cracking performance in relation to performance grading to determine whether the rheology testing approaches provide properties that are representative of likely field performance. The following observations were made based on the testing of three plant-produced gap-graded asphalt rubber mixes:

- The dynamic and flexural moduli results were similar for all three mixes and were consistent with those measured on other RHMA-G mixes.
- The initial rates of cumulative permanent deformation with increasing loading cycles were similar for the three mixes, but thereafter one mix appeared to be more susceptible to rutting than the other two. Similar trends were recorded in the flow number tests and in tests to determine the number of cycles to 3% and 5% permanent axial strain. Rankings in these tests were consistent with the true high-temperature grade results of the binders.
- Two of the mixes had similar fatigue life results that were somewhat lower than expected for RHMA-G mixes, when compared with other mixes recently tested at the UCPRC. The

remaining mix had a slightly higher fatigue life that was more consistent with other RHMA-G mixes tested.

- The semicircular beam flexibility index results showed the same ranking and trends as the beam fatigue results.

Given that only three plant-produced binders and the mixes produced with them were tested in this phase, the database of results was considered to be insufficient for in-depth analysis purposes. Additional plant-produced mixes were programed for testing in Phase 2g (this report) and Phase 3.

2.9 Conclusions

Based on the results obtained from Phase 1 and Phase 2 testing, the concentric cylinder geometry appears to be a potentially appropriate alternative to the parallel plate geometry for quantifying the properties of asphalt rubber binders produced per Caltrans specifications, and specifically for assessing the performance properties of binders containing crumb rubber particles larger than 250 µm (particles retained on the #60 sieve). Additional testing of a larger number of binders, planned for Phase 2g (this report) and Phase 3 of the project, is required to confirm these initial findings. The concentric cylinder geometry requires a larger binder sample for testing, and it takes longer to complete than testing with the parallel plate geometry. Incompletely digested rubber particles, which have different sensitivities to temperature and applied stress and strain than the base asphalt binder, appear to dominate the test results, and this will need to be factored into the analyses and interpretation of rheology and mix performance test results. The proposed modifications to the short- and long-term aging procedures and to the BBR specimen preparation procedures are considered to be more aligned with the original intent of the tests and will likely reduce the variability between replicate specimens during testing.

2.10 Recommendations

Initial results from Phase 1 and Phase 2 support the continuation of testing to assess the appropriateness of using the concentric cylinder geometry to measure the performance properties of asphalt rubber binders that are produced according to Caltrans specifications using a wet process with crumb rubber particles larger than 0.25 mm (#60 mesh). This testing should

be in line with the original workplan and objectives prepared for this project, and work should continue to refine the testing procedures on additional plant-produced binders, assess the repeatability and reproducibility of measurements from any proposed test methods, and evaluate the applicability of the results to the actual performance properties of mixes produced with asphalt rubber binders. The potential influence of incompletely digested rubber particles dominating the results will need to be carefully considered in any testing and analysis procedures.

3. TESTING PLANS

3.1 Introduction

The testing plan included testing of an additional 19 plant-produced asphalt rubber binders and five plant-produced RHMA-G mixes listed in Table 3.1. The testing plan included four binders produced for chip seal projects. The reference number in the table depicts the order of sampling. This number is also used in the result tables and plots in Chapter 5 through Chapter 9.

Table 3.1: List of Projects for Binder and Mix Samples

Ref. #	District	Project	Binder	Mix	Ref. #	District	Project	Binder	Mix
4	3	BUT-162	xx	xx	14	6	TUL-99	xx	—
5	10	MER-33	xx	xx	15	3	YOL-84	xx	—
6	1	LAK-20	xx	xx	16	5	SBT-156	xx	—
7	9	INY-395	xx	xx	17	6	KIN-41	xx	—
8	11	IMP-111	xx	xx	18	11	IMP-86	xx	—
9	1	HUM-96[a]	xx	—	19	5	SCR-9	xx	—
10	11	IMP-111[a]	xx	—	20	11	IMP-86[a]	xx	—
11	1	HUM-101	xx	—	21	11	IMP-86[a]	xx	—
12	8	RIV-86	xx	—	22	3	YUB-20	xx	—
13	3	UCPRC-TT[b]	xx	xx					

[a] Chip seal project

[b] Mix testing results for test track materials are documented in separate reports

Samples of crumb rubber, base binder and asphalt rubber binder were collected from the plants on all projects, and loose mix was collected from the plants on five projects. Projects were selected from those available to ensure as much statewide representation of climate, binders, aggregates, and asphalt plants as possible.

Note that the three binders tested in Phase 2f (Reference #1, #2, and #3) *(3)* are not covered in this report.

3.2 Sampling

On each project, excluding the UCPRC test track project, binders were sampled on three different days over the duration of the project to allow testing for variation if required. This provided three lots of binder per project. The lot used for testing was randomly selected. Seven projects were then randomly selected for testing of a second lot to check consistency between lots. Samples were collected in either 3.5-gallon o5 5-gallon metal buckets, which were stored in a temperature-controlled room until tested.

3.3 Base Binder Testing

The base binder performance grade (PG) was verified following standard AASHTO procedures.

3.4 Asphalt Rubber Binder Testing

3.4.1 Crumb Rubber Particle Size Distribution

Samples of waste tire rubber and high natural rubber were collected from all projects. Scrap tire and high natural rubber gradations were both checked to confirm that they met Caltrans specifications. Samples were mixed in a ratio of 75% waste tire rubber to 25% high natural rubber, in line with Caltrans specifications. The gradation of the combined 200 g sample was then checked for reasonableness (Caltrans specifications do not require the reporting of a gradation of the combined rubber).

3.4.2 Rheology Testing

Binder testing followed the procedures developed in Phase 1 and Phase 2 of the study *(3)*, summarized in Chapter 2. High-temperature tests (Phase 1 and Phase 2a), intermediate-temperature tests (Phase 2c), and multiple stress creep recovery (MSCR) tests (Phase 2d) included both concentric cylinder and parallel plate geometries. Difficulties with testing at intermediate temperatures with the concentric cylinder geometry were anticipated due to torque limitations of the equipment. Specimens for the low-temperature tests were fabricated using the modified mold configuration (Phase 2b).

Dynamic shear rheometer (DSR) geometries used for the different tests included the following:

- Concentric cylinder
  - High-temperature tests: 29 mm diameter cup with 17 mm spindle and 6 mm gap between the spindle and cup edges
  - Intermediate-temperature tests: 29 mm diameter cup with 10 mm spindle and 9.5 mm gap between the spindle and cup edges
  - MSCR tests: 29 mm diameter cup with 17 mm spindle and 6 mm gap between the spindle and cup edges
- Parallel plate
  - High-temperature tests: 25 mm diameter plate with 3 mm gap
  - Intermediate-temperature tests: 8 mm diameter plate with 3 mm gap
  - MSCR tests: 25 mm diameter plate with 3 mm gap

3.4.3 Binder Preparation

Asphalt rubber binders were heated at 190°C in 1-gallon cans and then split into 16 ounce cans. These smaller cans were then used one by one to conduct RTFO and PAV aging, and DSR and BBR testing. No can was heated more than twice to avoid unnecessary binder aging. Observations during binder preparation indicated that the 1-gallon container always had some phase separation between the binder and the incompletely digested rubber particles, which resulted in the first two smaller cans having either more phase-separated binder or more free binder. Consequently, the first two small cans of each pour were discarded to ensure that only homogenous binders were tested. Samples for concentric cylinder and parallel plate tests were poured alternately from single cans, RTFO bottles, and PAV pans to further randomize the samples.

Three replicates, sampled from multiple cans, were tested in each test to ensure that variability between samples was considered.

3.4.4 Precision Analysis

The precision and bias statements provided in AASHTO T 315 (summarized in Table 3.2) were developed primarily for unmodified binders tested using parallel plate geometry. Separate statements for polymer-modified binders based on MSCR testing and provided in ASTM D7405 (summarized in Table 3.3) were developed with the same geometry. To date, statements have not been developed for testing asphalt rubber binders with concentric cylinder or parallel plate (with 3 mm plate gap) geometries. These can only be developed through multi-laboratory round robin testing once the procedures have been finalized.

Preliminary single-operator precision analyses were attempted in this phase of the study to obtain a better understanding of the results. The difference between two replicates for each geometry, expressed as a percent of their respective means, was calculated for all unaged, RTFO-aged, and PAV-aged asphalt rubber binders tested in this phase of the study. The current AASHTO and ASTM statements were used as a benchmark to compare against. It should be noted that higher variability in test results is generally expected for modified binders given that the MSCR test, which was specifically developed for polymer-modified binders, allows for up to a 26%

difference in the non-recoverable creep compliance (J_{nr} at 3.2 kPa) results between two tests of the same sample for a single operator and up to 42.6% for multi-laboratory tests.

Table 3.2: AASHTO T 315 Precision Estimates for Unmodified Binders

Precision Level	Condition	Coefficient of Variation	Acceptable Range of Two Test Results
Single Operator	Unaged binder: G*/sin(δ)	2.3	6.4
	RTFO-aged binder: G*/sin(δ)	3.2	9.0
	PAV-aged binder: G*×sin(δ)	4.9	13.8
Multi-Laboratory	Unaged binder: G*/sin(δ)	6.0	17.0
	RTFO-aged binder: G*/sin(δ)	7.8	22.2
	PAV-aged binder: G*×sin(δ)	14.2	40.2

Table 3.3: ASTM D7405 Precision Estimates for Unmodified Binders

Precision Level	Condition	Coefficient of Variation	Acceptable Range of Two Test Results
Single Operator	Average percent recovery at 0.1 kPa	2.4	6.7
	Average percent recovery at 3.2 kPa	3.0	8.5
	Jnr at 0.1 kPa if result is >1.00	4.6	12.8
	Jnr at 0.1 kPa if result is 0.26 – 1.00	5.4	15.2
	Jnr at 0.1 kPa if result is 0.10 – 0.25[a]	13.7	38.3
	Jnr at 3.2 kPa if result is >1.00	5.7	16.0
	Jnr at 3.2 kPa if result is 0.26 – 1.00	5.5	15.3
	Jnr at 3.2 kPa if result is 0.10 – 0.25[a]	9.5	26.6
Multi-laboratory	Average percent recovery at 0.1 kPa	5.4	15.0
	Average percent recovery at 3.2 kPa	6.5	18.1
	Jnr at 0.1 kPa if result is >1.00	9.1	25.6
	Jnr at 0.1 kPa if result is 0.26 – 1.00	12.7	35.6
	Jnr at 0.1 kPa if result is 0.10 – 0.25[a]	16.7	46.8
	Jnr at 3.2 kPa if result is >1.00	7.9	22.0
	Jnr at 3.2 kPa if result is 0.26 – 1.00	13.9	39.0
	Jnr at 3.2 kPa if result is 0.10 – 0.25[a]	15.2	42.6

[a] If J_{nr} values are <0.10, binders should be tested at a temperature that is 6°C higher.

The process used to determine single-operator precision was as follows:

- Test three replicates of each binder sample
- Assemble three possible pairs of the three replicates (i.e., Rep1 and Rep2, Rep2 and Rep3, and Rep1 and Rep3). Determine the percentage difference of the pairs as follows:
  + Calculate the average of two rutting parameters (G*/sin(δ), G*×sin(δ), or J_{nr} at 3.2%) for each temperature using Equation 3.1.

$$A = \frac{Rut.Parameter\ Rep1 + Rut.Paremeter\ Rep2}{2} \quad \textbf{(3.1)}$$

  + Calculate the difference between two rutting parameters for each temperature using Equation 3.2.

$$D = Rut.Parameter\ Rep1 - Rut.Parameter\ Rep2 \quad \textbf{(3.2)}$$

+ Calculate the difference between two rutting parameters as a percentage of their respective average using Equation 3.3.

$$Percentage\ Difference\ = \left(\frac{D}{A}\right) \times 100 \quad \textbf{(3.3)}$$

3.5 RHMA-G Mix Testing

Mix testing followed the same procedures used in the Phase 2f testing *(3)*. The testing factorial is summarized in Table 3.4.

Table 3.4: Tests Performed on Plant-Produced Mixes

Test	Replicates	Air Voids (%)[a]	Test Variables
Stiffness • Dynamic modulus - AASHTO T 378	3	7.0±1.0	• 1 temperature sequence (4, 20, 45°C) • 1 stress level[a] • No confining pressure
Stiffness • Beam flexural frequency sweep - AASHTO T 321	2	7.0±1.0	• 3 temperatures (10, 20, 30°C) • 2 strain levels (100 µstrain at 10 and 20°C; 200 µstrain at 30°C)
Rutting Performance • Flow number from repeated load triaxial results - AASHTO T 378	3	7.0±1.0	• 1 temperature (52°C) • 1 deviator stress (600 kPa [87 psi])[b] • 1 contact stress (30 kPa [4 psi]) • No confining pressure
Cracking Performance • Beam fatigue - AASHTO T 321	3	7.0±1.0	• 1 temperature (20°C) • 3 strain ranges (high, medium, low) based on the mix stiffness • 1 frequency (10 Hz)
Cracking Performance • Semicircular Beam (SCB) test - AASHTO T 393	3	7.0±1.0	• 1 temperature (25°C)

[a] Based on saturated surface-dry bulk specific gravity.
[b] Deviator stress controlled by AMPT software to get 75 to 125 µstrain peak-to-peak axial strain.

3.5.1 Performance Testing Specimen Preparation

Specimen preparation details for the different tests were as follows:

- Asphalt mix performance tester (AMPT) tests were conducted on specimens with 100 mm (≈4 in.) diameter and 150 mm (≈6 in.) height, cored from 150 mm and 175 mm (≈7 in.) gyratory-compacted specimens.
- Beam fatigue specimens were cut from ingots compacted with a steel-wheel roller to target air void contents of 7.0±1.0%. The beams were 380 mm (≈15 in.) in length, 50 mm (≈2 in.) in height, and 63 mm (≈2.5 in.) in width.
- Semicircular bend (SCB) specimens were cut from gyratory-compacted specimens with 150 mm diameter and 175 mm height. Two 50 mm (≈2 in.) thick discs were cut from the compacted specimen, from which four SCB specimens were cut. A 15 mm × 1.5 mm notch was cut into each SCB specimen.

3.5.2 Mix Testing Details

Specimen Air Void Contents

Air void contents were determined according to AASHTO T 269. Bulk specific gravity was determined using both saturated surface-dry (AASHTO T 166) and automatic vacuum sealing methods (AASHTO T 331).

Mix Stiffness: Dynamic Modulus

Tests to determine dynamic modulus (*E**) and phase angle of the RHMA-G mixes were performed using an AMPT at 10, 1, and 0.1 Hz when testing at 4°C and 20°C (39°F and 68°F) and at 10, 1, 0.1, and 0.01 Hz when testing at 45°C (113°F). In this test, the specimen is subjected to a haversine axial-compressive load with fixed amplitude under controlled-strain conditions. The axial deformation of the specimen during cyclic loading is measured using three linear variable displacement transducers (LVDTs) mounted around the specimen 120° apart. The dynamic modulus is calculated by dividing the peak stress (σ_{max}) by the peak strain (ε_{max}) during each loading cycle. Three replicate specimens from each mix were tested.

Dynamic modulus master curves were developed using Equation 3.4 through Equation 3.6. The measured modulus values were used to construct master curves at the reference temperature of 20°C by fitting the data to the sigmoidal function shown in Equation 3.4. The testing frequencies at any testing temperature were converted to the reduced frequency at the reference temperature using the time-temperature superposition principle (Equation 3.5) with the aid of the Arrhenius shift factor (Equation 3.6).

$$log(|G^*(f_r)|) = \delta + \frac{\alpha}{1+e^{\beta+\gamma\times log(f_r)}} \quad \textbf{(3.4)}$$

where: δ, α, β, and y are sigmoidal function parameters
f_r is the reduced frequency at reference temperature T_r (°C)

$$log(f_r) = log\big(a_T(T)\big) + log(f) \quad \textbf{(3.5)}$$

where: f is the testing frequency at testing temperature T (°C)

$$log(a_T(T)) = \frac{E_a}{Ln(10)\times R}\left(\frac{1}{T} - \frac{1}{T_r}\right) \quad \textbf{(3.6)}$$

where: $aT(T)$ is the shift factor value for temperature T (°K)
E_a is an activation energy term (Joules [J]/mol)
R is the universal gas constant (J/(mol·K)
T_r is the reference temperature (°K)

The parameters of the sigmoidal function as well as the activation energy term in the Arrhenius shift factor equation were estimated using the *Solver* feature in *Microsoft Excel* by minimizing the sum of square error between predicted and measured values.

Mix Stiffness: Flexural Modulus

Four-point-bending beam frequency sweep tests were conducted to measure the stiffness (flexural dynamic modulus) of the RHMA-G beams under different frequencies and various temperatures. Two replicates were tested at temperatures of 10°C, 20°C, and 30°C and over frequencies of 15, 10, 5, 2, 1, 0.5, 0.2, 0.1, 0.05, 0.02 and 0.01 Hz. Tests were performed in strain control mode (100 µstrain at 10°C and 20°C, and 200 µstrain at 30°C).

A sigmoidal function similar to that used to determine the dynamic modulus was used to construct the flexural dynamic modulus master curve at a reference temperature of 20°C. The shift factor equation used for generating the master curves is shown in Equation 3.7.

$$log(a_T(T)) = C \times (T - T_r) \quad \textbf{(3.7)}$$

where: C is a shift factor constant
T_r is the reference temperature (°C)
T is the testing temperature (°C)

Rutting Performance: Repeated Load Triaxial

The flow number test (AASHTO T 378) provides an indication of the resistance of an asphalt mix to permanent deformation (rutting). The accumulation of permanent deformation is assumed to occur in primary, secondary, and tertiary phases. Permanent strain typically accumulates rapidly in the primary phase, followed by a lower constant rate through the secondary phase, and then accumulates rapidly again in the tertiary phase. The flow number is defined as the number of cycles at which the tertiary phase starts. Higher flow number values imply that a mix has better rutting (permanent deformation) resistance. In this study, unconfined specimens were subjected to a repeated compressive deviator stress of 600 kPa (87 psi) and a 30 kPa (4.4 psi) contact stress. The resulting cumulative permanent deformation versus the number of loading cycles was recorded with flow number calculations performed automatically by the AMPT software. The numbers of cycles to 1%, 3%, and 5% permanent axial strain were also analyzed to obtain a better understanding of the likely rutting behavior of each of the mixes. According to the test method,

the selected testing temperature should be based on the adjusted high PG temperature of the binder identified for the pavement location. Since testing for specific project locations was not included as part of the workplan, all tests were performed at 52°C to obtain a good understanding of how damage accumulated during the test. Running the test at higher temperatures (e.g., 64°C or the high PG temperatures determined in Chapter 5) could have resulted in accelerated evolution of permanent deformation, which would not provide a comprehensive indication of how damage accumulated with load repetition. Running the test at lower temperatures would extend the testing time but would probably not provide any additional useful information.

Cracking Performance: Four-Point Beam

The beam fatigue test (AASHTO T 321) provides an indication of the resistance of an asphalt mix to fatigue cracking at a constant deformation (strain). Beam specimens are subjected to four-point bending by applying sinusoidal loading at three different strain levels (high, intermediate, and low) at a frequency of 10 Hz and temperature of 20°C (68°F). The fatigue life for each strain level was selected by multiplying the maximum stiffness value for that strain level by the number of cycles at which that stiffness value occurred. Laboratory test results will generally correspond with field fatigue or reflection cracking performance for overlays thinner than about 75 mm (0.25 ft.) but may not correspond with expected field performance for thicker layers of asphalt. For thicker layers, the interaction of the pavement structure, traffic loading, temperature, and mix stiffness with the controlled-strain beam fatigue results needs to be simulated using mechanistic analysis in order to rank mixes for expected field performance.

In this UCPRC study, the testing approach currently specified in AASHTO T 321 was modified to optimize the quantity and quality of the data collected. Replicate specimens were first tested at high- and medium-strain levels to develop an initial regression relationship between fatigue life and strain (Equation 3.8). Strain levels were selected, based on experience, to achieve fatigue lives between 10,000 and 100,000 load cycles and between 300,000 and 500,000 load cycles for high and medium strains, respectively. Additional specimens were then tested at lower strain levels selected based on the results of the initial linear regression relationship to achieve a fatigue life of about 1 million load repetitions. The final regression relationship was then refined to accommodate the measured stiffness at the lower strain level.

$$LnN = A + B \times \varepsilon \quad \textbf{(3.8)}$$

where: N is fatigue life (number of cycles)
ε is the strain level (microstrain [μstrain])
A and B are model parameters

Cracking Performance: Semicircular Bend

The semicircular bend (SCB, AASHTO T 393) test can be used to determine the fracture resistance parameters of asphalt mixtures at intermediate temperature and to rank the cracking resistance of asphalt mixtures containing different binders, modifiers, aggregate gradations, and recycled asphalt pavement. The UCPRC is currently investigating the SCB, IDEAL-CT (ASTM D8225) and other simple cracking tests that relate to beam fatigue test results and can be used for mix design, quality control, and quality assurance purposes *(7)*. The SCB fracture energy (G_f) and flexibility index (FI) test parameters were selected to compare the performance of mixes. Fracture energy is the area under the load-displacement curve and shows the overall resistance of the mix to crack-related damage. The flexibility index is calculated from the fracture energy and post-peak slope of the load-displacement curve that represents the average crack growth rate. Increasing fracture energy and flexibility index implies increasing cracking resistance that can be used to identify brittle mixes.

4. RUBBER GRADATIONS

Rubber gradation results are summarized in Table 4.1. The project number in the table refers to the project that the binder/mix was produced for, as listed in Table 3.1.

Table 4.1: Rubber Gradations Used in Plant-Produced Binders

Sieve Size (mm)	Sieve Size (US)	Project						
		R4	R5	R6	R7	R8	R9	R10
		Percent Passing						
2.36	#8	100.0	100.0	100.0	100.0	100.0	100.0	100.0
2.00	#10	100.0	99.9	100.0	99.5	100.0	100.0	100.0
1.18	#16	74.0	66.2	82.2	59.4	76.8	54.2	54.2
0.6	#30	45.8	40.2	40.2	31.7	42.2	31.2	31.2
0.3	#50	13.3	10.5	8.8	11.5	15.1	10.4	10.4
0.15	#100	1.9	1.6	0.9	2.8	4.3	2.0	2.0
0.075	#200	0.6	0.2	0.1	1.4	1.2	0.4	0.4
Max. particle size (mm)		1.6	2.0	1.6	2.0	1.6	1.6	1.6
Sieve Size (mm)	Sieve Size (US)	Project						
		R11	R12	R13	R14	R15	R16	R17
		Percent Passing						
2.36	#8	100.0	100.0	100.0	100.0	100.0	100.0	100.0
2.00	#10	100.0	100.0	100.0	100.0	100.0	100.0	99.9
1.18	#16	71.7	75.2	69.4	59.2	77.7	91.3	65.7
0.6	#30	40.5	48.7	35.5	26.5	19.5	22.9	29.8
0.3	#50	15.9	20.1	12.3	11.8	3.9	5.1	12.3
0.15	#100	3.6	5.2	2.9	4.8	0.9	0.9	4.0
0.075	#200	0.6	1.0	0.5	1.1	0.2	0.1	0.7
Max. particle size (mm)		1.6	1.6	1.6	1.6	1.6	1.6	2.0
Sieve Size (mm)	Sieve Size (US)	Project						
		R18	R19	R20	R21	R22		
		Percent Passing						
2.36	#8	100.0	100.0	100.0	100.0	100.0		
2.00	#10	100.0	100.0	100.0	100.0	98.6		
1.18	#16	67.8	65.3	66.0	75.6	67.0		
0.6	#30	35.1	32.8	38.1	48.6	34.1		
0.3	#50	13.8	11.7	12.1	17.5	17.8		
0.15	#100	4.0	2.4	2.8	4.2	4.2		
0.075	#200	0.8	0.1	0.5	0.8	0.0		
Max. particle size (mm)		1.6	1.6	1.6	1.6	2.0		

Although the combined rubber formulations differed between asphalt plants across the different sieves, all gradations were considered reasonable. Maximum particle sizes met Caltrans specification requirements.

5. HIGH-TEMPERATURE PERFORMANCE GRADE TESTING

5.1 Introduction

This chapter covers rheology testing to determine the high-temperature performance grades of the 19 plant-produced asphalt rubber binders and the base binders used to produce them. The concentric cylinder and parallel plate geometry results are compared through a simple correlation and single-operator precision analyses of the asphalt rubber binder test results.

5.2 Base Binders

High-temperature performance grade and continuous grade results for the base binders are summarized in Table 5.1 and plotted in Figure 5.1 through Figure 5.3. The base binder from Source 15 could not be sampled.

Table 5.1: Base Binder High-Temperature PG and CG Results

Source	High PG	High CG	G*/sin(δ) Results (kPa) at Different Temperatures					
			Unaged			RTFO-Aged		
			64°C	70°C	76°C	64°C	70°C	76°C
B4	64	66.9	1.4	0.7	—	4	1.5	—
B5	64	65.4	1.5	0.7	—	2.6	1.1	—
B6	64	67.6	1.6	0.7	—	3.8	1.8	—
B7	64	65.5	1.4	0.6	—	2.7	1.2	—
B8	64	68.2	3.1	1.4	0.6	3.9	1.7	—
B9	64	68.0	1.7	0.8	—	4.3	2.0	—
B10	70	71.5	2.7	1.2	0.6	6.3	2.7	1.3
B11	64	69.4	4.3	2.0	1.0	4.3	2.0	—
B12	64	67.2	1.5	0.7	—	3.5	1.6	—
B13	64	66.4	3.1	1.4	0.7	3.0	1.4	—
B14	64	65.5	1.4	0.6	—	2.7	1.2	—
B15[a]	—	—	—	—	—	—	—	—
B16	64	64.8	1.4	0.6	—	2.5	1.1	—
B17	64	65.4	1.2	0.5	—	2.6	1.1	—
B18	70	70.8	2.5	1.1	0.5	6.2	2.7	1.2
B19	64	67.6	1.5	0.7	0-	4.9	2.3	1.1
B20	64	66.0	1.3	0.6	—	3.4	1.5	—
B21	70	72.3	3.0	1.3	0.6	6.9	3.0	1.4
B22	64	67.8	1.6	0.8	—	3.9	1.8	—

[a] The B15 base binder was not sampled by the plant

All but three of the binders had a high-temperature PG of 64°C, with the other binders having a high-temperature PG of 70. Continuous grades varied between 64.8 and 72.3, all higher than the PG.

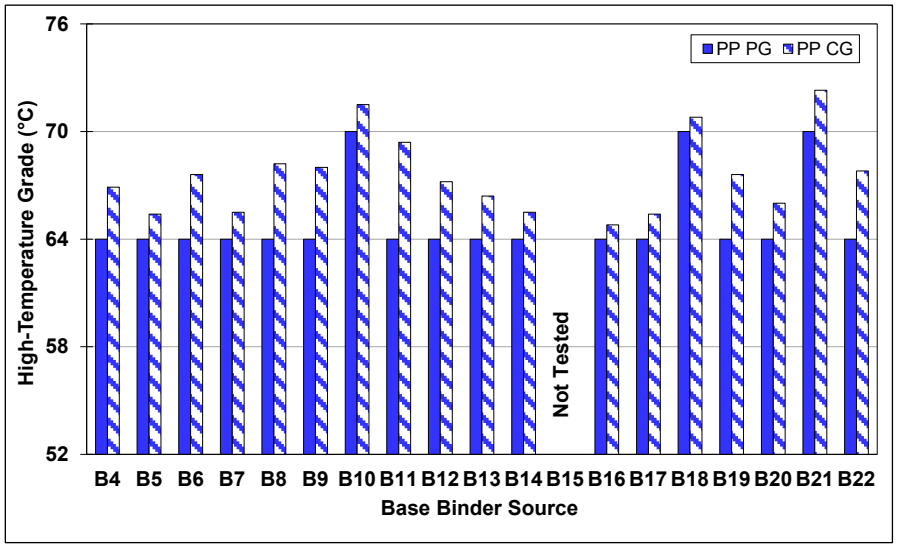

Figure 5.1: Base binder high-temperature PG and CG.

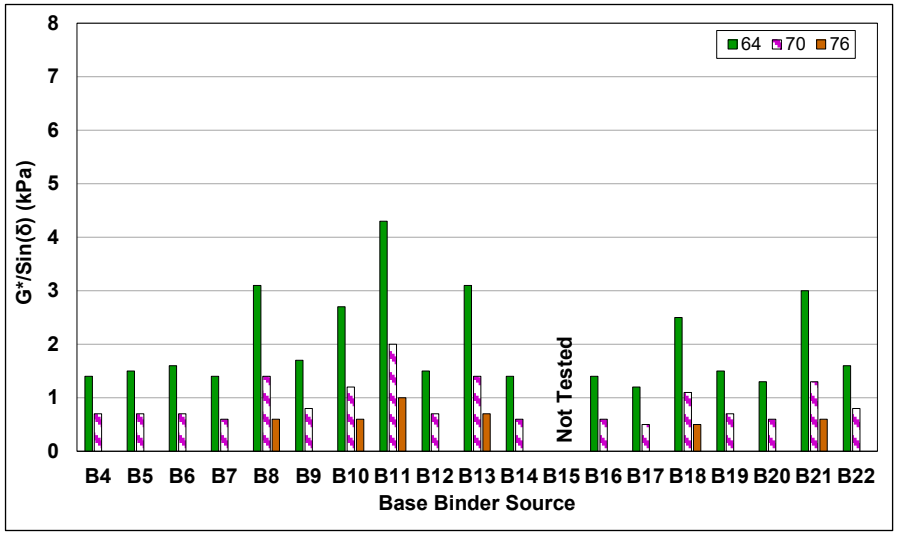

Figure 5.2: Base binder unaged high-temperature.

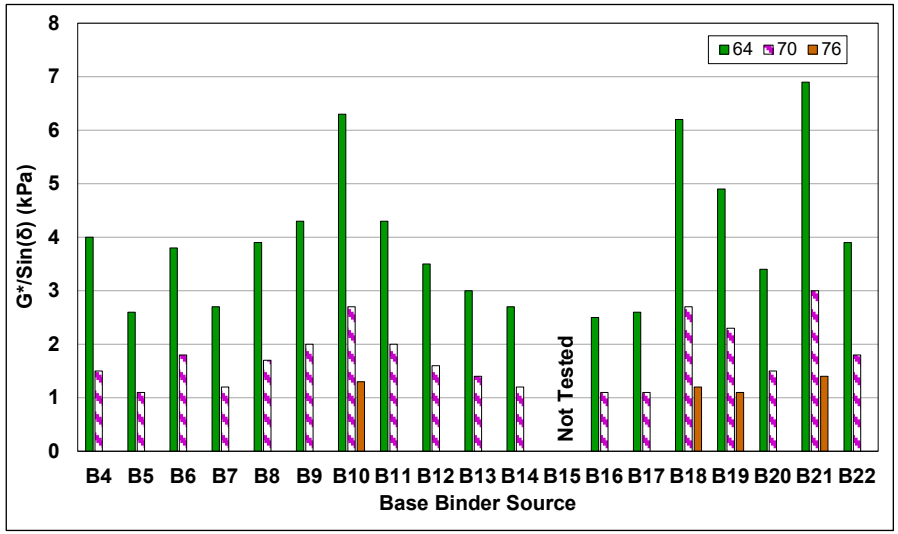

Figure 5.3: Base binder RTFO-aged high-temperature.

5.3 Asphalt Rubber Binders

High-temperature performance and continuous grade results determined with the two geometries are listed in Table 5.2.

Table 5.2: AR Binder High-Temperature PG and CG Results

Concentric Cylinder			Parallel Plate		
Source	**High PG**	**High CG**	**Source**	**High PG**	**High CG**
R4	94	99.8	R4	100	103.1
R5	82	84.8	R5	82	86.0
R6	94	99.8	R6	100	101.9
R7	76	81.9	R7	82	83.4
R8	88	88.1	R8	88	89.9
R9	88	90.4	R9	88	93.3
R10	88	88.3	R10	88	92.0
R11	94	97.8	R11	94	99.0
R12	88	90.2	R12	88	89.7
R13	88	89.9	R13	88	89.5
R14	82	82.3	R14	76	80.8
R15	88	90.0	R15	88	89.0
R16	76	81.6	R16	76	77.5
R17	76	81.5	R17	76	81.5
R18	94	98.6	R18	100	100.5
R19	88	93.6	R19	94	96.8
R20	88	89.9	R20	82	84.8
R21	88	90.2	R21	88	91.3
R22	88	92.3	R22	88	93.4

The results (G*/sin(δ)) for the unaged and RTFO-aged binders tested at different temperatures are summarized in Table 5.3 through Table 5.6. Performance grade and average continuous grade of the asphalt rubber binders are plotted in Figure 5.4 and Figure 5.5. Results for the unaged and RTFO-aged binders tested with both concentric cylinder and parallel plate geometries are plotted in Figure 5.6 through Figure 5.13.

A review of the data led to the following observations:

- All of the asphalt rubber binders had higher high-temperature PGs than their respective base binders, with results differing between the two geometries for seven of the binders. Performance grades measured with the concentric cylinder geometry were higher than those measured with the parallel plate geometry for two of the binders and lower than the parallel plate geometry for five of the binders.
- Fourteen of the binders tested with concentric cylinder geometry and 13 tested with parallel plate geometry had PGs higher than the maximum grade of 82°C listed in the AASHTO M 320 standard. Grades higher than 82 are considered to be unrealistically high

and probably not a true indication of likely high-temperature performance (i.e., rut resistance under heavy loads on hot days).

Table 5.3: AR Binder Unaged High-Temperature Testing Results: Concentric Cylinder

Source	G*/sin(δ) Results (kPa) at Temperatures							
	64°C	70°C	76°C	82°C	88°C	94°C	100°C	106°C
R4	22.9	13.7	8.0	4.7	2.7	1.6	1.0	—
R5	8.7	4.9	2.8	1.6	1.0	—	—	—
R6	19.5	11.8	6.8	4.0	2.3	1.4	0.8	—
R7	6.0	3.2	1.7	1.0	—	—	—	—
R8	9.3	5.2	2.9	1.7	1.0	—	—	—
R9	14.3	7.5	3.9	2.2	1.2	0.7	—	—
R10	9.4	5.4	3.1	1.8	1.0	0.6	—	—
R11	20.2	12.0	6.9	4.0	2.3	1.4	0.8	—
R12	14.8	9.1	5.5	3.3	2.0	1.3	0.8	—
R13	12.6	6.9	3.8	2.1	1.2	0.7	—	—
R14	7.2	4.2	2.5	1.5	1.0	—	—	—
R15	13.1	7.0	3.7	2.1	1.2	0.7	—	—
R16	6.3	3.6	2.1	1.3	0.8	—	—	—
R17	4.9	2.8	1.7	1.0	0.7	—	—	—
R18	25.9	14.4	7.9	4.4	2.5	1.5	0.9	—
R19	17.3	9.5	5.2	2.9	1.6	0.9	—	—
R20	11.7	6.5	3.6	2.0	1.2	0.7	—	—
R21	11.9	6.6	3.7	2.1	1.2	0.8	—	—
R22	14.9	8.2	4.5	2.6	1.5	0.9	—	—

Table 5.4: AR Binder Unaged High-Temperature Testing Results: Parallel Plate

Source	G*/sin(δ) Results (kPa) at Different Temperatures							
	64°C	70°C	76°C	82°C	88°C	94°C	100°C	106°C
R4	25.6	15.3	9.0	5.3	3.2	1.9	1.4	—
R5	9.3	5.3	3.1	1.9	1.2	—	—	—
R6	19.6	12.0	7.4	4.4	2.6	1.5	0.9	—
R7	6.5	3.5	1.9	1.1	0.7	—	—	—
R8	9.2	5.5	3.2	1.9	1.2	0.7	—	—
R9	25.6	15.3	9.0	5.3	3.2	1.9	1.4	—
R10	11.4	6.5	3.8	2.2	1.4	0.9	—	—
R11	22.2	12.8	7.4	4.3	2.5	1.5	0.9	—
R12	14.1	8.3	4.8	2.9	1.7	1.1	0.7	—
R13	11.9	6.4	3.5	2.0	1.2	0.7	—	—
R14	7.2	4.1	2.5	1.5	1.0	—	—	—
R15	11.0	5.8	3.2	1.8	1.1	0.7	—	—
R16	6.3	3.5	2.2	1.3	0.8	—	—	—
R17	—	—	2.2	1.4	0.9	—	—	—
R18	27.9	15.5	8.6	4.9	2.9	1.7	1.1	0.7
R19	—	—	6.4	3.5	2.1	1.2	0.8	—
R20	—	—	2.2	1.3	0.8	—	—	—
R21	—	—	3.9	2.2	1.3	0.8	—	—
R22	15.2	8.4	5.0	2.6	1.7	0.9	—	—

Table 5.5: AR Binder RTFO-Aged High-Temperature Testing Results: Concentric Cylinder

Source	G*/sin(δ) Results (kPa) at Different Temperatures									
	64°C	70°C	76°C	82°C	88°C	94°C	100°C	106°C	112°C	118°C
R4	66.8	45.1	30.2	20.1	13.2	8.6	5.6	3.6	2.3	1.5
R5	14.4	8.7	4.9	2.8	1.7	—	—	—	—	—
R6	61.5	41.5	27.9	18.8	12.6	8.4	5.6	3.7	2.4	1.6
R7	14.4	8.4	4.8	2.8	1.7	—	—	—	—	—
R8	27.6	15.7	8.8	4.9	2.8	1.6	—	—	—	—
R9	49.3	29.8	17.5	10.1	5.8	3.4	2.0	—	—	—
R10	29.4	16.8	10.0	6.6	4.2	2.2	1.9	—	—	—
R11	66.6	43.4	28.7	18.4	11.7	7.3	4.5	2.8	1.7	—
R12	20.0	12.1	7.2	4.3	2.6	1.6	—	—	—	—
R13	30.3	18.4	11.0	6.5	3.9	2.3	1.4	—	—	—
R14	11.3	6.4	3.7	2.2	—	—	—	—	—	—
R15	23.2	14.8	9.5	6.1	3.9	2.5	1.6	—	—	—
R16	11.7	6.5	3.6	2.1	—	—	—	—	—	—
R17	12.6	7.3	4.2	2.5	1.5	—	—	—	—	—
R18	77.5	47.3	28.3	16.7	9.9	5.8	3.4	2.1	—	—
R19	—	—	25.5	16.2	10.2	6.3	3.9	2.4	1.5	—
R20	—	—	9.8	6.0	3.6	2.2	—	—	—	—
R21	—	—	12.6	7.4	4.4	2.6	1.6	—	—	—
R22	32.3	19.8	11.9	7.1	4.2	2.5	1.5	—	—	—

Table 5.6: AR Binder RTFO-Aged High-Temperature Testing Results: Parallel Plate

Source	G*/sin(δ) Results (kPa) at Different Temperatures (°C)									
	64°C	70°C	76°C	82°C	88°C	94°C	100°C	106°C	112°C	118°C
R4	71.6	50.0	34.4	23.3	15.5	10.0	6.5	4.1	2.6	1.9
R5	16.2	9.2	5.3	3.1	1.8	—	—	—	—	—
R6	54.4	38.1	27.2	19.2	13.3	9.1	6.1	4.0	2.6	1.9
R7	15.4	8.6	4.9	2.8	1.6	—	—	—	—	—
R8	25.1	14.2	8.0	4.5	2.6	1.5	—	—	—	—
R9	46.8	28.2	16.6	9.7	5.6	3.3	—	—	—	—
R10	30.1	17.9	10.6	6.3	3.8	2.3	—	—	—	—
R11	63.2	41.7	27.1	17.3	10.8	6.7	4.1	2.6	1.6	—
R12	21.0	12.7	7.4	4.4	2.6	1.6	—	—	—	—
R13	33.2	20.5	12.3	7.4	4.4	2.7	1.6	—	—	—
R14	11.5	6.4	3.5	2.0	—	—	—	—	—	—
R15	32.9	19.2	11.0	6.4	3.7	2.2	—	—	—	—
R16	—	—	4.5	2.6	1.6	—	—	—	—	—
R17	—	—	3.6	2.1	—	—	—	—	—	—
R18	—	—	30.3	18.6	12.1	7.2	4.3	2.6	1.7	—
R19	—	—	27.6	17.1	10.6	6.4	4.0	2.5	1.6	—
R20	—	—	10.2	6.2	3.8	2.3	1.5	—	—	—
R21	—	—	11.9	6.9	4.0	2.4	—	—	—	—
R22	34.7	21.2	12.9	7.6	4.5	2.7	1.7	—	—	—

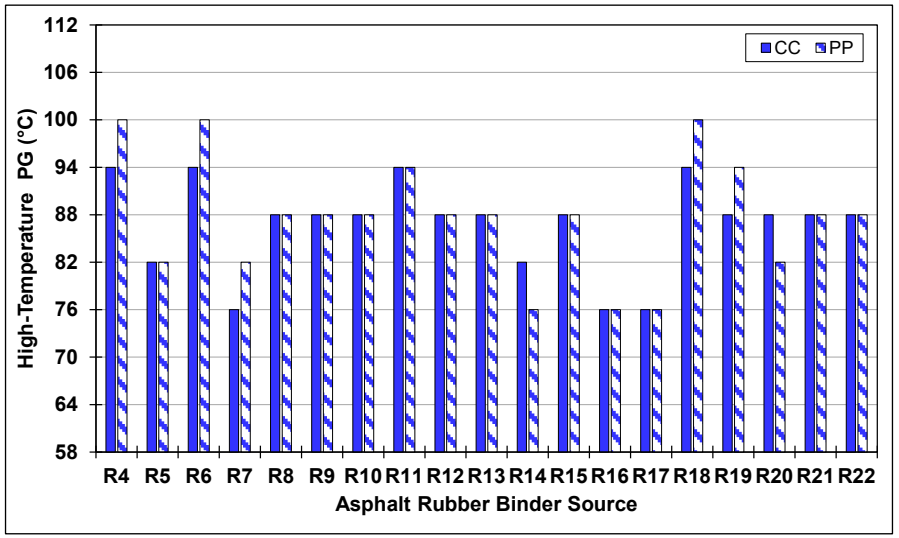

Figure 5.4: AR binder high-temperature PG.

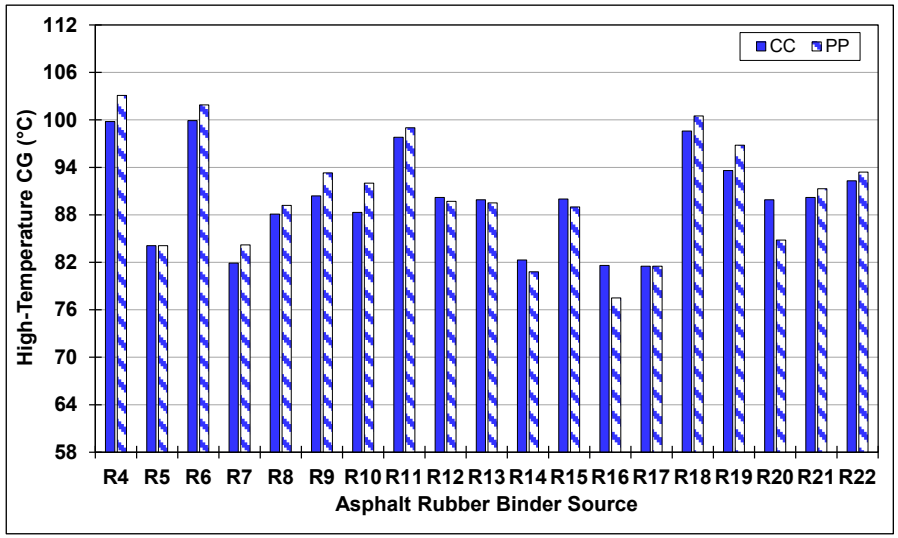

Figure 5.5: AR binder high-temperature CG.

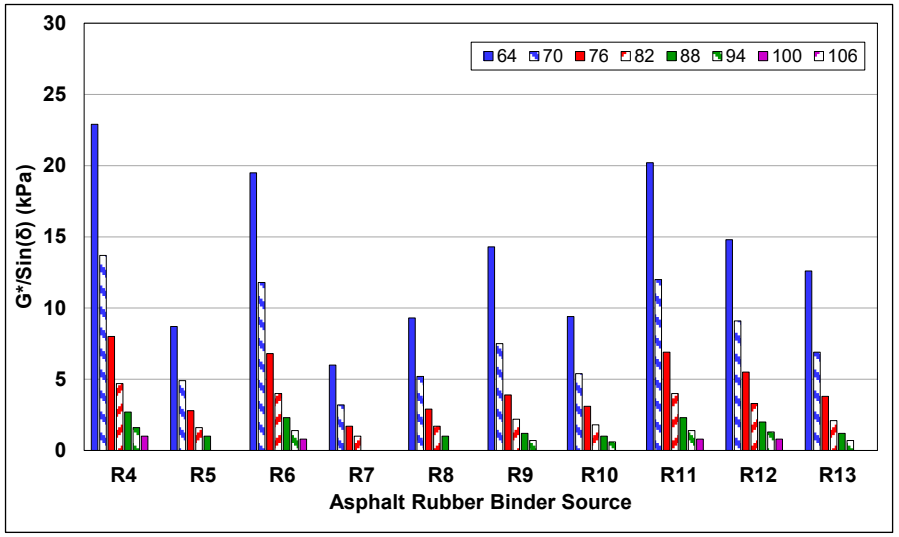

Figure 5.6: AR binder high-temperature (unaged): Concentric cylinder (R4-R13).

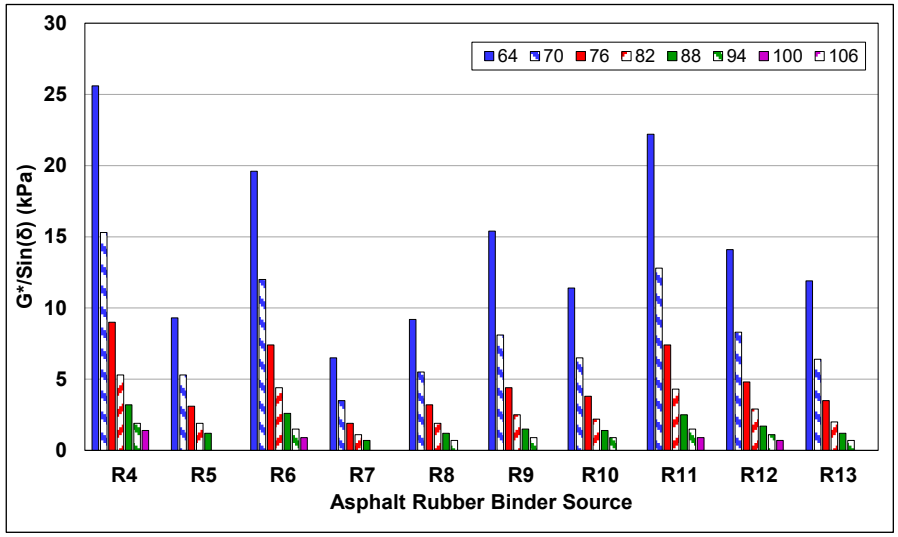

Figure 5.7: AR binder high-temperature (unaged): Parallel plate (R4-R13).

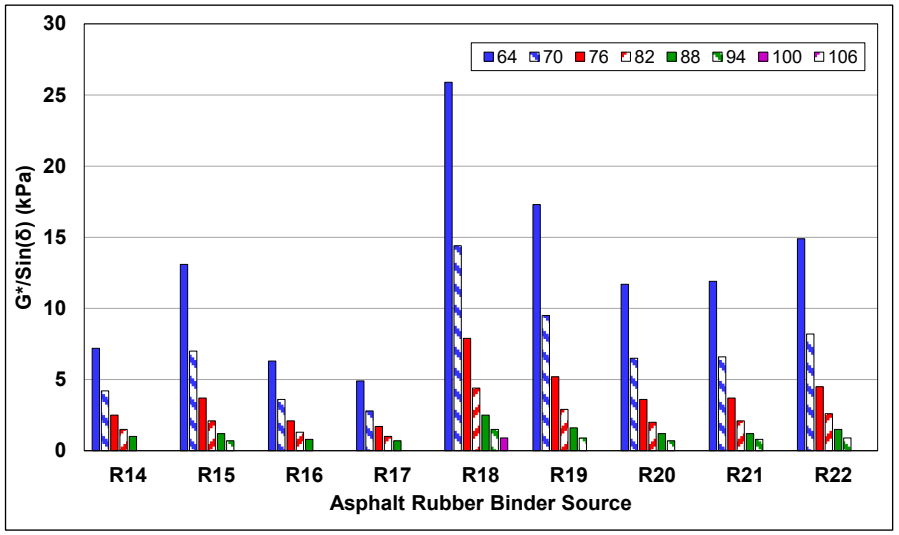

Figure 5.8: AR binder high-temperature (unaged): Concentric cylinder (R14-R22).

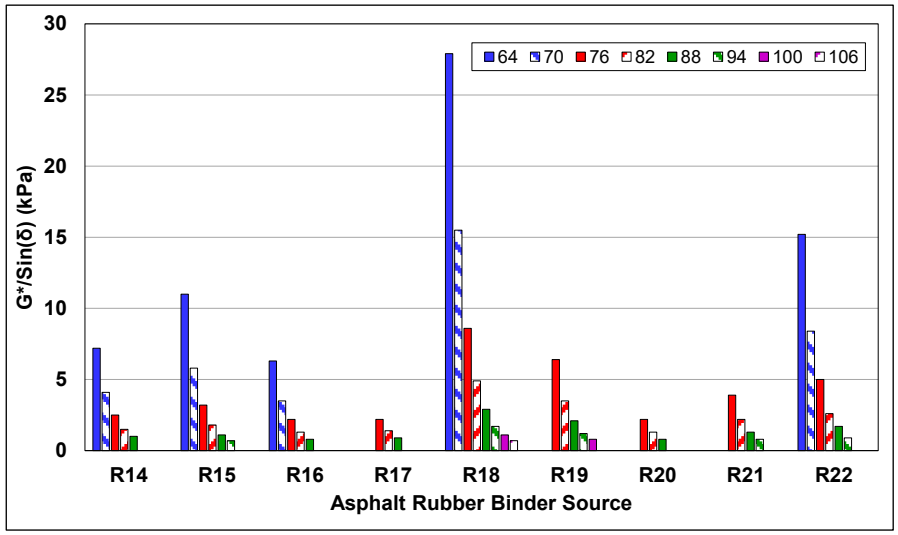

Figure 5.9: AR binder high-temperature (unaged): Parallel plate (R14-R22).

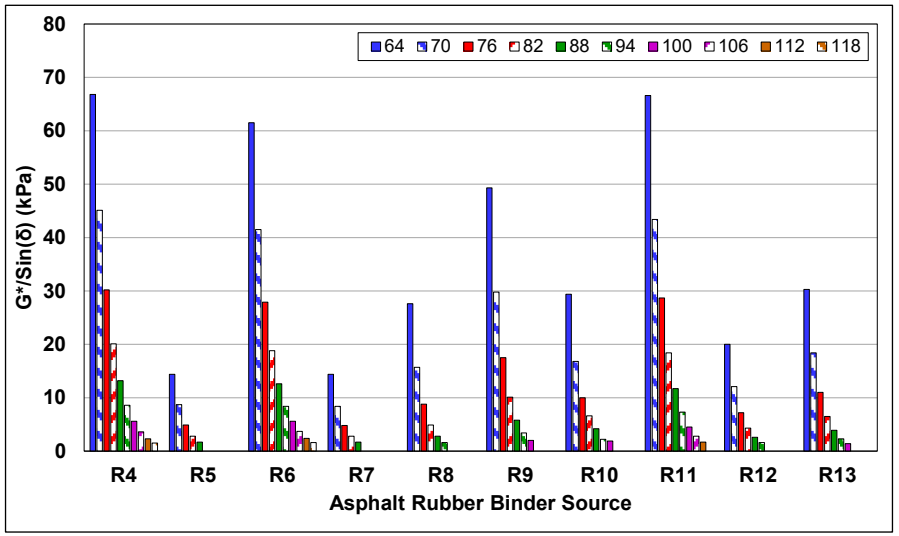

Figure 5.10: AR binder high-temperature (RTFO-aged): Concentric cylinder (R4-R13).

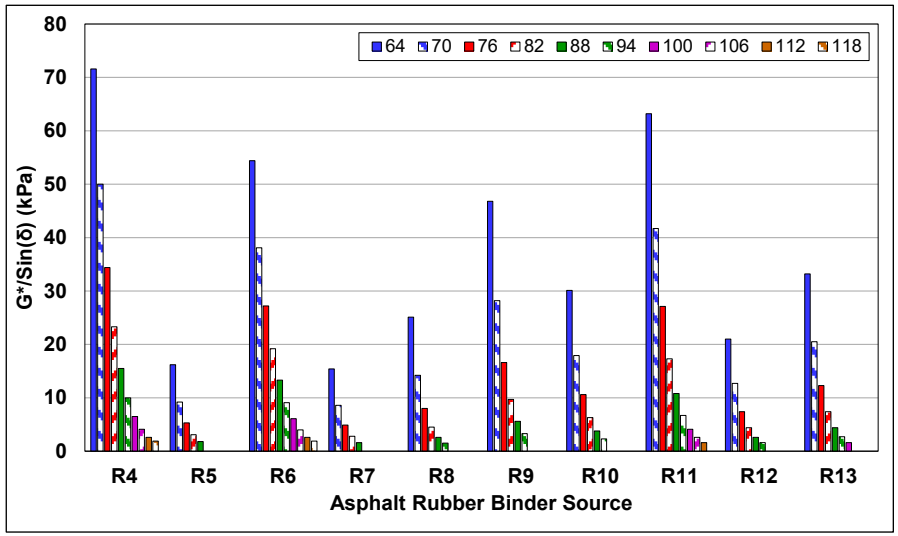

Figure 5.11: AR binder high-temperature (RTFO-aged): Parallel plate (R4-R13).

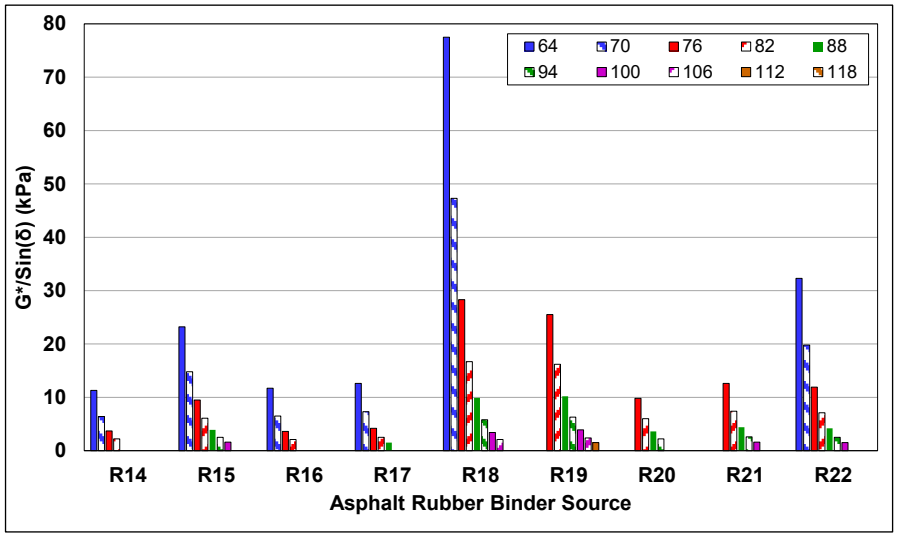

Figure 5.12: AR binder high-temperature (RTFO-aged): Concentric cylinder (R14-R22).

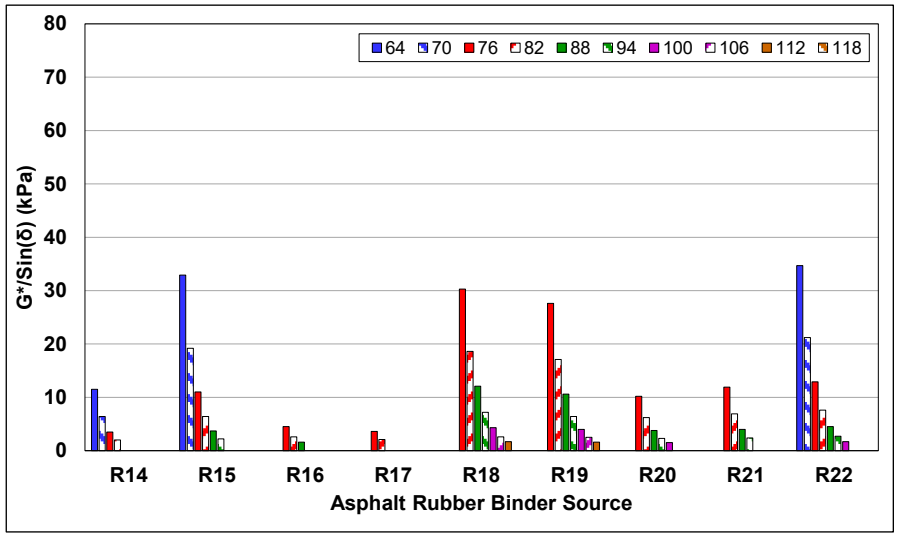

Figure 5.13: AR binder high-temperature (RTFO-aged): Parallel plate (R14-R22).

- Incompletely digested rubber particles and the degree of digestion of the particles in the tested sample appear to have had a considerable influence on the high-temperature testing results for both geometries when compared to the base binders. This would probably have had a bigger impact on the parallel plate geometry results because of the smaller gap (i.e., 3 mm versus 6 mm in the concentric cylinder).
- Three of the binders tested at five grades higher than their respective base binders using concentric cylinder geometry. Two of those binders tested six grades higher when tested with the parallel plate geometry, with three binders testing at five grades higher.
- Eight binders tested four grades higher than the base binder with the concentric cylinder geometry compared to five binders with the parallel plate geometry. Four binders tested three grades higher with the concentric cylinder geometry compared to five binders with the parallel plate geometry. Three binders tested two grades higher with both geometries.
- Continuous grades varied between 81.5 and 99.8 using concentric cylinder geometry and between 77.5 and 103.1 using parallel plate geometry. Continuous grades measured with the concentric cylinder were lower than those measured with the parallel plate for 11 of the binders, equal for four of the binders, and higher for four of the binders. The difference between the results from each geometry did not exceed 6°C for any of the binders. No clear reasons for the differences across the 19 binders were identified. No consistent rankings were identified, including comparisons with rubber gradations.
- Stiffness/rut resistance (G*/sin[δ]) decreased with increasing test temperature in all instances, as expected. Trends at individual temperatures were consistent between the two geometries across the 19 binders, but there were no apparent trends in the differences between the two geometries for individual binders.

5.4 Comparison of Testing Geometries

Scatter plots comparing the performance and continuous grades determined with the two geometries are shown in Figure 5.14 and Figure 5.15. A box-and-whisker plot showing variability between the concentric cylinder and parallel plate results is shown in Figure 5.16. Scatter plots comparing the two geometries when used to test the unaged and RTFO-aged binders are shown in Figure 5.17 and Figure 5.18. The percent differences in G*/sin(δ) between the concentric cylinder and parallel plate geometries, calculated using the formula in Equation 5.1, are shown in Figure 5.19 and Figure 5.20 for the unaged samples and in Figure 5.21 and Figure 5.22 for the RTFO-aged samples. The differences in midpoint G*/sin(δ) for the two geometries are shown in Figure 5.23 and Figure 5.24 for the unaged and RTFO-aged binders, respectively.

$$\frac{CC[G^*/\sin(\delta)] - PP[G^*/\sin(\delta)]}{PP[G^*/\sin(\delta)]} \times 100 \quad \textbf{(5.1)}$$

A review of the data led to the following observations:

- A statistical comparison of the performance grade results from the two geometries indicated a reasonable linear correlation (R^2 of 0.79), but demonstrated that the two geometries will list different grades for the same binder in some instances. The correlation for continuous grade results was stronger (R^2 0.91).
- When performance and continuous grade results are compared with a box-and-whisker plot (Figure 5.16), it is clear that the results from the concentric cylinder geometry were less variable than the parallel plate and had less scatter in the data.
- A statistical comparison of the unaged and RTFO-aged binder results from the two geometries indicated strong linear correlations (R^2 of 0.98 and 0.96, respectively), which implies that the two geometries are testing the same properties.
- When comparing the two geometries at individual testing temperatures on unaged binders, G*/sin(δ) values determined with concentric cylinder were mostly lower than those determined with parallel plate (14 of the 19 binders). The difference between the two geometries generally increased with increasing test temperature. On RTFO-aged binders, the differences between the two geometries were inconsistent and no clear trends were apparent, indicating that the rubber particles age differently to the asphalt and that the degree of digestion of the larger rubber particles probably influenced the results.
- When comparing the two geometries in terms of the midpoint testing temperature, the difference in G*/sin(δ) values determined was small for the unaged binders, with nine of the 19 binders testing slightly higher with the concentric cylinder geometry and nine testing slightly higher with the parallel plate geometry. One sample had the same result for both geometries. The results for RTFO-aged binders show larger differences in stiffness between the two geometries for each binder, with the parallel plate geometry recording higher midpoint stiffnesses than the concentric cylinder geometry for 13 of the 19 binders.

5.5 Single-Operator Precision Results

Single-operator precision results for the two geometries used to test unaged binders are plotted in Figure 5.25 and Figure 5.26 and for both geometries combined in Figure 5.27. Results for RTFO-aged binders are plotted in Figure 5.28 through Figure 5.30.

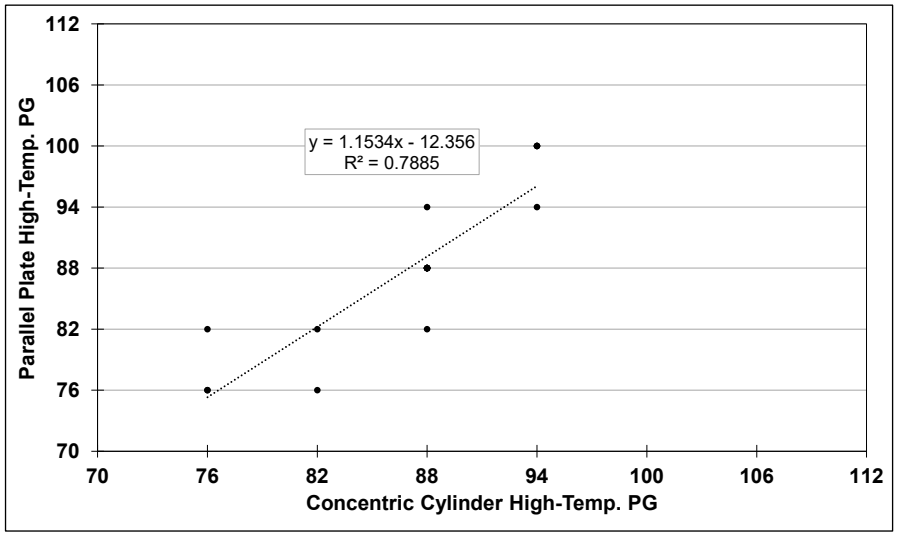

Figure 5.14: AR binder high-temperature PG: Geometry comparison.

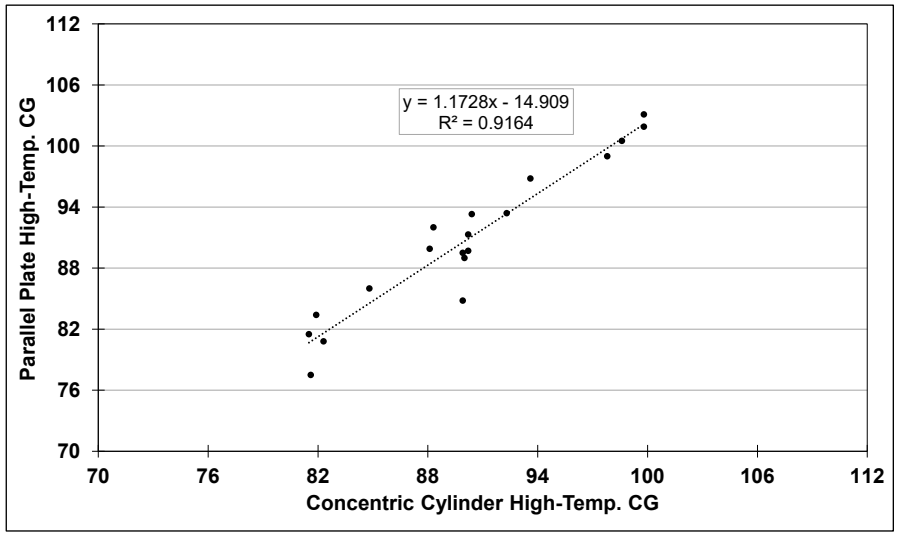

Figure 5.15: AR binder high-temperature CG: Geometry comparison.

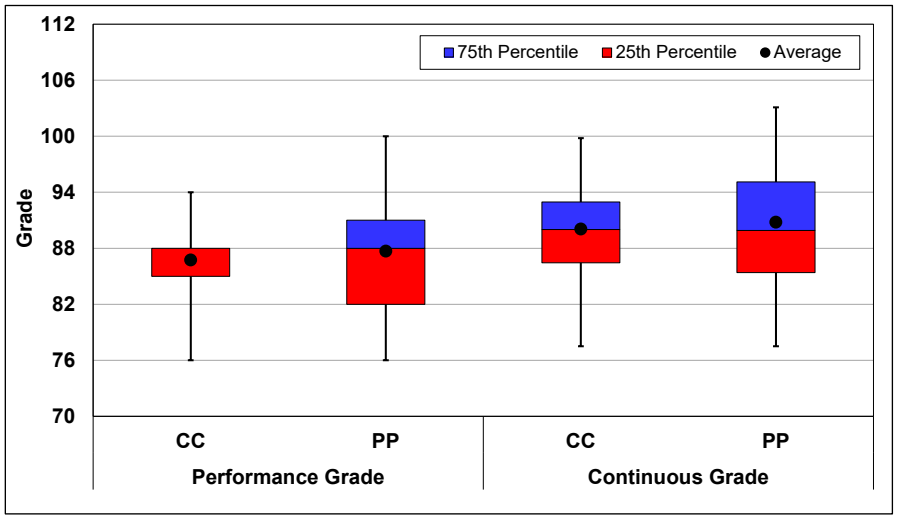

Figure 5.16: AR binder high-temperature PG and CG: Geometry comparison.

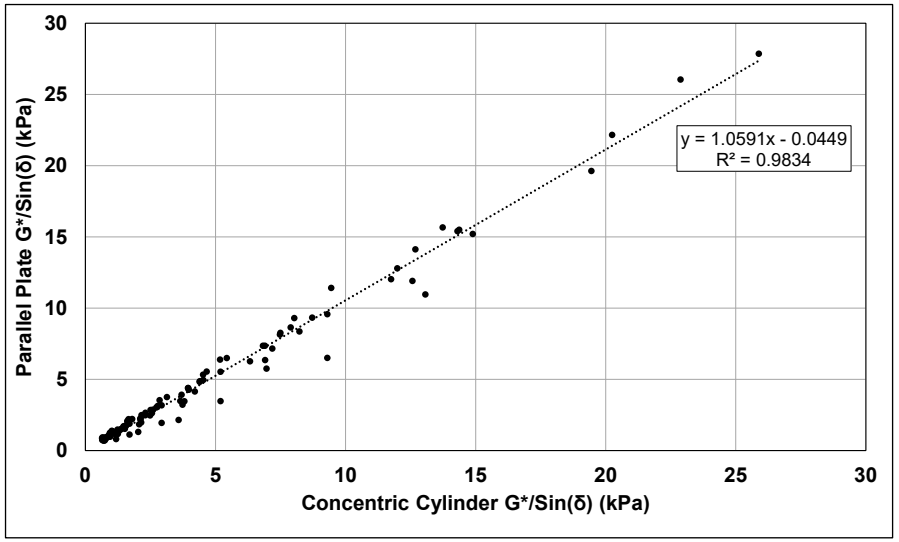

Figure 5.17: AR binder high-temperature (unaged): Geometry comparison.

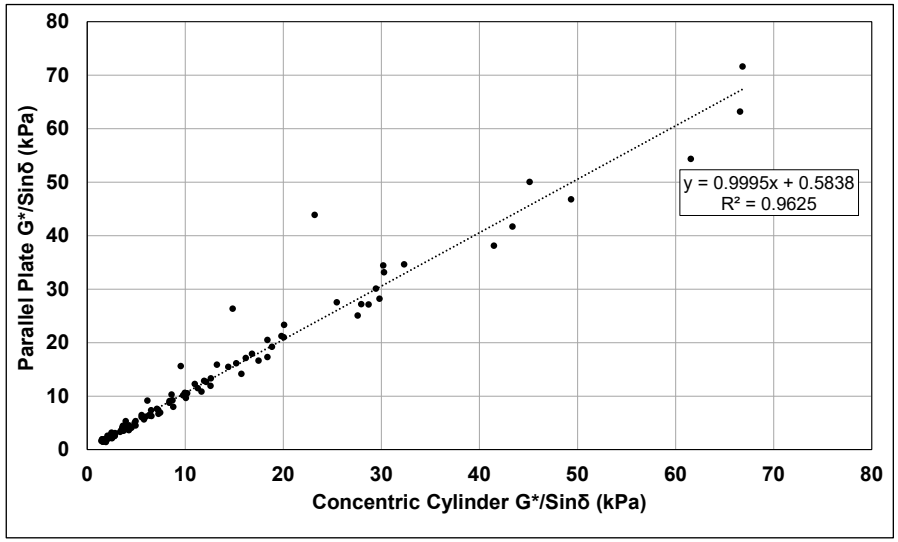

Figure 5.18: AR binder high-temperature (RTFO-aged): Geometry comparison.

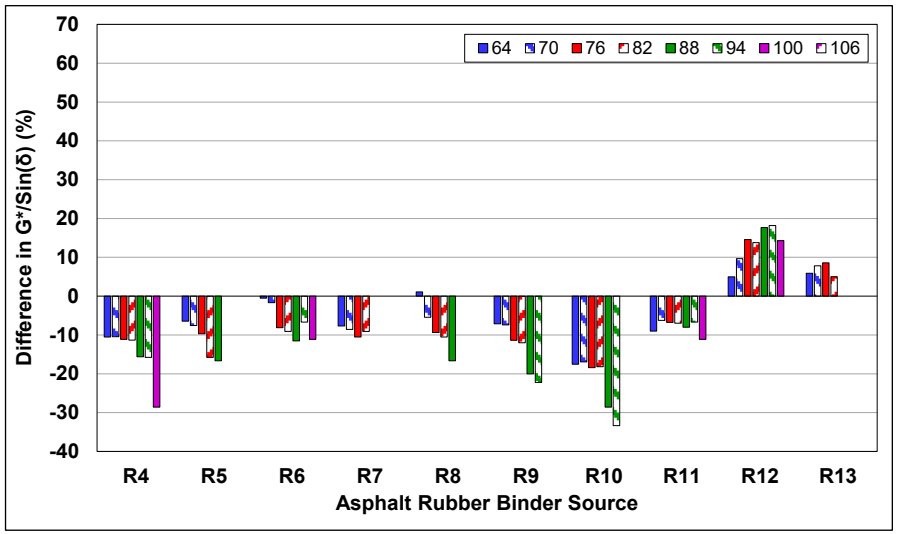

Figure 5.19: AR binder high-temperature (unaged): Geometry difference (R4-R13).

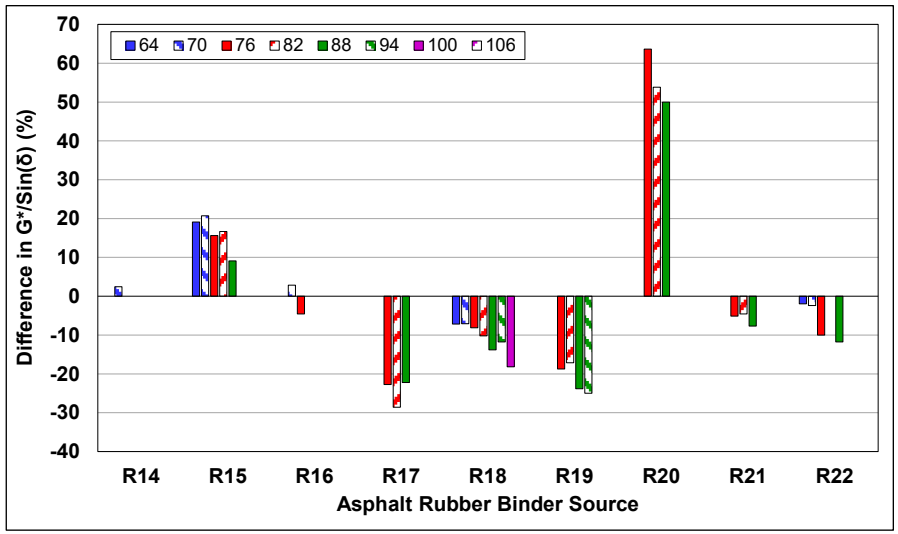

Figure 5.20: AR binder high-temperature (unaged): Geometry difference (R14-R22).

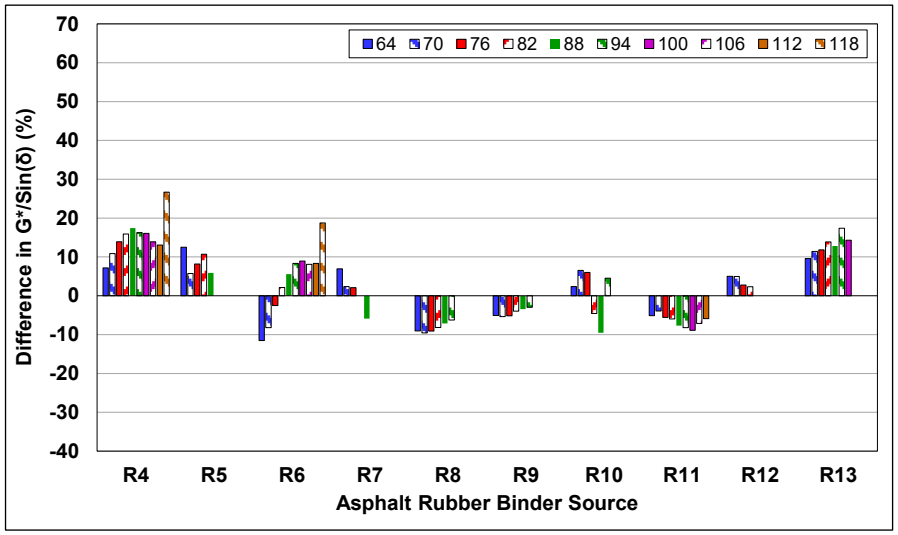

Figure 5.21: AR binder high-temperature (RTFO-aged): Geometry difference (R4-R13).

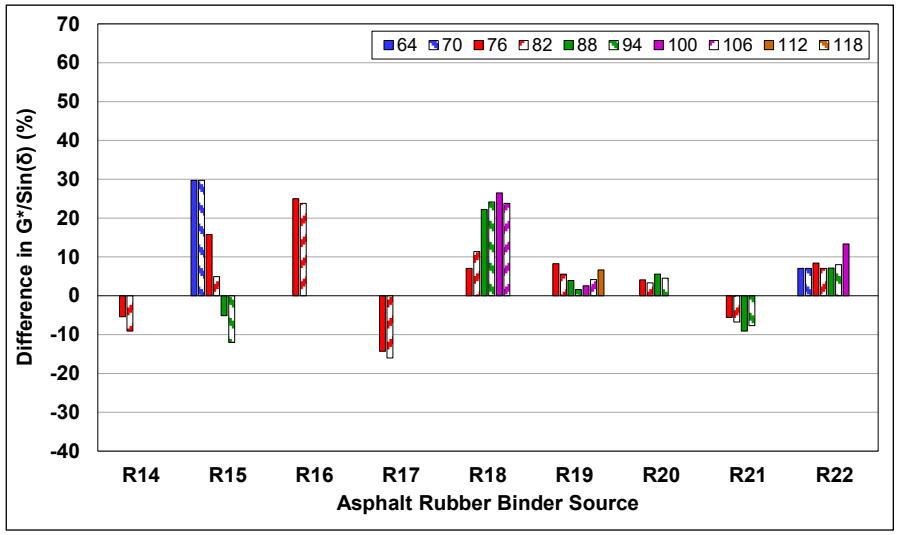

Figure 5.22: AR binder high-temperature (RTFO-aged): Geometry difference (R14-R22).

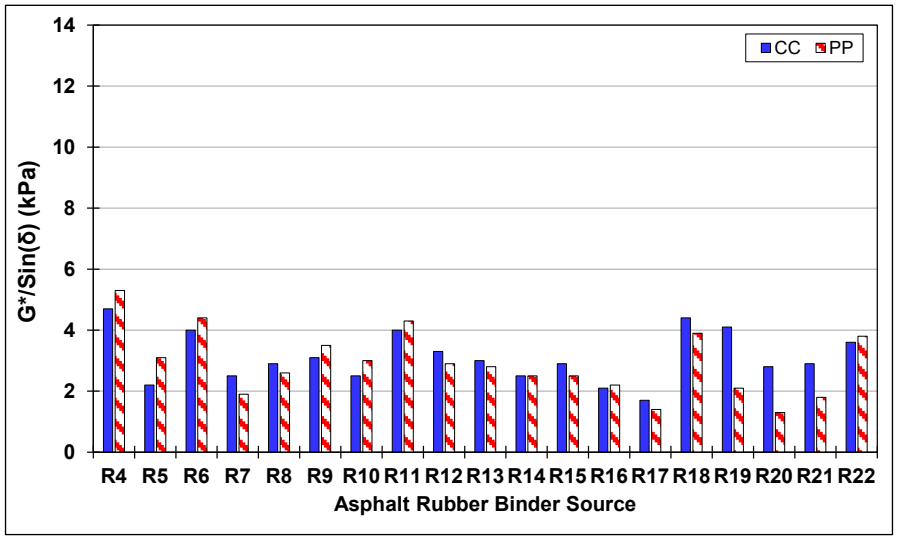

Figure 5.23: AR binder high-temperature (unaged): Difference in midpoint G*/sin(δ).

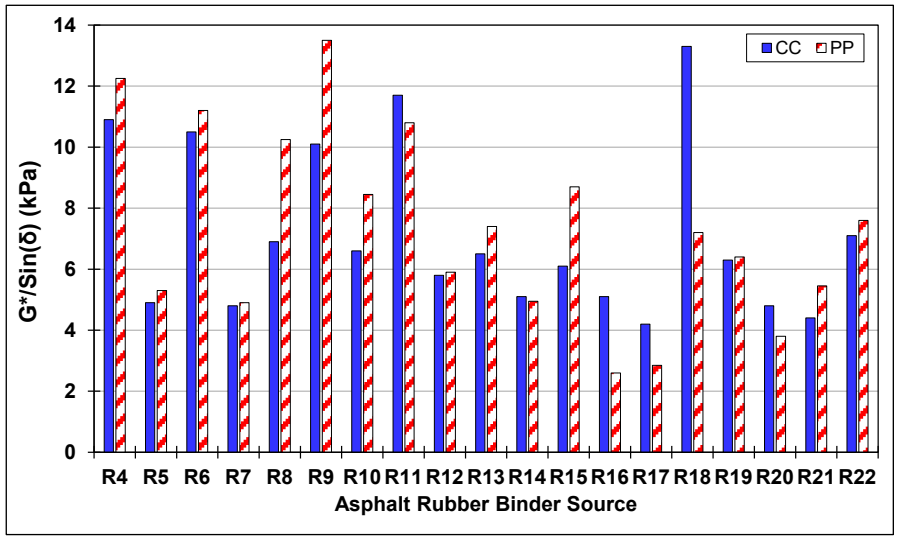

Figure 5.24: AR binder high-temperature (RTFO-aged): Difference in midpoint G*/sin(δ).

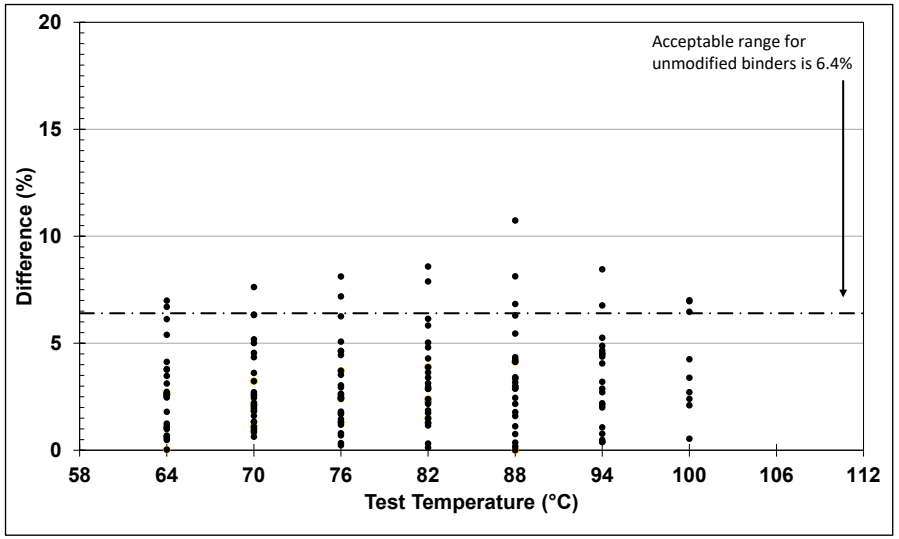

Figure 5.25: Precision results for unaged AR binders: Concentric cylinder.

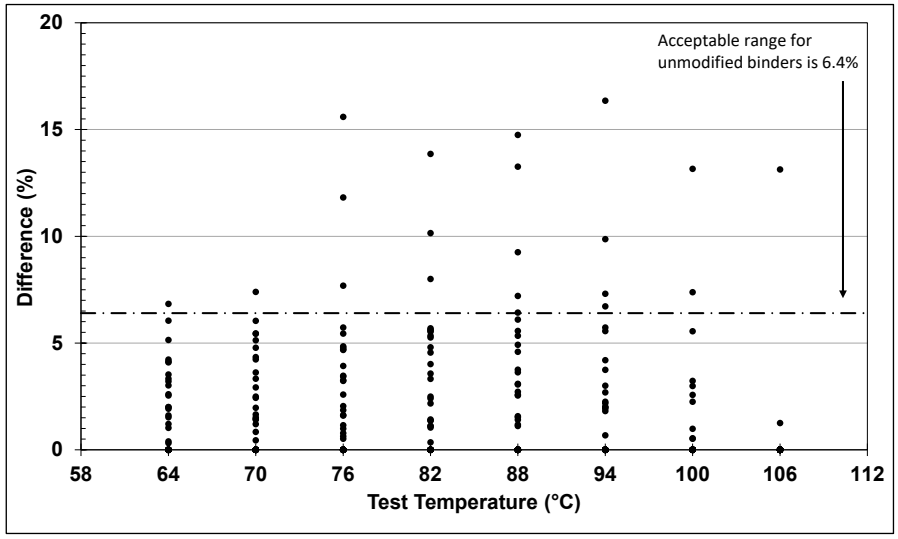

Figure 5.26: Precision results for unaged AR binders: Parallel plate.

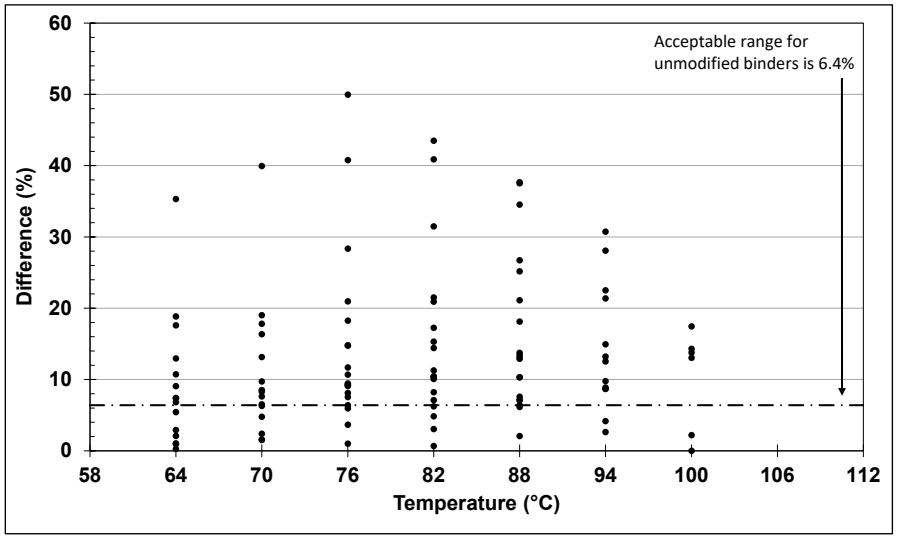

Figure 5.27: Precision results for unaged AR binders: Combined results.

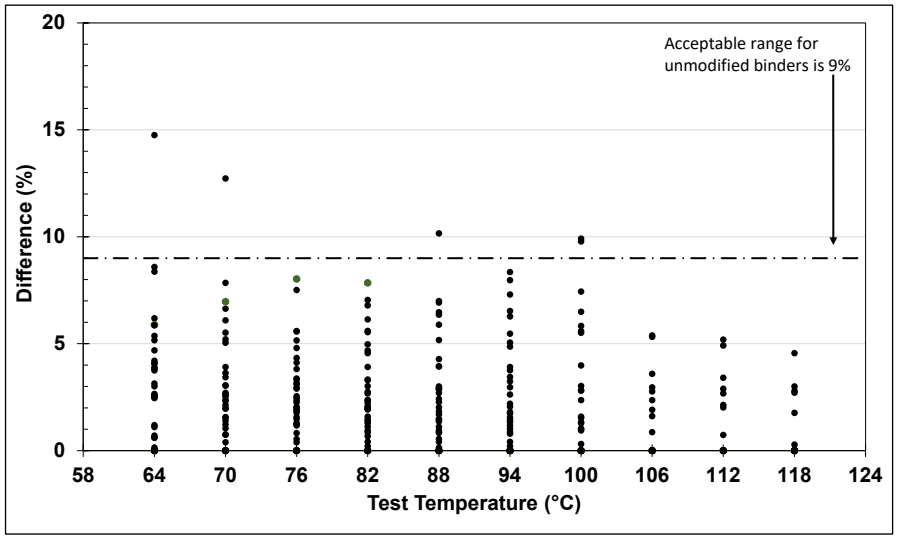

Figure 5.28: Precision results for RTFO-aged AR binders: Concentric cylinder.

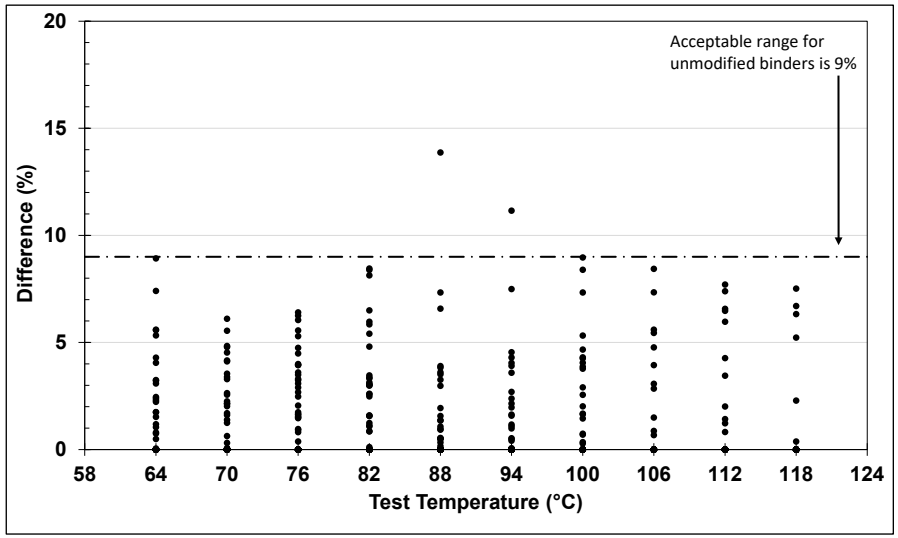

Figure 5.29: Precision results for RTFO-aged AR binders: Parallel plate.

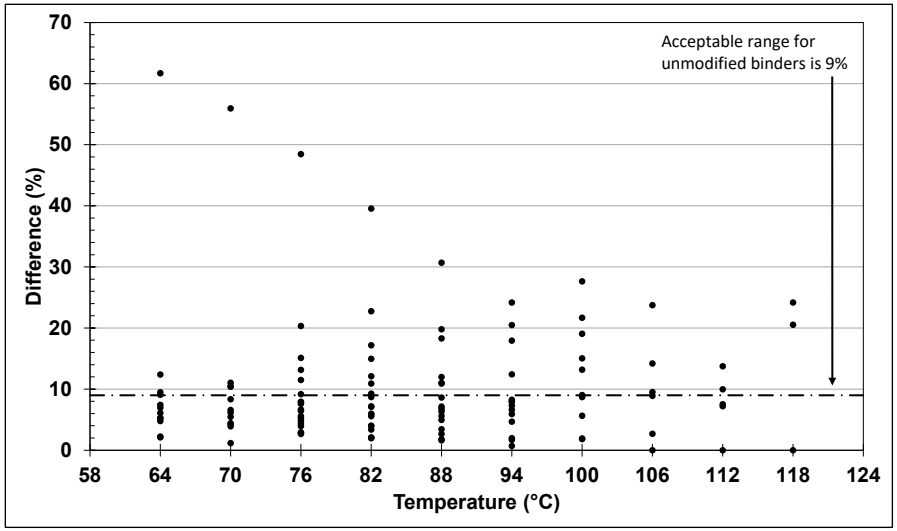

Figure 5.30: Precision results for RTFO-aged AR binders: Combined results.

A review of the data led to the following observations:

- For the unaged binder testing:
  - The percentage difference between two replicates exceeded 6.4% for 21 of the 350 concentric cylinder test results and for 23 of the 147 parallel plate results. This equates to 94% and 84% of the respective results falling within this acceptable range for unmodified binders.
  - Increasing the acceptable range limit to 9% would increase the acceptance rate of the concentric cylinder test results to 98% and the parallel plate results to 92%. The acceptance rate for parallel plate results would need to be increased to 15% to achieve the same 98% acceptance if it as based on this data.
  - When the results are combined (i.e., all the results from both geometries for one binder at one temperature are considered as replicates), the percentage difference between two replicates exceeded 6.4% for 80 of the 105 results, or 24%. The acceptable range would need to be increased to 42% to achieve 98% acceptance if it was based on this data.
  - Although the size of the data sets were different, the results indicate that variation in the parallel plate results were higher than those in the concentric cylinder results and that the two geometries yield significantly different results. This implies that the two geometries should not be used interchangeably for high-temperature testing.
- For the RTFO-aged binder. testing indicated the following:
  - The percentage difference between two replicates exceeded 9% for five of the 234 concentric cylinder test results, and for two of the 195 parallel plate results. This equates to 98% and 99% of the respective results falling within this acceptable range for unmodified binders. Based on this dataset, the variability between results appears to be reasonable and the acceptable range would not need to be changed if it was based on this data.
  - When the results are combined, the percentage difference between two replicates exceeded 9% for 72 of the 116 results, or 6%. The acceptable range would therefore need to be increased significantly to achieve 98% acceptance. This indicates that the two geometries yield significantly different results, which confirms that the two geometries should not be used interchangeably for high-temperature testing.

6. INTERMEDIATE-TEMPERATURE PERFORMANCE GRADE TESTING

6.1 Introduction

This chapter covers rheology testing to determine the intermediate-temperature performance grades of the 19 plant-produced asphalt rubber binders and the base binders used to produce them. The concentric cylinder and parallel plate geometry results are compared through a simple correlation and single-operator precision analyses of the test results.

6.2 Base Binders

Intermediate-temperature performance and continuous grade results for the 19 base binders are summarized in Table 6.1 and plotted in Figure 6.1. Results (G*×sin[δ]) for the PAV-aged binders tested at the different temperatures are plotted in Figure 6.2 and Figure 6.3. Two binders had an intermediate-temperature PG of 22, four graded at 25, three graded at 28, seven graded at 31, and two graded at 34, indicating that the fatigue properties of binders used in California varies considerably. Continuous grades varied between 20.4 and 31.5 and were all lower than the PG.

Table 6.1: Base Binder Intermediate-Temperature PG and CG Results

Source	Int. PG	Int. CG	G*×sin(δ) Results (kPa) at Different Temperatures				
			19°C	22°C	28°C	25°C	34°C
B4	22	20.4	5,952	4,113	2,791	—	—
B5	31	29.1	—	—	—	6,007	3,642
B6	25	22.3	—	5,204	3,629	2,504	1,728
B7	31	29.2	—	—	—	6,120	3,685
B8	31	30.5	—	—	—	7,094	4,666
B9	25	23.6	—	6,089	4,166	2,784	1,840
B10	34	31.5	—	—	—	—	5,279
B11	22	21.4	6,698	4,648	3,137	—	—
B12	28	26.0	—	—	5,709	3,785	2,533
B13	31	28.3	—	—	—	5,228	3,565
B14	31	28.8	—	—	—	5,735	3,467
B15[a]	—	—	—	—	—	—	—
B16	31	28.6	—	—	—	5,570	3,303
B17	28	27.7	—	—	7,739	4,730	2,779
B18	31	30.0	—	—	—	6,542	4,398
B19	25	22.4	—	5,243	3,581	2,394	—
B20	28	25.5	—	—	5,359	3,450	2,165
B21	34	31.0	—	—	—	—	5,019
B22	25	24.3	—	6,807	4,537	—	—

[a] The B15 base binder was not sampled by the plant

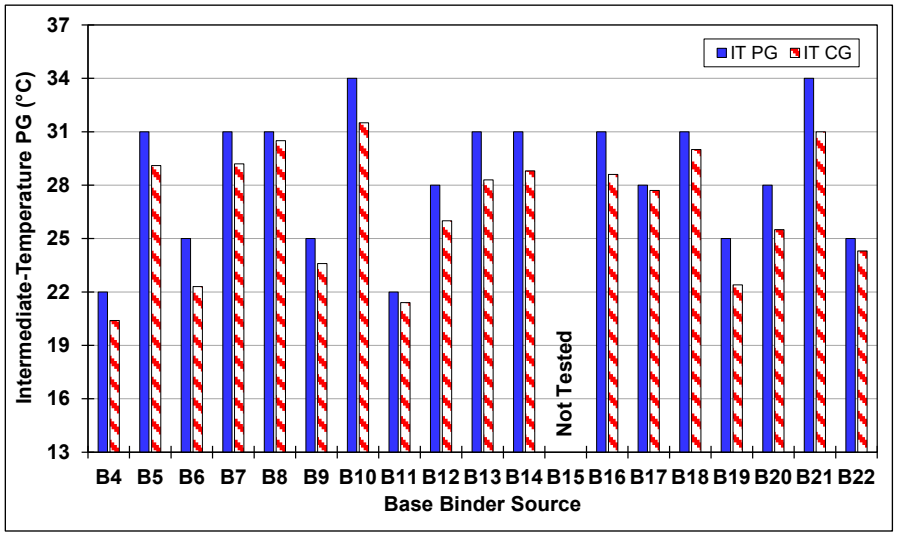

Figure 6.1: Base binder intermediate-temperature PG and CG.

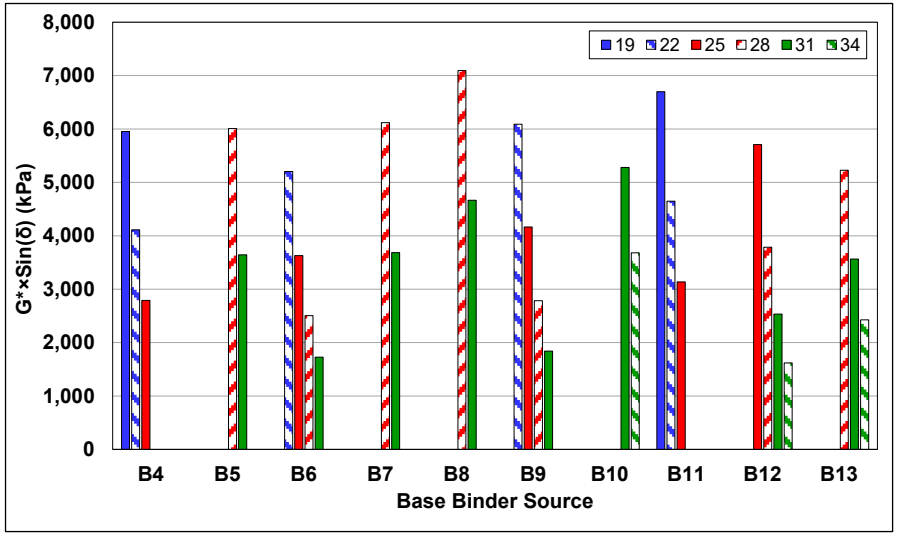

Figure 6.2: Base binder intermediate-temperature testing (B4-B13).

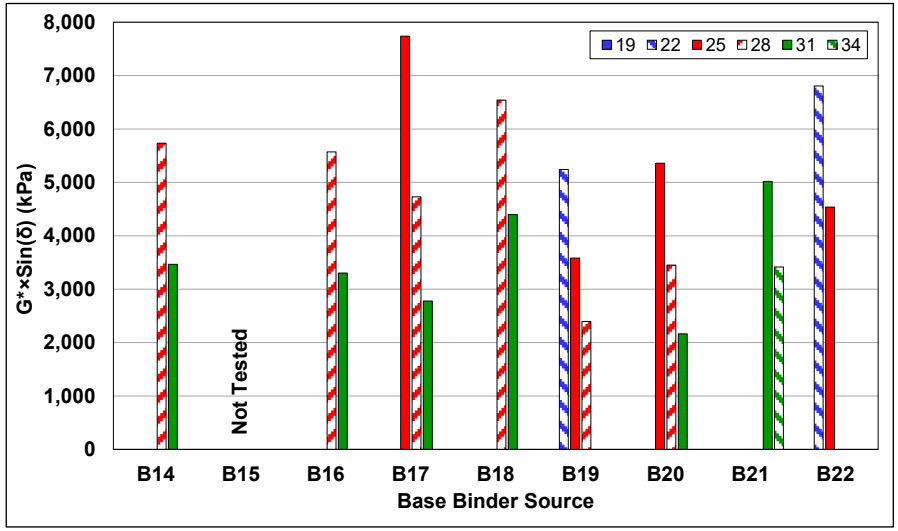

Figure 6.3: Base binder intermediate-temperature testing (B14-B22).

6.3 Asphalt Rubber Binders

Intermediate-temperature performance and continuous grade results for the 19 asphalt rubber binders determined using concentric cylinder and parallel plate geometries are listed in Table 6.2 and plotted in Figure 6.4 and Figure 6.5, respectively.

Table 6.2: AR Binder Intermediate-Temperature PG and CG Results

Concentric Cylinder			Parallel Plate		
Source	**Int. PG**	**Int. CG**	**Source**	**Int. PG**	**Int. CG**
R4	16	13.6	R4	13	11.5
R5	22	21.2	R5	22	19.7
R6	22	19.9	R6	19	17.7
R7	22	20.4	R7	22	19.7
R8	22	20.9	R8	22	20.8
R9	19	16.0	R9	13	11.6
R10	22	21.9	R10	22	19.0
R11	22	19.0	R11	19	17.1
R12	22	19.8	R12	19	17.3
R13	19	17.5	R13	16	15.1
R14	25	22.4	R14	22	19.2
R15	22	19.3	R15	16	15.4
R16	25	22.5	R16	22	19.7
R17	25	22.3	R17	22	20.2
R18	25	23.1	R18	22	20.3
R19	19	16.1	R19	16	14.9
R20	19	18.2	R20	19	16.7
R21	25	22.2	R21	22	20.2
R22	22	20.6	R22	19	17.1

The results (G*×sin(δ)) for the PAV-aged binders tested at different temperatures with the two geometries are summarized in Table 6.3 and Table 6.4, respectively, and plotted in Figure 6.6 through Figure 6.9. Lower intermediate-temperature grades imply improved fatigue and reflective cracking resistance, which is expected when testing asphalt rubber binders.

A review of the data led to the following observations:

- The asphalt rubber binders had intermediate-temperature PGs that were between one and five grades lower than their respective base binders, with the exception of one binder (R11), which had the same intermediate temperature as the base binder when tested with the concentric cylinder geometry. The results were the same for both geometries for five of the binders, with the concentric cylinder geometry reporting consistently higher intermediate temperatures than the parallel plate geometry on the other 13 binders.

Table 6.3: AR Binder Intermediate-Temperature Testing Results: Concentric Cylinder

Source	G*×sin(δ) Results (kPa) at Different Temperatures					
	10°C	13°C	16°C	19°C	22°C	25°C
R4	—	6,110	4,712	3,624	2,775	2,043
R5	—	—	—	6,460	4,527	2,977
R6	—	6,245	4,867	3,707	2,813	2,031
R7	—	—	—	5,940	4,084	2,638
R8	—	—	—	6,066	4,487	—
R9	—	5,022	3,832	2,908	2,121	—
R10	—	—	—	6,596	4,972	3,644
R11	—	—	—	5,014	3,830	2,864
R12	—	—	—	5,399	4,020	2,878
R13	—	—	5,741	4,351	3,295	2,384
R14	—	—	—	—	5,326	3,468
R15	—	—	—	5,118	3,880	2,843
R16	—	—	—	—	5,341	3,471
R17	—	—	—	—	5,222	3,363
R18	—	—	—	—	5,606	4,107
R19	—	—	5,037	3,871	2,968	2,171
R20	—	—	6,299	4,592	3,324	2,235
R21	—	—	—	—	5,101	3,805
R22	—	—	—	5,820	4,393	3,223

Table 6.4: AR Binder Intermediate-Temperature Testing Results: Parallel Plate

Source	G*×sin(δ) Results (kPa) at Different Temperatures					
	10°C	13°C	16°C	19°C	22°C	25°C
R4	—	3,013	4,561	3,435	2,562	1,867
R5	—	—	—	5,444	3,770	2,532
R6	—	5,475	4,135	3,090	2,287	1,639
R7	—	—	—	5,480	3,738	2,478
R8	—	—	—	5,977	4,416	3,173
R9	5,724	4,410	3,371	2,550	—	—
R10	—	—	—	5,020	3,766	2,728
R11	—	—	5,531	4,221	3,184	2,347
R12	—	—	5,674	4,219	3,085	2,181
R13	—	6,086	4,589	3,430	2,528	—
R14	—	—	—	5,154	3,561	2,480
R15	—	6,052	4,753	3,584	2,662	—
R16	—	—	—	5,447	3,730	2,443
R17	—	—	—	5,821	3,970	2,581
R18	—	—	—	5,724	4,217	2,999
R19	—	5,923	4,506	3,404	2,539	—
R20	—	—	5,408	3,900	2,764	1,880
R21	—	—	—	5,571	4,225	3,146
R22	—	—	5,512	4,181	3,118	2,228

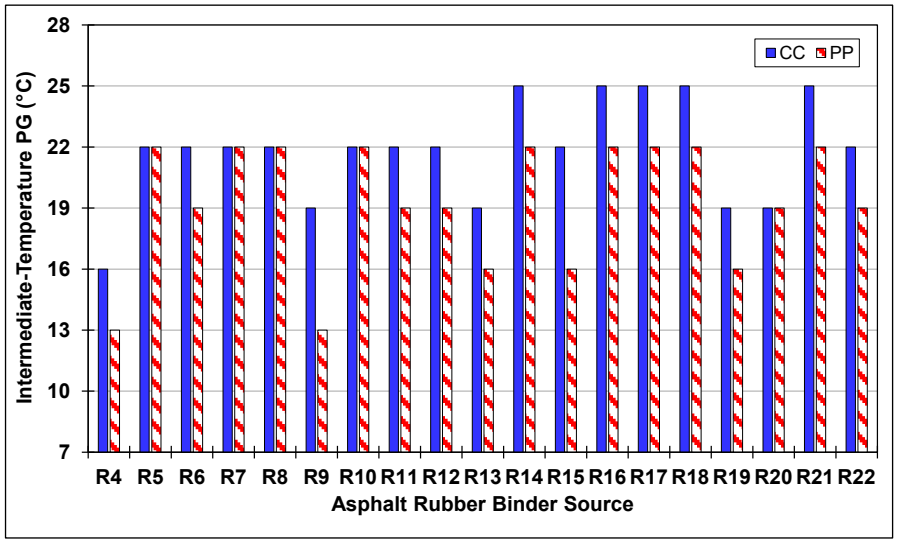

Figure 6.4: AR binder intermediate-temperature PG.

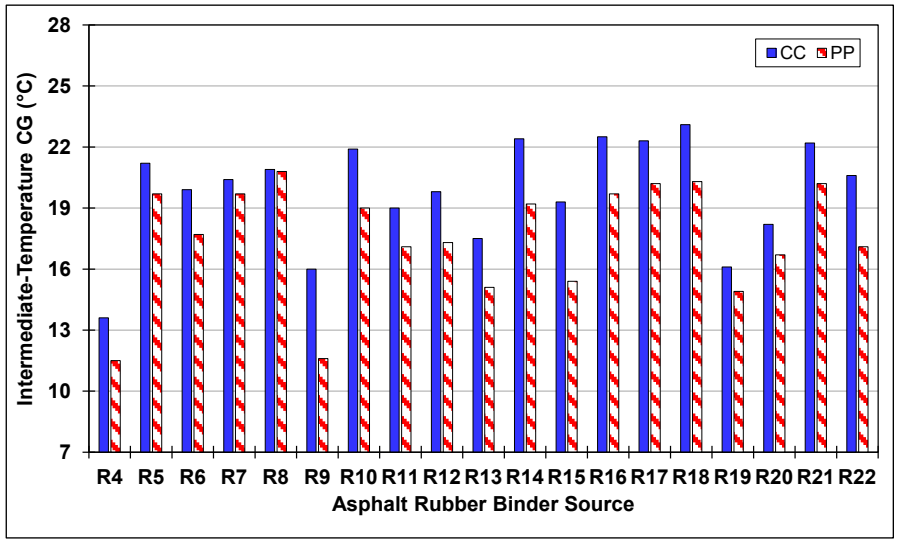

Figure 6.5: AR binder intermediate-temperature CG.

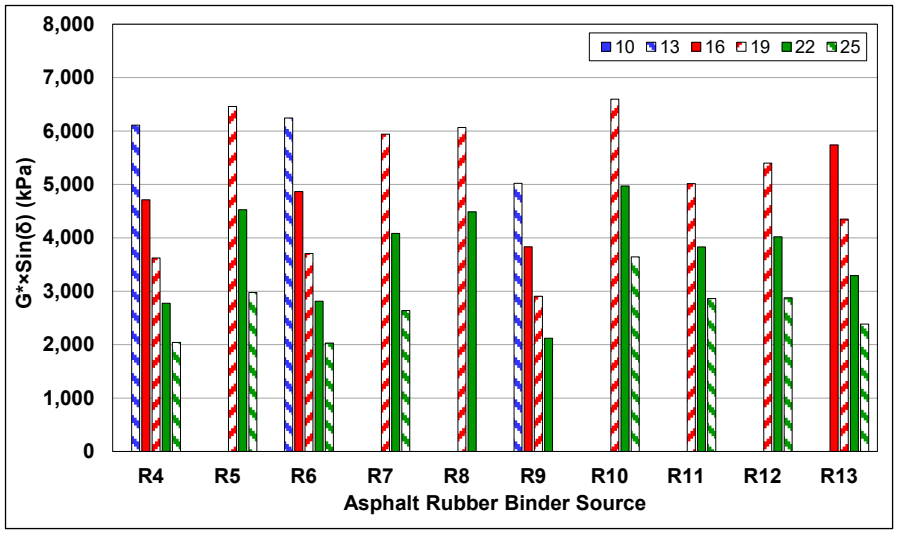

Figure 6.6: AR binder intermediate-temperature: Concentric cylinder (R4-R13).

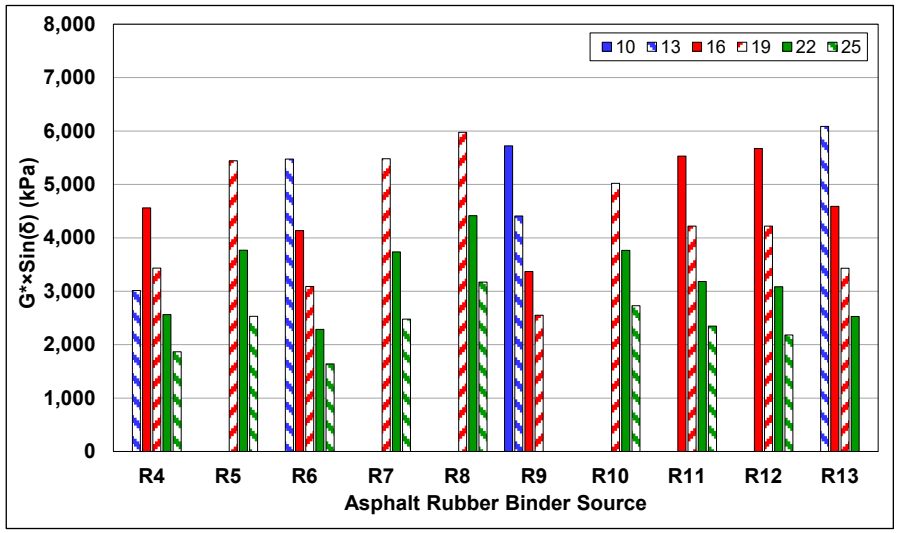

Figure 6.7: AR binder intermediate-temperature: Parallel plate (R4-R13).

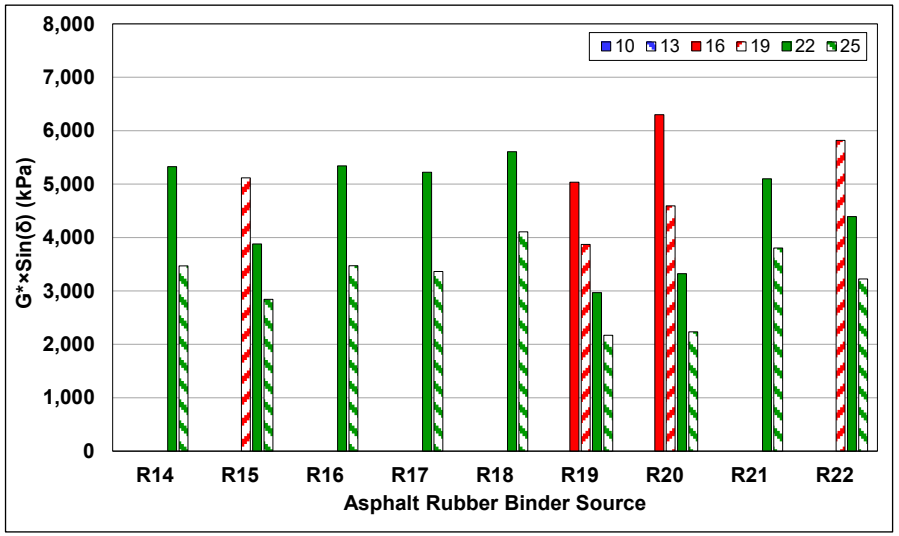

Figure 6.8: AR binder intermediate-temperature: Concentric cylinder (R14-R22).

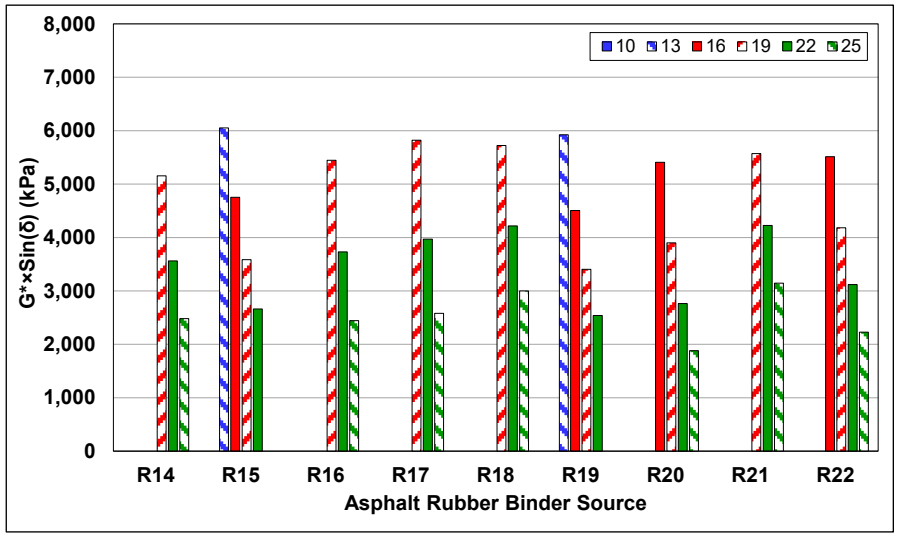

Figure 6.9: AR binder intermediate-temperature: Parallel plate (R14-R22).

- One binder (R13) tested at five grades lower than its base binder using parallel plate geometry. Testing with the concentric cylinder provided a result that was four times lower than the base binder. Another three binders tested at three grades lower than the base binder using the parallel plate geometry, with one of them (R10) giving the same result when tested with the concentric cylinder geometry. Using the concentric cylinder geometry, five binders tested at three grades lower than the base binder, seven tested at two grades lower, and three tested at one grade lower. With the parallel plate geometry, 10 binders tested at three grades lower than the base binder, three tested at two grades lower, and one tested at one grade lower.
- There were no apparent trends between intermediate PG and rubber gradation.
- The continuous grades measured with the concentric cylinder were higher than those measured with the parallel plate for all binders. Continuous grades varied between 13.6 and 23.1 when tested with concentric cylinder geometry and between 11.5 and 20.8 when tested with parallel plate geometry. Parallel plate continuous grade results were all lower than the concentric cylinder results. Continuous grade rankings were not the same for the two geometries, and neither geometry had the same ranking with each other or with the respective base binder.
- No clear trends were observed when comparing high- and intermediate-temperature results.
- Fatigue resistance (G*×sin[δ]) decreased with decreasing test temperature in all instances, as expected.

6.4 Comparison of Testing Geometries

Scatter plots comparing the performance and continuous grades determined with the two geometries are shown in Figure 5.14 and Figure 5.15. A box-and-whisker plot showing variability between the concentric cylinder and parallel plate results is shown in Figure 5.16. A scatter plot comparing the two geometries when used to test the PAV-aged binders at different temperatures is shown in Figure 6.13. The percent differences in G*×sin(δ) between the concentric cylinder and parallel plate geometries, calculated using the formula in Equation 5.1, are shown in Figure 6.14 and Figure 6.15. The differences in midpoint G*×sin(δ) for the two geometries are shown in Figure 6.16.

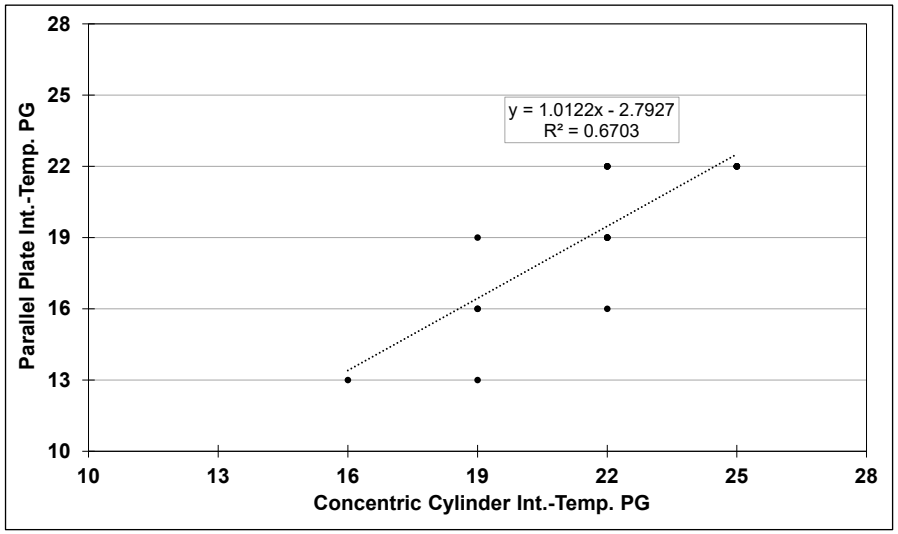

Figure 6.10: AR binder intermediate-temperature PG: Geometry comparison.

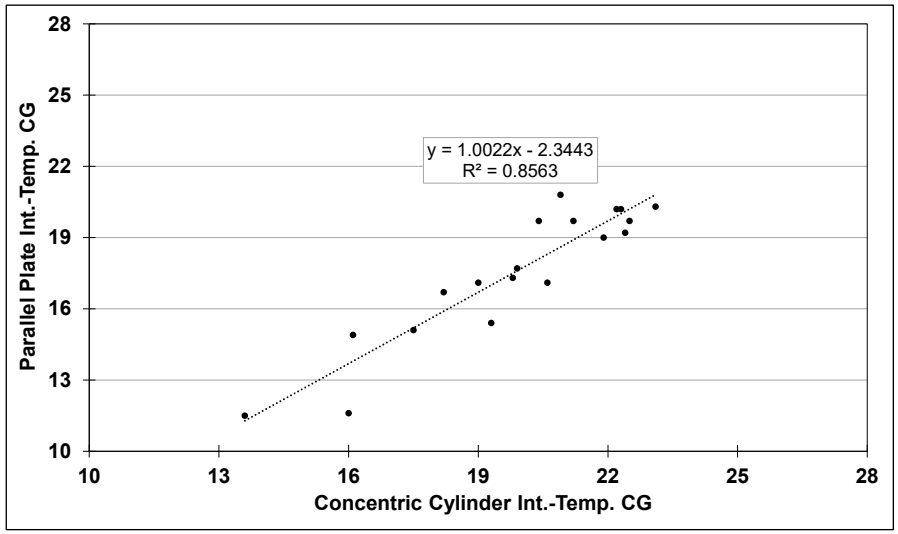

Figure 6.11: AR binder intermediate-temperature CG: Geometry comparison.

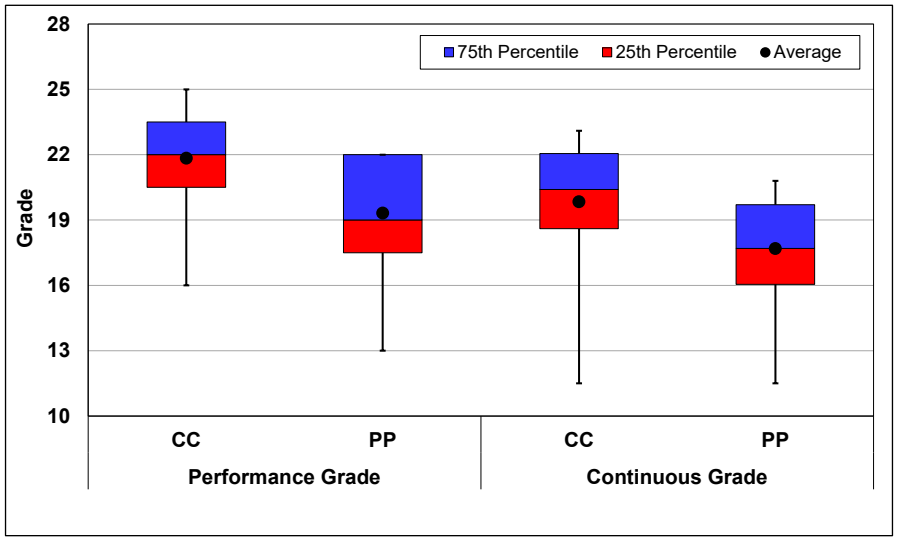

Figure 6.12: AR binder intermediate-temperature PG and CG: Geometry comparison.

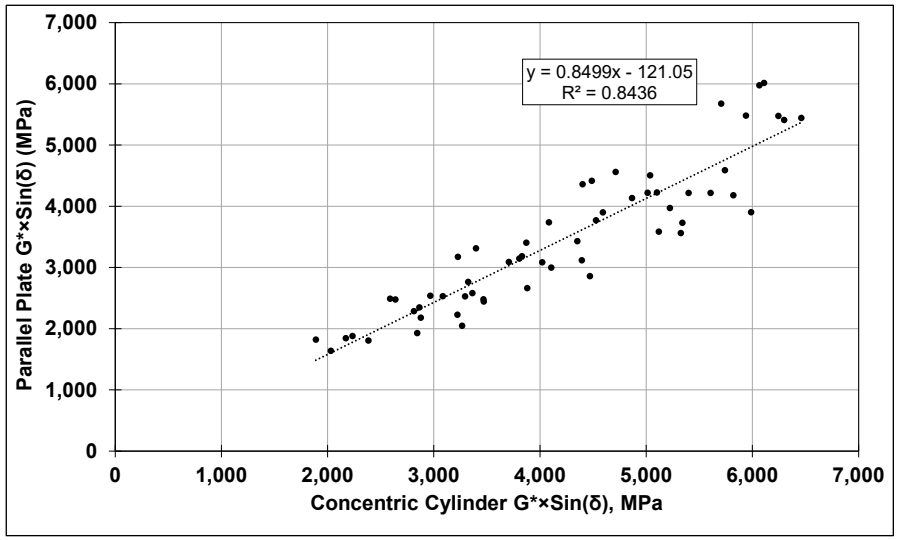

Figure 6.13: AR binder intermediate-temperature: Geometry comparison.

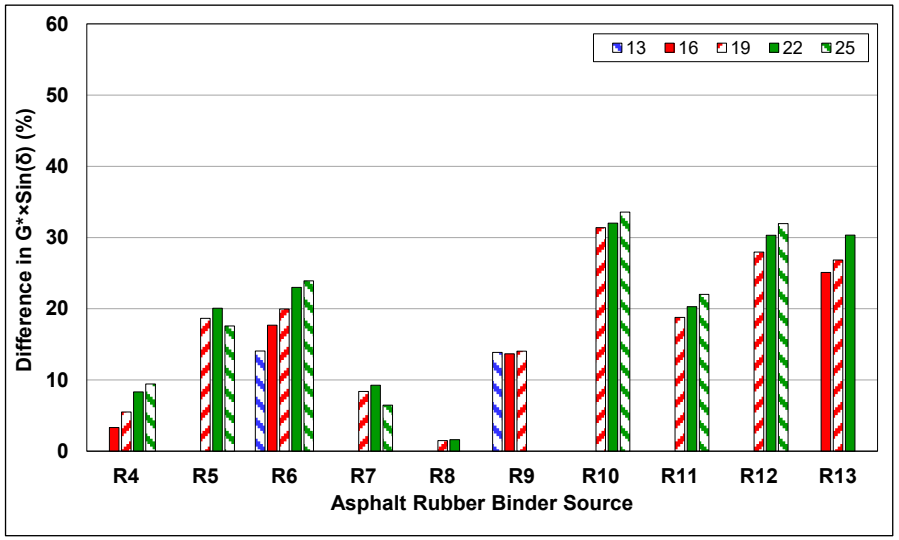

Figure 6.14: AR binder intermediate-temperature: Geometry difference (R4-R13).

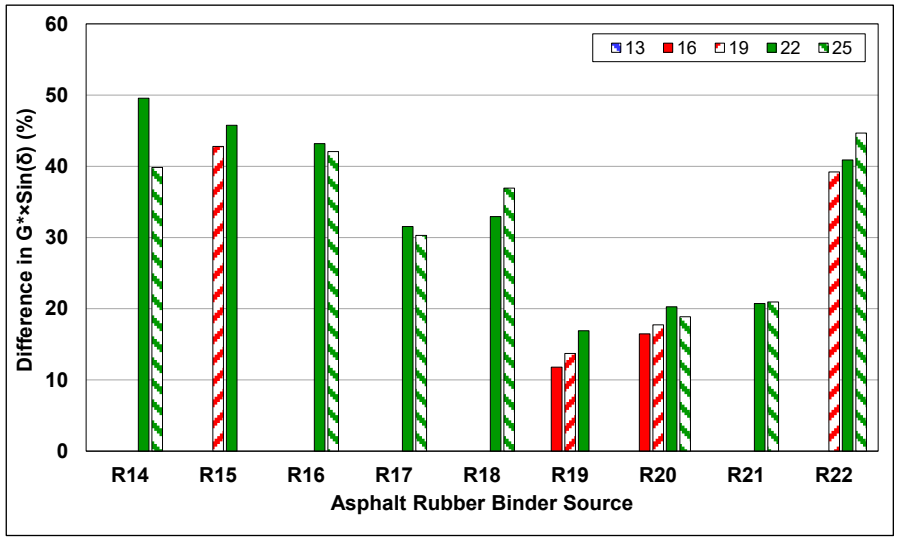

Figure 6.15: AR binder intermediate-temperature: Geometry difference (R14-R22).

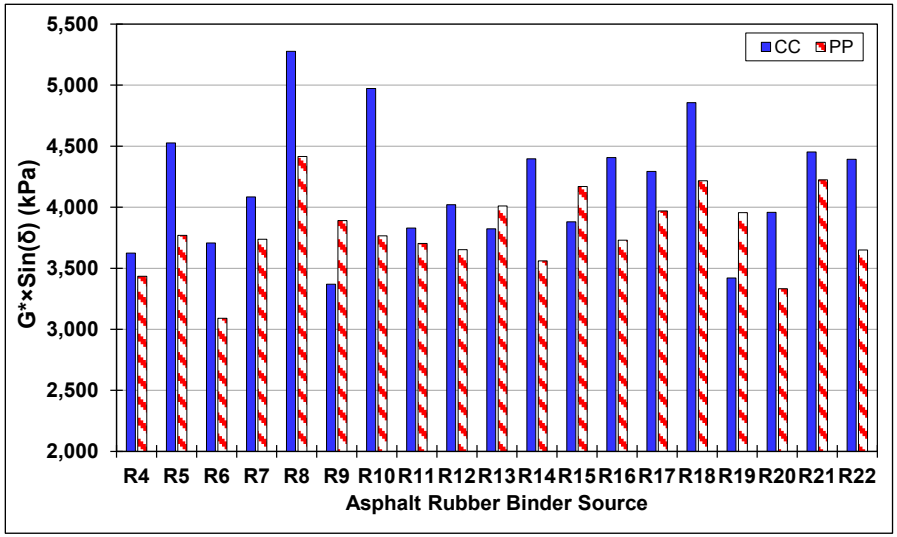

Figure 6.16: AR binder intermediate-temperature: Difference in midpoint G*×sin(δ).

A review of the data led to the following observations:

- A statistical comparison of the performance grade results from the two geometries indicated a marginal linear correlation (R^2 of 0.67), indicating that the two geometries will list different grades for the same binder in some instances. The correlation for continuous grade results was stronger (R^2 0.85) but insufficient to justify that the geometries can be used interchangeably.
- When performance and continuous grade results are compared with a box-and-whisker plot (Figure 6.12), it is clear that the concentric cylinder geometry listed higher intermediate-temperature performance and continuous grades than the parallel plate geometry, but results from both geometries had relatively high variability.
- A statistical comparison of the PAV-aged binder results from the two geometries indicated a reasonable linear correlation (R^2 of 0.84), which implies that the two geometries are testing the same properties.
- When comparing the two geometries at individual testing temperatures, G*×sin(δ) values determined with concentric cylinder were consistently higher than those determined with parallel plate.
- When comparing the two geometries in terms of the midpoint testing temperature, G*×sin(δ) values determined with concentric cylinder were higher than those determined with parallel plate for 15 of the 19 binders.

6.5 Single-Operator Precision Results

Single-operator precision results for the two geometries are plotted in Figure 6.17 and Figure 6.18 and for both geometries combined in Figure 6.19. A review of the data led to the following observations:

- The percentage difference between two replicates was below the 13.8% limit for the concentric cylinder test results. Six of the 118 parallel plate results were above the limit, which equates to 95% of the results falling within this acceptable range for unmodified binders.
- When the results are combined (i.e., all the results from both geometries for one binder at one temperature are considered as replicates), the percentage difference between two replicates exceeded 13.8% for 42 of the 61 results or 69%. The acceptable range would need to be increased to 40.2% to achieve 95% acceptance if it was based on this data.
- Although the size of the data sets were different, the results indicate that variation in the parallel plate results were higher than those in the concentric cylinder results and that the two geometries yield significantly different results. This implies that the two geometries should not be used interchangeably for intermediate-temperature testing.

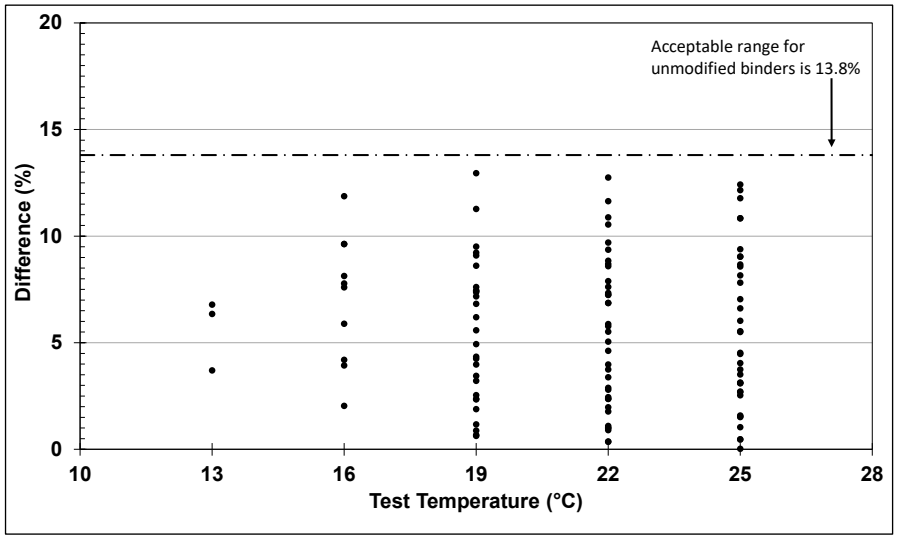

Figure 6.17: Precision results for PAV-aged AR binders: Concentric cylinder.

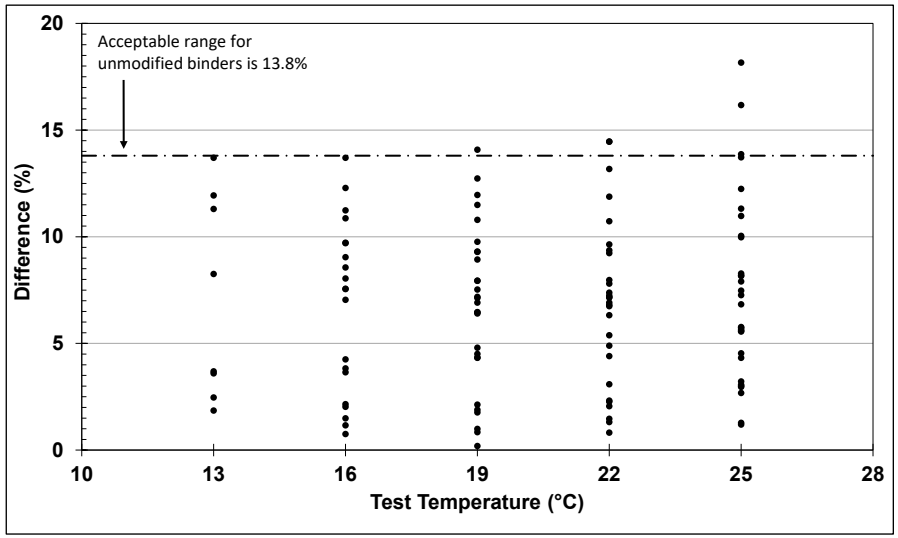

Figure 6.18: Precision results for PAV-aged AR binders: Parallel plate.

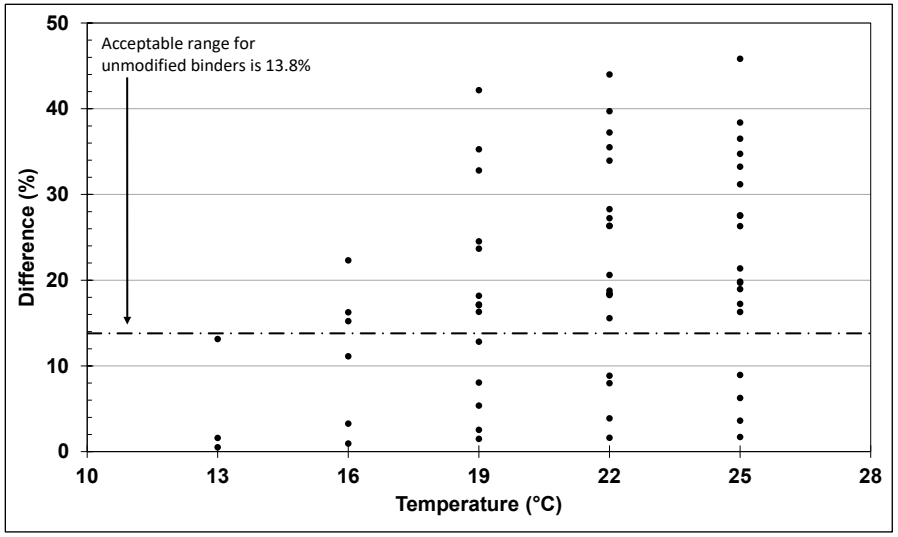

Figure 6.19: Precision results for PAV-aged AR binders: Combined results.

7. MULTIPLE STRESS CREEP RECOVERY TESTING

7.1 Introduction

This chapter covers rheology testing to determine the multiple stress creep recovery (MSCR) and high performance high-temperature grades of the 19 plant-produced asphalt rubber binders and the base binders used to produce them. The concentric cylinder and parallel plate geometry results are compared through a simple correlation and single-operator precision analyses of the test results.

7.2 Base Binders

Although the MSCR test was developed primarily for quantifying the benefits of modified binders (polymer), the base binders were also tested for comparative purposes. Average percent recovery (APR), non-recoverable creep compliance (J_{nr}), and MSCR grade for the base binders are listed in Table 7.1. Average percent recovery non-recoverable creep compliance are plotted in Figure 7.1 and Figure 7.2, respectively.

Table 7.1: Base Binder MSCR Results

Source	APR		J_{nr}			75% of 0.1 kPa	Grade
	0.1 kPa	3.2 kPa	0.1 kPa	3.2 kPa	Difference		
B4	10.92	1.31	1.89	2.46	0.57	1.42	64S
B5	0.77	0.00	3.44	3.60	0.16	2.58	64S
B6	10.43	1.10	1.95	2.49	0.55	1.46	64S
B7	0.00	0.00	3.66	3.76	0.10	2.75	64S
B8	7.06	2.00	0.98	1.09	0.11	0.74	64H
B9	4.95	0.63	1.87	2.11	0.24	1.41	64S
B10	4.45	0.68	1.41	1.55	0.13	1.06	64H
B11	9.64	1.30	1.82	2.28	0.46	1.37	64S
B12	3.61	0.03	2.46	2.80	0.34	1.85	64S
B13	2.87	0.00	2.97	3.35	0.39	2.22	64S
B14	0.00	0.00	3.51	3.63	0.11	2.63	64S
B15[a]	—	—	—	—	—	—	—
B16	0.00	0.00	3.93	4.05	0.12	2.95	Fail
B17	0.00	0.00	3.97	4.09	0.11	2.98	Fail
B18	6.09	1.07	1.40	1.57	0.18	1.05	64H
B19	9.48	1.43	1.72	2.13	0.41	1.29	64S
B20	2.99	0.00	2.62	2.95	0.33	1.96	64S
B21	6.14	0.89	1.22	1.41	0.19	0.91	64H
B22	3.48	0.12	2.34	2.63	0.29	1.76	64S

[a] The B15 base binder was not sampled by the plant

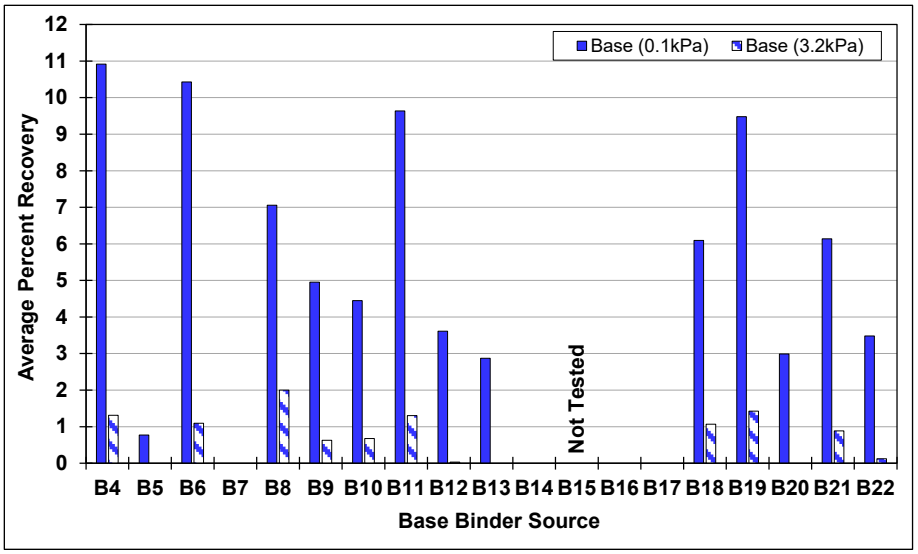

Figure 7.1: Base binder: Average percent recovery at 64°C.

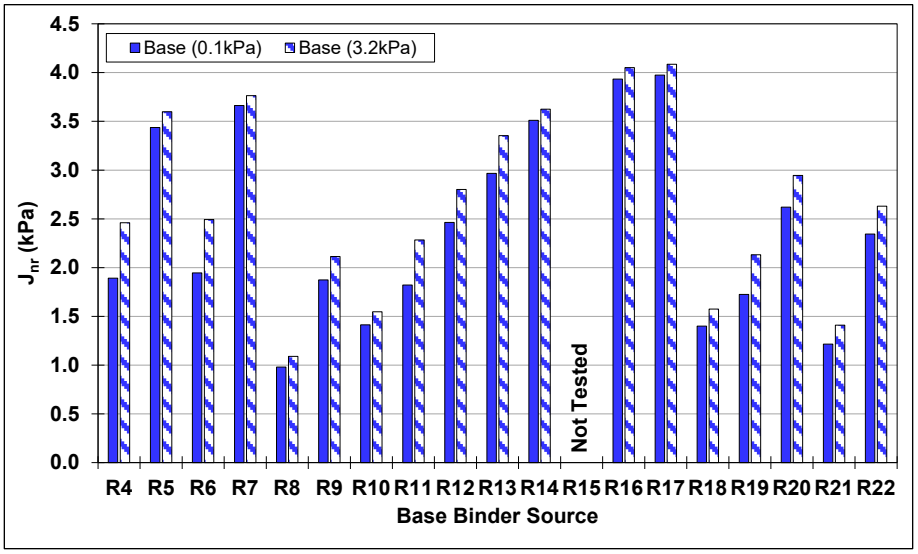

Figure 7.2: Base binder: Non-recoverable creep compliance at 64°C.

A review of the data led to the following observations:

- The average percent recoveries tested at the low stress level (0.1 kPa) ranged from zero (four binders) up to 10.9, consistent with results for unmodified binders in general. Percent recoveries at the higher stress level (3.2 kPa) ranged from 0% (seven binders) up to 2.0%.
- Variability in average percent recovery between replicates of the same base binder samples was small at both stress levels.
- The non-recoverable creep compliance showed some variation across the different base binders with little difference between the two stress levels. Creep compliance at 3.2 kPa was higher than that at 0.1 kPa for all binders, as expected.

- Twelve of the binders graded in the standard category, four met the requirements for the heavy traffic category, and two failed (J_{nr} greater than 4.0 per AASHTO M 322).

7.3 Asphalt Rubber Binders

Average percent recovery, non-recoverable creep compliance, and MSCR grade for the asphalt rubber binders are listed in Table 7.2 and Table 7.3 for tests using the concentric cylinder and parallel plate geometries, respectively. Average percent recovery and non-recoverable creep compliance results are plotted in Figure 7.3 through Figure 7.6 for the two geometries, respectively. A review of the data led to the following observations:

- The average percent recoveries measured on the asphalt rubber binders were significantly higher than those recorded on the base binders, as expected.
- All of the binders graded in the "E" (extremely heavy traffic) category according to AASHTO M 322, regardless of the testing geometry used.
- A comparison of Figure 7.3 and Figure 7.4 show that trends between the two geometries were similar although results for individual binders were different.
- The average percent recoveries tested at the low stress level (0.1 kPa) ranged from 59.9 to 94.2 for tests with the concentric cylinder geometry and from 73.6 to 95.5 for tests with the parallel plate geometry. Percent recoveries at the higher stress level (3.2 kPa) ranged from 42.6 to 91.7 and from 39.2 to 92.7 for the two geometries, respectively.
- Average percent recoveries tested at 0.1 kPa with concentric cylinder geometry were mostly lower than those tested with parallel plate geometry (17 of the 19 binders). Concentric cylinder results ranged from 30% lower to 7% higher than those determined with the parallel plate geometry. At the higher stress level, the concentric cylinder geometry produced lower values on nine of the binders, with concentric cylinder results ranging from 13% lower to 21% higher than those determined with the parallel plate.
- The asphalt rubber binders had significantly lower creep compliances than their respective base binders, as expected. Non-recoverable creep compliance was close to zero for all binders when tested at both stress levels. A comparison of Figure 7.5 and Figure 7.6 show that trends between the two geometries were similar although results for individual binders were different.
- The difference in non-recoverable creep compliance tested at 0.1 kPa between the two geometries was significant. At the higher stress level, the difference was much lower but still significant in most instances. There were no clear trends in the data.
- There were no apparent trends between rubber gradation and average percent recovery or non-recoverable creep compliance.

Table 7.2: AR Binder MSCR Results: Concentric Cylinder

Source	APR		J_{nr}			75% of 0.1 kPa	Grade
	0.1 kPa	3.2 kPa	0.1 kPa	3.2 kPa	Difference		
R4	94.18	91.72	0.00	0.01	0.00	0.00	64E
R5	92.60	45.57	0.00	0.20	0.19	0.00	64E
R6	88.02	83.10	0.00	0.02	0.02	0.00	64E
R7	59.97	42.64	0.14	0.26	0.12	0.10	64E
R8	91.43	73.82	0.01	0.05	0.03	0.01	64E
R9	70.40	74.54	0.02	0.03	0.01	0.02	64E
R10	81.95	73.03	0.03	0.06	0.02	0.03	64E
R11	88.81	86.62	0.00	0.01	0.01	0.00	64E
R12	73.50	65.16	0.05	0.10	0.05	0.04	64E
R13	86.16	74.40	0.02	0.04	0.02	0.02	64E
R14	64.42	47.31	0.21	0.33	0.12	0.16	64E
R15	82.94	72.59	0.03	0.04	0.02	0.02	64E
R16	71.58	49.56	0.15	0.27	0.12	0.11	64E
R17	76.53	53.24	0.13	0.27	0.14	0.10	64E
R18	87.49	82.90	0.01	0.01	0.00	0.01	64E
R19	91.32	86.60	0.01	0.01	0.00	0.00	64E
R20	84.23	74.28	0.03	0.05	0.02	0.02	64E
R21	81.84	72.70	0.03	0.04	0.01	0.02	64E
R22	80.93	72.90	0.03	0.04	0.01	0.02	64E

Table 7.3: AR Binder MSCR Results: Parallel Plate

Source	APR		J_{nr}			75% of 0.1 kPa	Grade
	0.1 kPa	3.2 kPa	0.1 kPa	3.2 kPa	Difference		
R4	95.53	92.70	0.00	0.00	0.00	0.00	64E
R5	86.31	52.63	0.04	0.16	0.12	0.03	64E
R6	94.25	86.14	0.01	0.01	0.01	0.00	64E
R7	85.68	42.04	0.05	0.26	0.21	0.04	64E
R8	89.48	70.82	0.02	0.05	0.03	0.01	64E
R9	89.56	76.91	0.01	0.02	0.02	0.01	64E
R10	83.68	70.23	0.03	0.06	0.03	0.02	64E
R11	93.89	89.67	0.00	0.01	0.00	0.00	64E
R12	90.34	66.96	0.02	0.08	0.06	0.02	64E
R13	89.29	71.04	0.02	0.05	0.03	0.01	64E
R14	73.56	39.19	0.14	0.37	0.24	0.10	64E
R15	86.22	66.48	0.02	0.06	0.04	0.02	64E
R16	80.52	42.01	0.08	0.30	0.22	0.06	64E
R17	85.03	46.45	0.06	0.28	0.21	0.05	64E
R18	92.27	86.54	0.00	0.01	0.00	0.00	64E
R19	92.51	86.04	0.01	0.01	0.00	0.00	64E
R20	87.20	67.86	0.02	0.07	0.04	0.02	64E
R21	84.93	69.01	0.02	0.05	0.03	0.02	64E
R22	86.55	69.59	0.02	0.05	0.03	0.02	64E

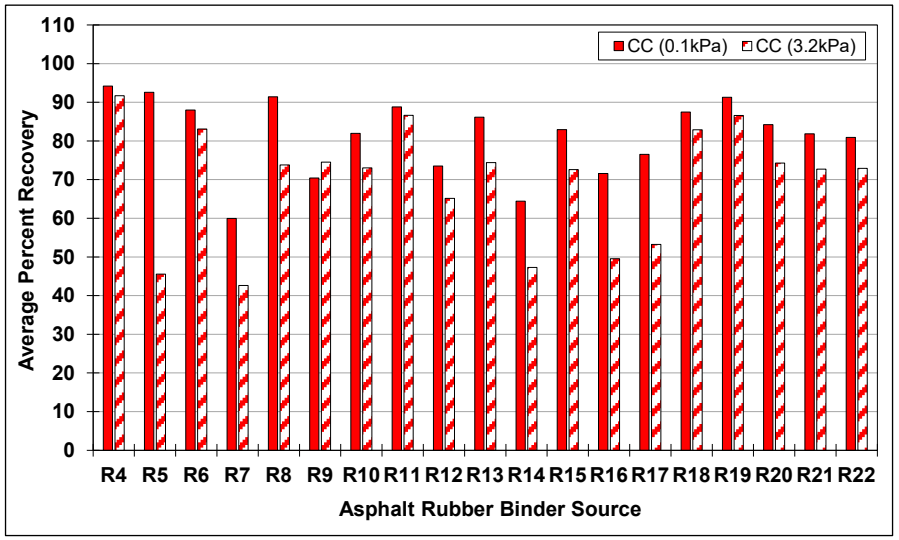

Figure 7.3: AR binder: Average percent recovery at 64°C: Concentric cylinder.

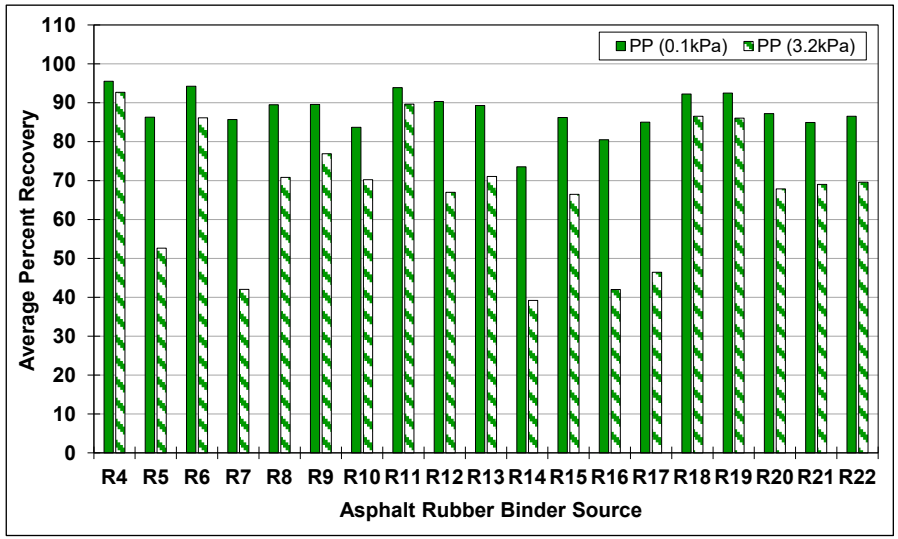

Figure 7.4: Average percent recovery at 64°C: Parallel plate.

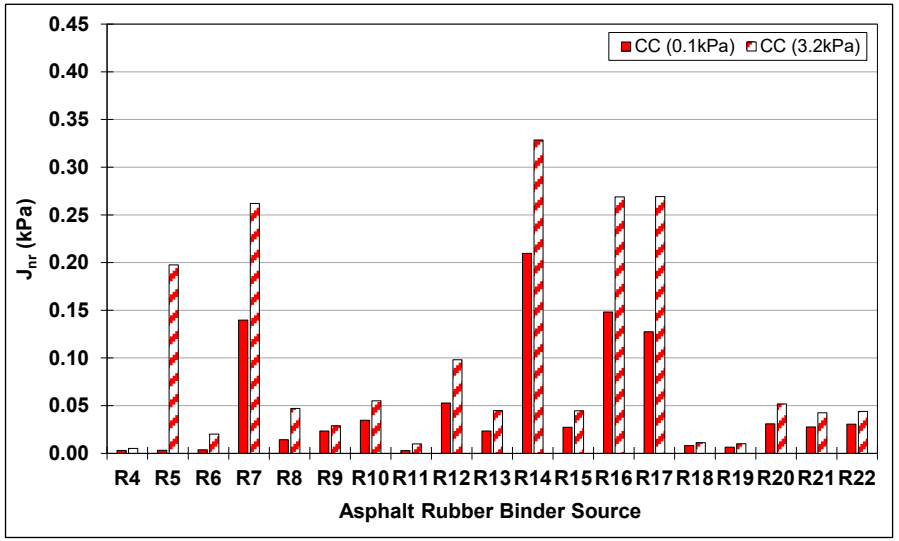

Figure 7.5: AR binder: Non-recoverable creep compliance at 64°C: Concentric cylinder.

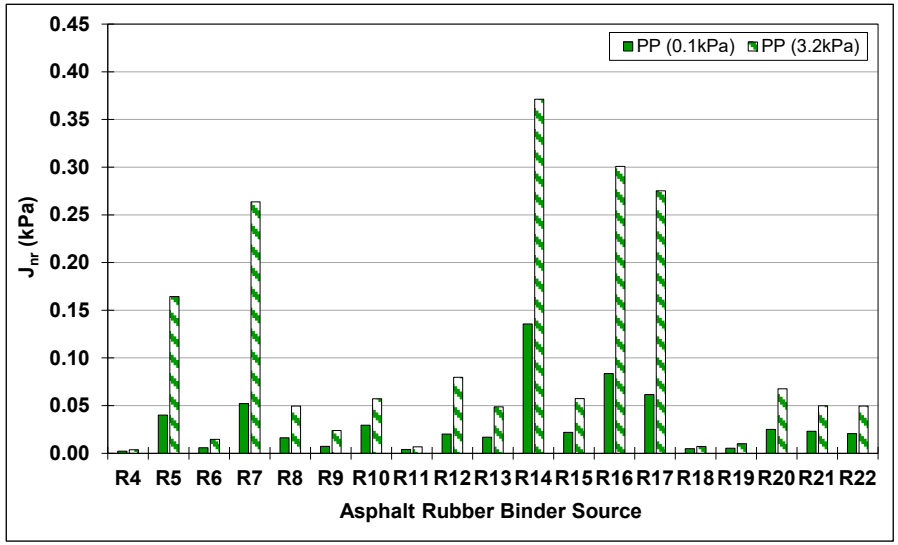

Figure 7.6: AR binder: Non-recoverable creep compliance at 64°C: Parallel plate.

7.4 Comparison of Testing Geometries

Scatter plots comparing the average percent recovery and non-recoverable creep compliance results from the two geometries are shown in Figure 7.7 and Figure 7.8. The percent difference in the two test parameters when tested with the concentric cylinder and parallel plate geometries, calculated using the formula in Equation 5.1, are shown in Figure 7.9 and Figure 7.10. A review of the data led to the following observations:

- A statistical comparison of the average percent recoveries tested at 3.2 kPa indicated a reasonable linear correlation (R^2 of 0.92), which implies that the two geometries are testing the same properties. The comparison of non-recoverable creep compliances tested at 3.2 kPa indicated a good correlation (R^2 of 0.95).
- Average percent recoveries tested at 0.1 kPa with concentric cylinder geometry were mostly lower than those tested with parallel plate geometry (17 of the 19 binders), with results ranging from 30% lower to 7% higher. At the higher stress level, the concentric cylinder geometry produced lower values on nine of the binders, with results ranging from 13% lower to 21% higher than those determined with the parallel plate.
- The difference in non-recoverable creep compliance tested at 0.1 kPa between the two geometries was significant. At the higher stress level, the difference was much lower but still significant in most instances. There were no clear trends in the data, although the parallel plate results appeared to have higher variability at the higher stress level.

7.5 Single-Operator Precision Results

Single-operator precision results for average percent recovery and non-recoverable creep compliance tested with both geometries are plotted in Figure 7.11 and Figure 7.12 and for both geometries combined in Figure 7.13 and Figure 7.14. A review of the data led to the following observations:

- All but three of the average percent recovery results were on or above the 8.5% limit (two concentric cylinder and one parallel plate). Four of the non-recoverable creep compliance results (one concentric cylinder and three parallel plate) were above the 26.6% limit for test results between 0.10 and 0.25. Note that 13 of the 19 binders tested had results that were less than 0.10 for which no limit has been set (Table 3.3).
- When the results are combined (i.e., all the results from both geometries for one binder at one temperature are considered as replicates), the percentage difference between two replicates of the average percent recovery results exceeded 8.5% for seven of the results. Seven of the non-recoverable creep compliance results exceeded the 26.6% limit.

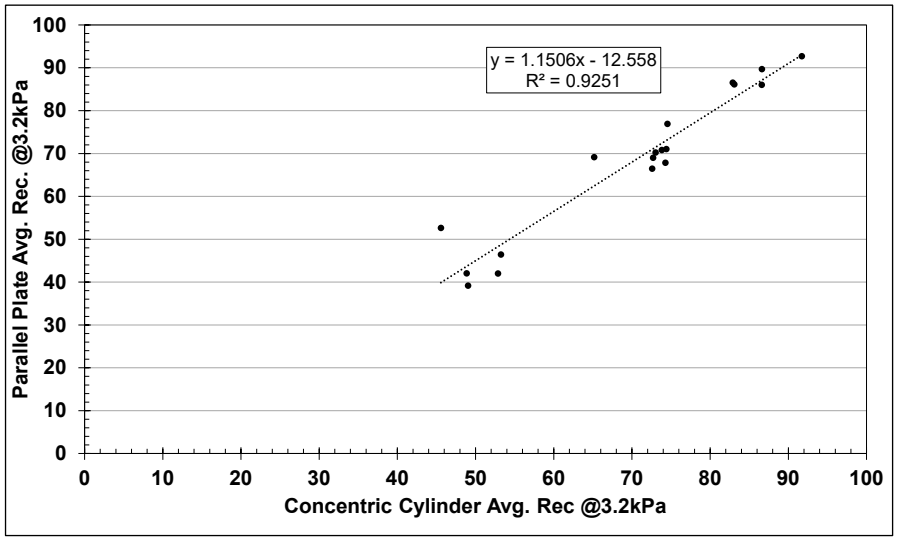

Figure 7.7: AR binder average percent recovery: Geometry comparison.

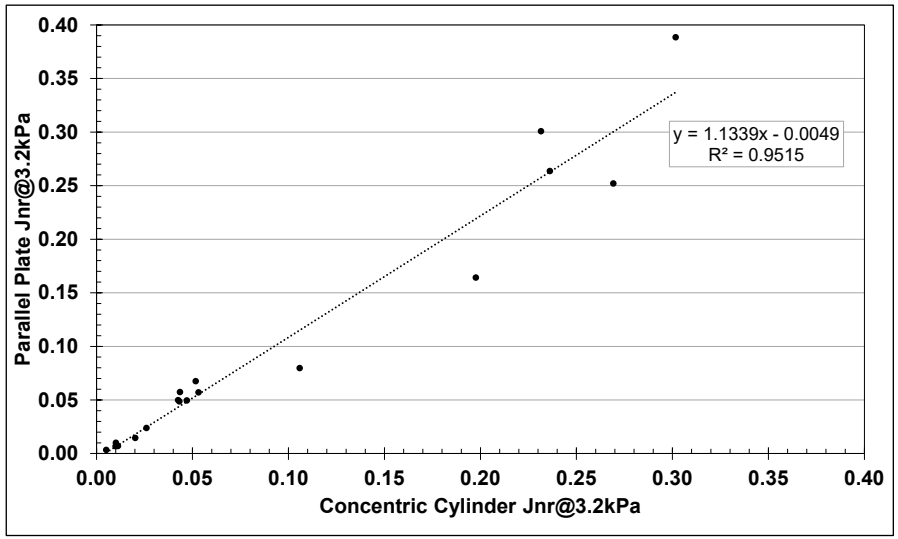

Figure 7.8: AR binder non-recoverable creep compliance: Geometry comparison.

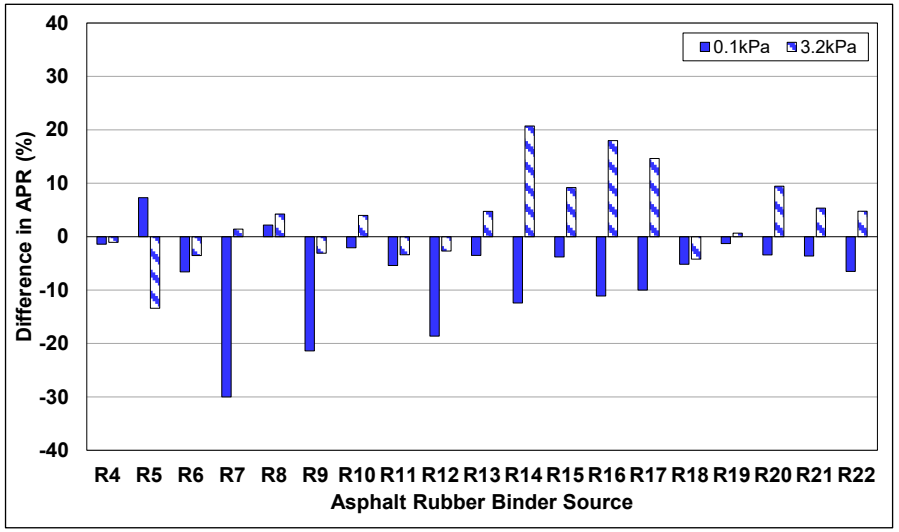

Figure 7.9: AR binder average percent recovery: Geometry difference.

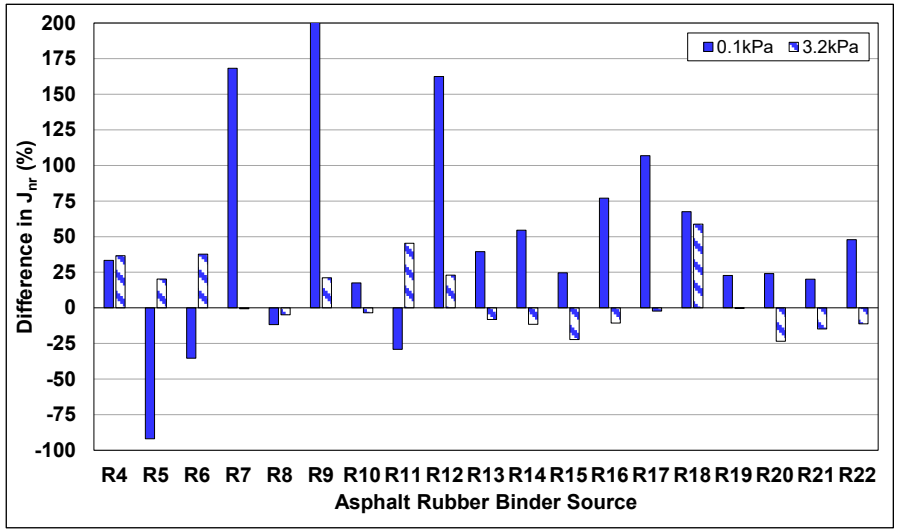

Figure 7.10: AR binder non-recoverable creep compliance: Geometry difference.

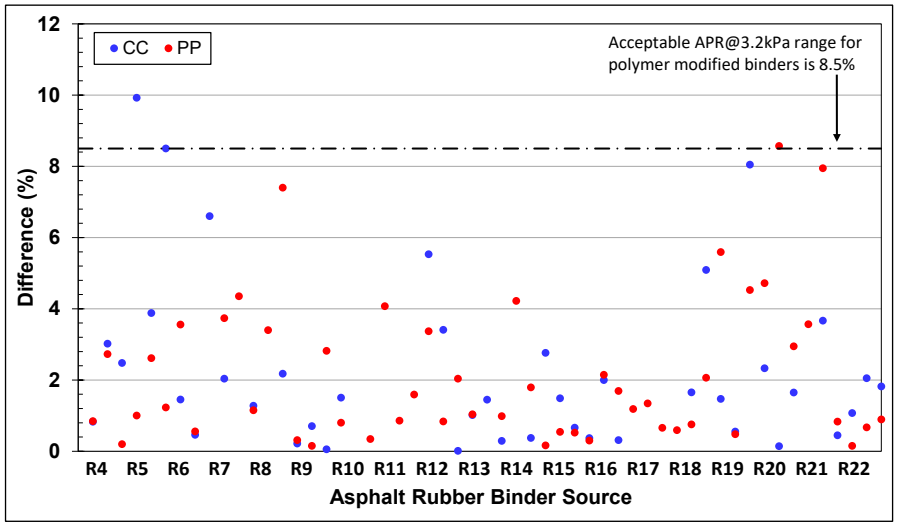

Figure 7.11: Precision results for average percent recovery.

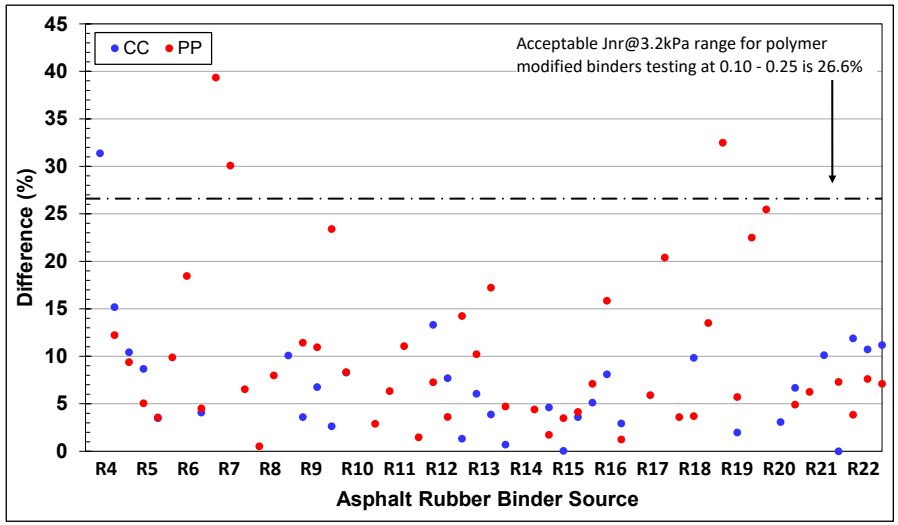

Figure 7.12: Precision results for non-recoverable creep compliance.

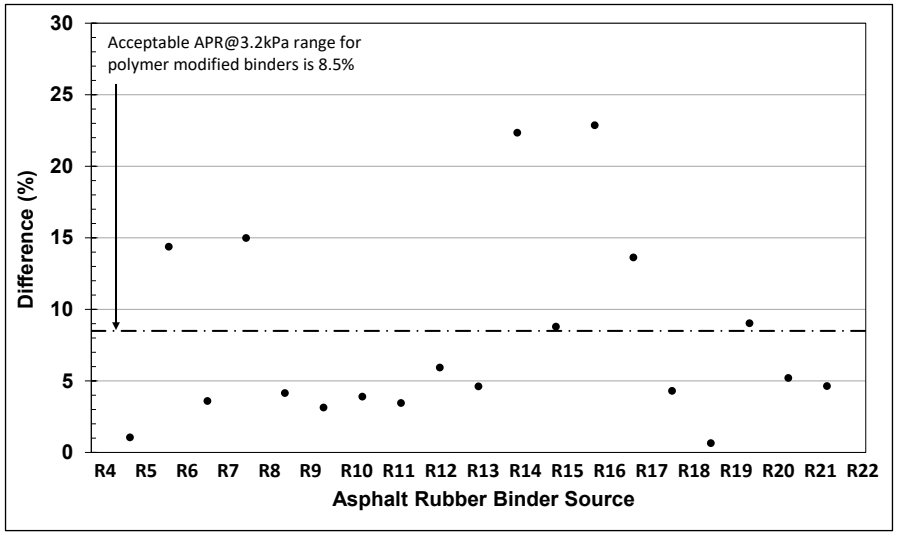

Figure 7.13: Precision results for average percent recovery: Combined results.

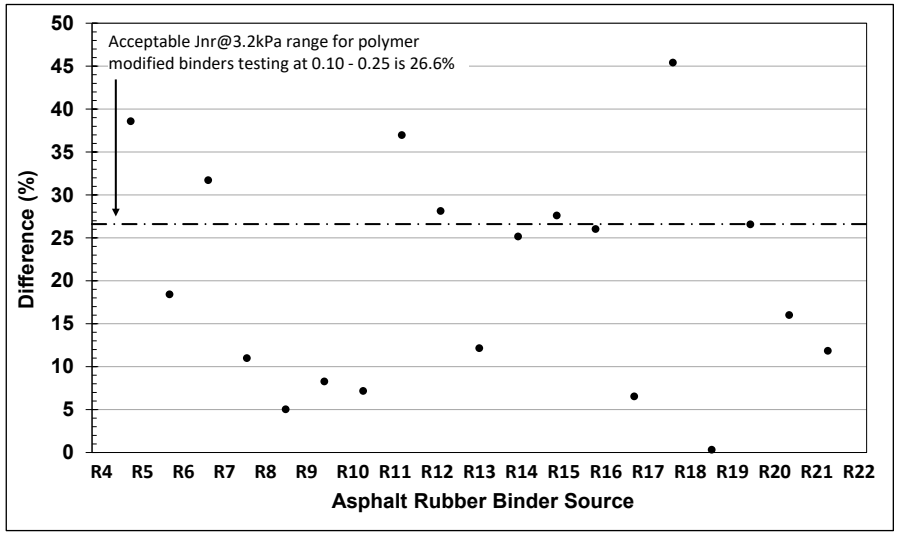

Figure 7.14: Precision results for non-recoverable creep compliance: Combined results.

8. LOW-TEMPERATURE PERFORMANCE GRADE TESTING

8.1 Introduction

Although low-temperature testing is not part of the comparison between dynamic shear rheometer geometries, this parameter is part of the performance grade and the results have therefore been included for completeness.

8.2 Base Binders

Low-temperature test results for the 19 base binders are summarized in Table 8.1. Low-temperature performance and continuous grade results are plotted in Figure 8.1. Stiffness and m-value test results are plotted in Figure 8.2 and Figure 8.4, respectively. Nine of the base binders had low-temperature PGs of -16, eight had low-temperature PGs of -22, and one graded at -28. Continuous grades varied between -16.3 and -28.6, all lower than the performance grade. Grades were dictated by the m-value (i.e., ≥ 0.30) for all base binders.

Table 8.1: Base Binder Low-Temperature PG and CG Results

Source	Low PG	Low CG	Stiffness (at °C)					m-value (at °C)				
			-6	-12	-18	-24	-30	-6	-12	-18	-24	-30
B4	-22	-25.1	48	104	219	468	—	0.408	0.353	0.286	0.259	—
B5	-16	-18.1	234	-	957	—	—	0.359	—	0.200	—	—
B6	-22	-28.6	65	161	278	562	—	0.389	0.337	0.303	0.244	-
B7	-16	-18.4	210	480	—	—	—	0.360	0.278	—	—	—
B8	-16	-18.5	206	—	673	—	—	0.330	—	0.209	—	—
B9	-22	-22.8	84	—	—	663	—	0.385	—	—	0.199	—
B10	-16	-16.3	161	—	461	—	—	0.303	—	0.228	—	—
B11	-28	-28.4	54	—	277	—	525	0.396	—	0.302	—	0.246
B12	-22	-23.6	101	—	462	—	—	0.384	—	0.261	—	—
B13	-22	-26.7	66	—	324	—	—	0.394	—	0.281	—	—
B14	-16	-18.2	233	464	—	-	—	0.328	0.272	—	—	—
B15[a]	—	—	—	—	—	—	—	—	—	—	—	—
B16	-16	-18.7	215	453	—	—	—	0.366	0.274	—	—	—
B17	-16	-20.0	175	391	—	—	—	0.397	0.292	—	—	—
B18	-16	-19.1	182	—	618	—	—	0.337	—	0.215	—	—
B19	-22	-26.2	67	—	316	—	—	0.395	—	0.286	—	—
B20	-22	-23.7	104	—	488	—	—	0.392	—	0.259	—	—
B21	-16	-17.2	157	310	—	—	—	0.311	0.259	—	—	—
B22	-22	-25.5	—	189	380	—	—	—	0.336	0.277	—	—

[a] The B15 base binder was not sampled by the plant

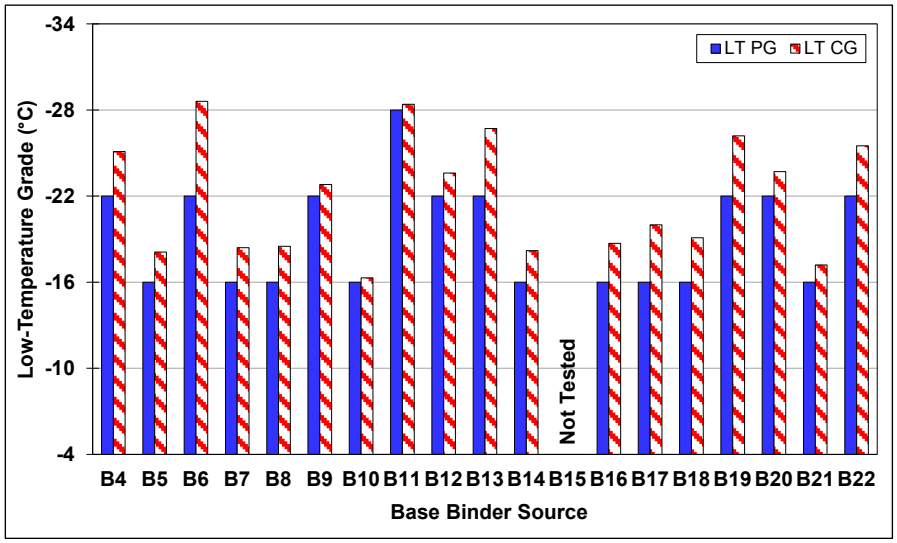

Figure 8.1: Base binder: Low-temperature performance and continuous grade.

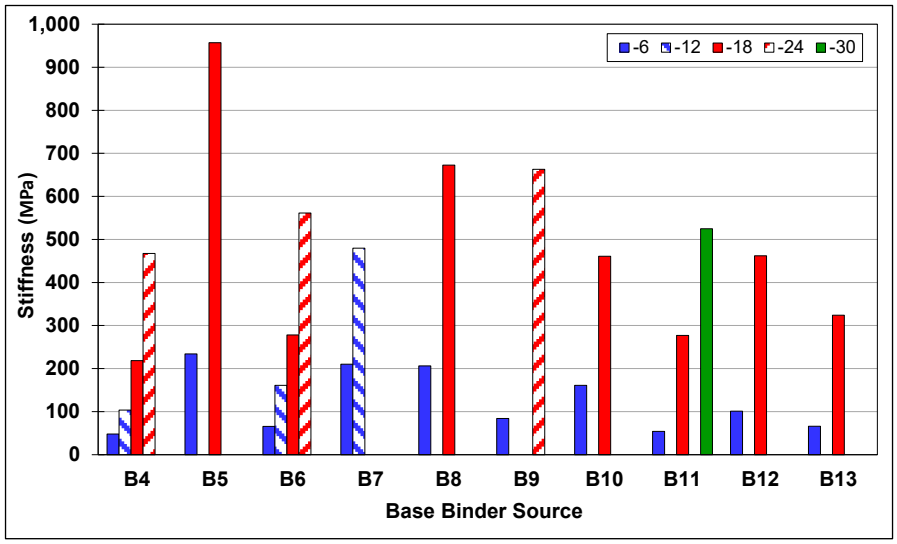

Figure 8.2: Base binder: Low-temperature stiffness (B4-B13).

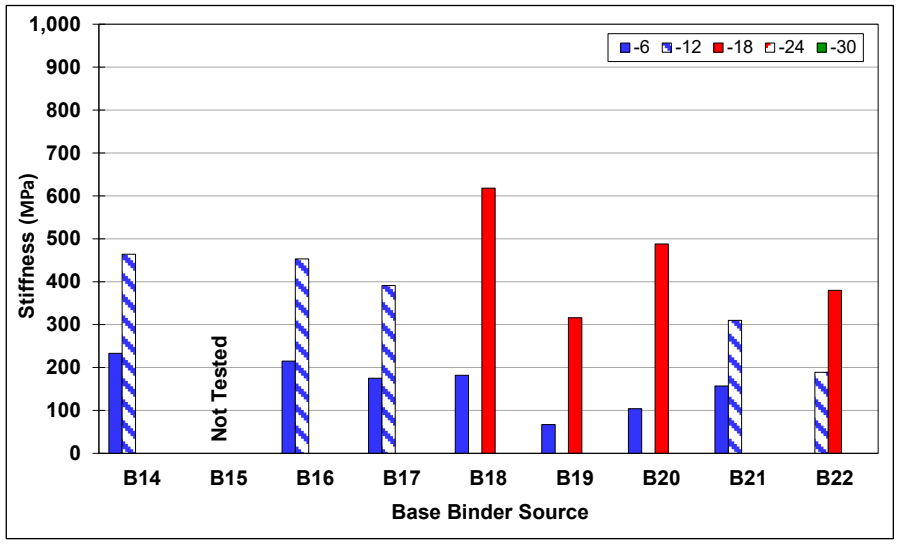

Figure 8.3: Base binder: Low-temperature stiffness (B14-B22).

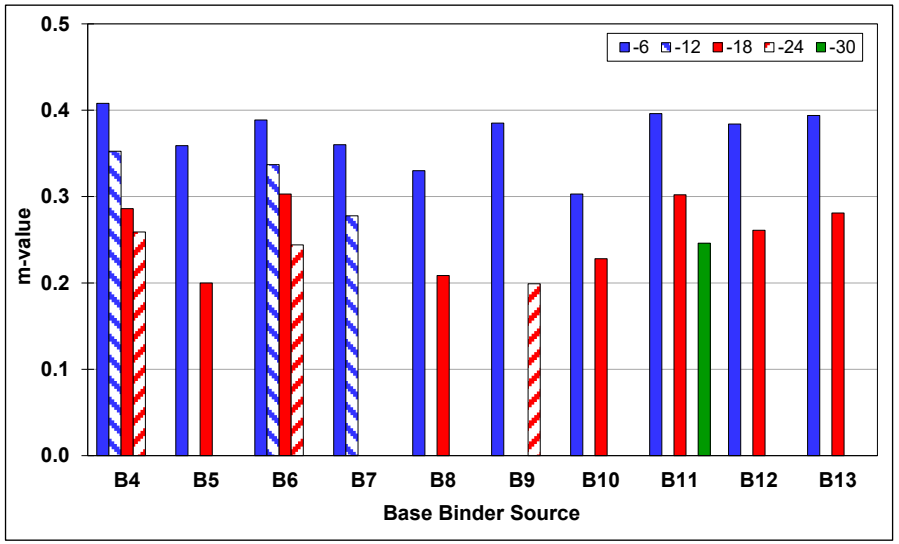

Figure 8.4: Base binder: Low-temperature m-value (B4-B13).

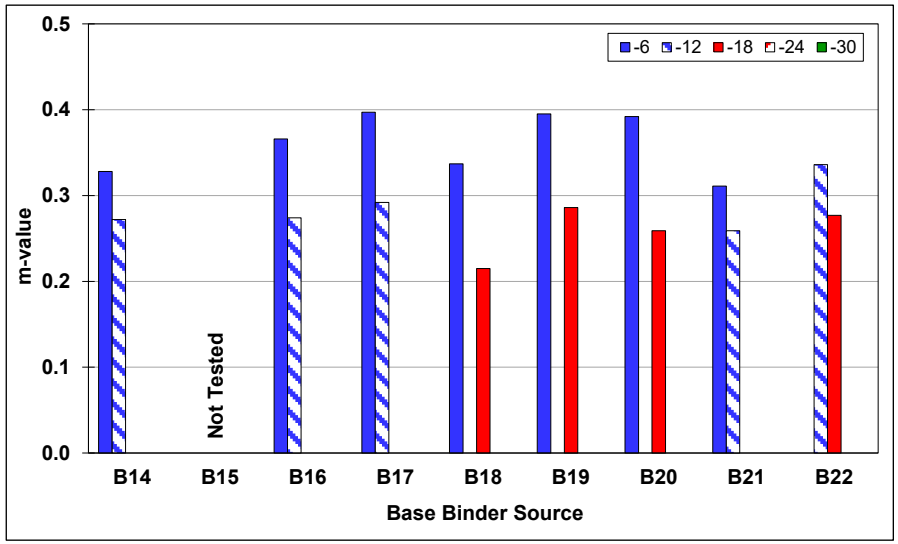

Figure 8.5: Base binder: Low-temperature m-value (B14-B22).

8.3 Asphalt Rubber Binders

Low-temperature performance and continuous grade results for the asphalt rubber binders are listed in Table 8.3 and plotted in Figure 8.6.

Table 8.2: AR Binder Low-Temperature PG and CG Results

Source	Low PG	Low CG	Source	Low PG	Low CG
R4	-22	-27.0	R14	-22	-26.6
R5	-22	-23.8	R15	-22	-26.0
R6	-22	-26.7	R16	-22	-27.2
R7	-22	-27.7	R17	-22	-21.8
R8	-22	-26.2	R18	-16	-21.5
R9	-22	-26.2	R19	-22	-25.2
R10	-22	-25.5	R20	-22	-26.5
R11	-22	-25.3	R21	-16	-18.9
R12	-22	-27.5	R22	-22	-22.8
R13	-28	-28.6			

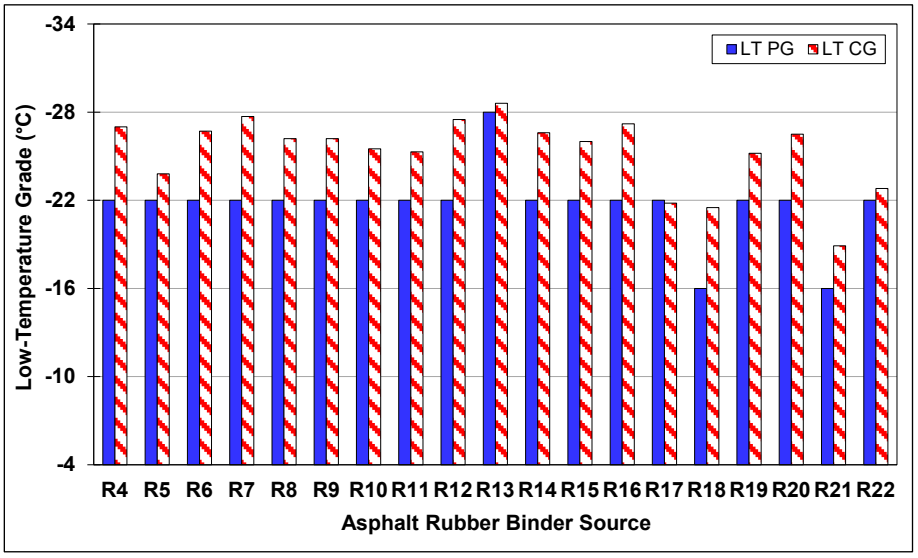

Figure 8.6: AR binder: Low-temperature performance and continuous grade.

Stiffness and m-value results at different test temperatures are listed in Table 8.3. Stiffness test results are plotted in Figure 8.7 and Figure 8.8. Results for m-value tests are plotted in Figure 8.9 and Figure 8.10. A review of the data led to the following observations:

- Two of the asphalt rubber binders had low-temperature PGs of -16 (same PG as their base binders), 16 had low-temperature PGs of -22, and one graded at -28. All of the asphalt rubber binders had the same low temperature PGs (-22). In total, nine of the binders had the same low temperature PG as their respective base binders, eight were one grade lower, and one was one grade higher.

Table 8.3: AR Binder Low-Temperature Testing Results

Source	Stiffness (at °C)						m-value (at °C)					
	-6	-12	-18	-24	-30	-36	-6	-12	-18	-24	-30	-36
R4	—	37	82	190	—	569	—	0.317	0.303	0.271	—	0.214
R5	—	135	274	414	—	—	—	0.319	0.261	0.221	—	—
R6	—	48	—	—	291	—	—	0.323	—	-	0.245	—
R7	—	103	—	393	—	—	—	0.363	—	0.243	—	—
R8	—	79	—	—	525	—	—	0.335	—	—	0.208	—
R9	36	—	121	198	544	—	0.331	—	0.270	0.235	0.194	—
R10	—	94	168	294	512	—	—	0.297	0.255	0.242	0.193	—
R11	—	64	104	—	368	—	—	0.317	0.287	—	0.228	—
R12	—	88	—	—	499	—	—	0.344	—	—	0.220	—
R13	—	51	116	—	376	—	—	0.344	0.304	—	0.233	—
R14	—	113	—	433	—	—	—	0.355	—	0.229	—	—
R15	—	70	—	235	380	—	—	0.330	—	0.249	0.207	—
R16	—	97	—	423	—	—	—	0.357	—	0.240	—	—
R17	—	101	—	385	—	—	—	0.360	—	0.246	—	—
R18	—	105	—	352	—	—	—	0.297	—	0.220	—	—
R19	—	51	—	171	518	—	—	0.319	—	0.253	0.197	—
R20	—	78	—	—	558	—	—	0.337	—	—	0.212	—
R21	—	95	—	—	440	—	—	0.281	—	—	0.190	—
R22	—	86	—	—	492	—	—	0.306	—	—	0.207	—

- Continuous grades varied between -18.9 and -28.6, all lower than the PG.
- Low-temperature cracking resistance decreased with decreasing test temperature in all instances, as expected.
- Stiffness values were well below the AASHTO M 320 criteria for determining the low-temperature grade ($S \leq 300$) and, consequently, grades were dictated by the m-value (≥ 0.30). The presence of incompletely digested rubber particles and potential phase separation between these particles and the asphalt binder probably contributed to the low stiffness values.
- There were no apparent trends between low-temperature PG and rubber gradation.
- Variability between replicate specimens was attributed in part to the rougher beam surfaces after trimming and to variation in the number, size, and degree of digestion of the rubber particles in each beam.
- The AASHTO M 320 procedure contains no recommendations for asphalt rubber binders. The minimum low-temperature grade in the standard table for conventional binders with a high-temperature grade equal to or greater than 76°C is -22°C, which was achieved for all 19 binders.

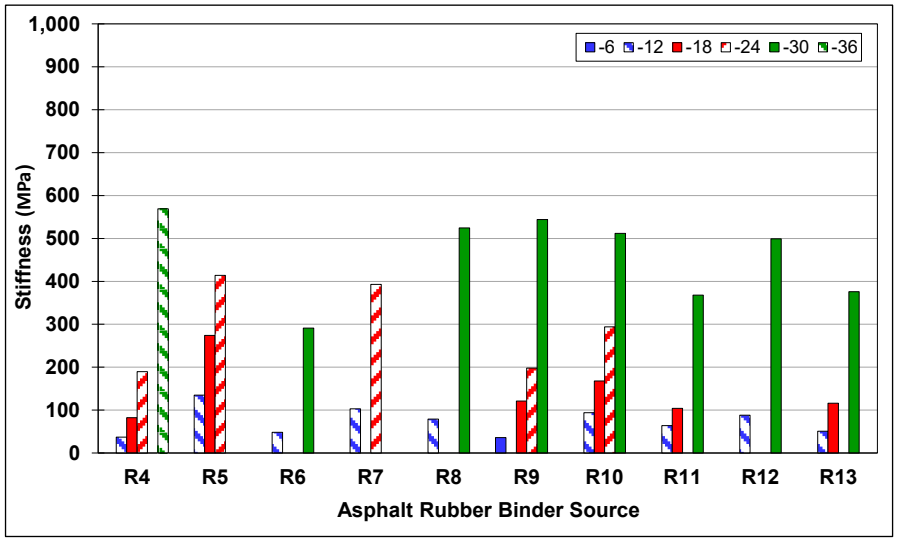

Figure 8.7: AR binder: Low-temperature stiffness (R4-R13).

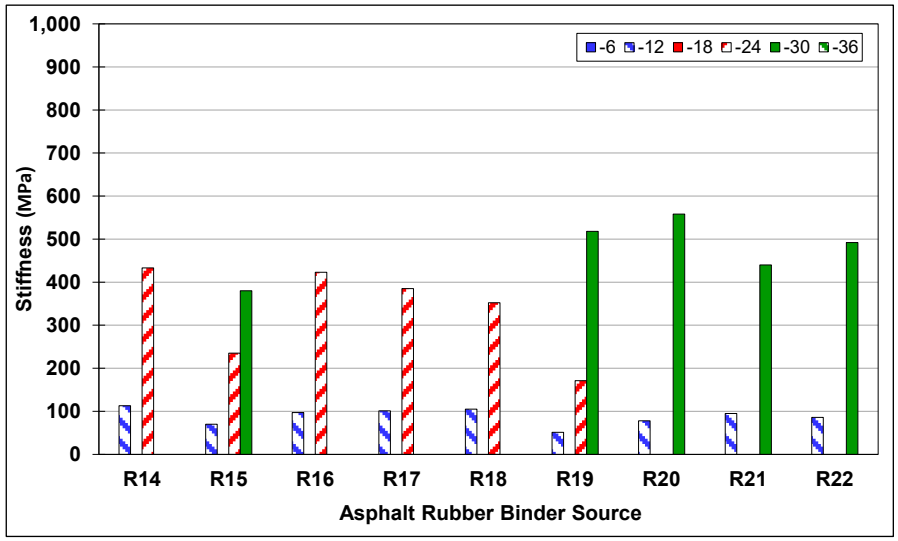

Figure 8.8: AR binder: Low-temperature stiffness (R14-R22).

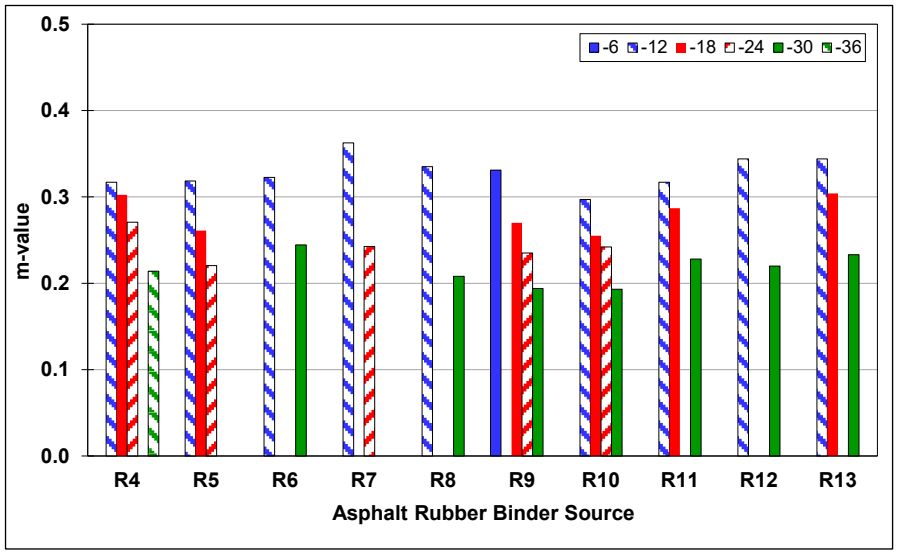

Figure 8.9: AR binder: Low-temperature m-value (R4-R13).

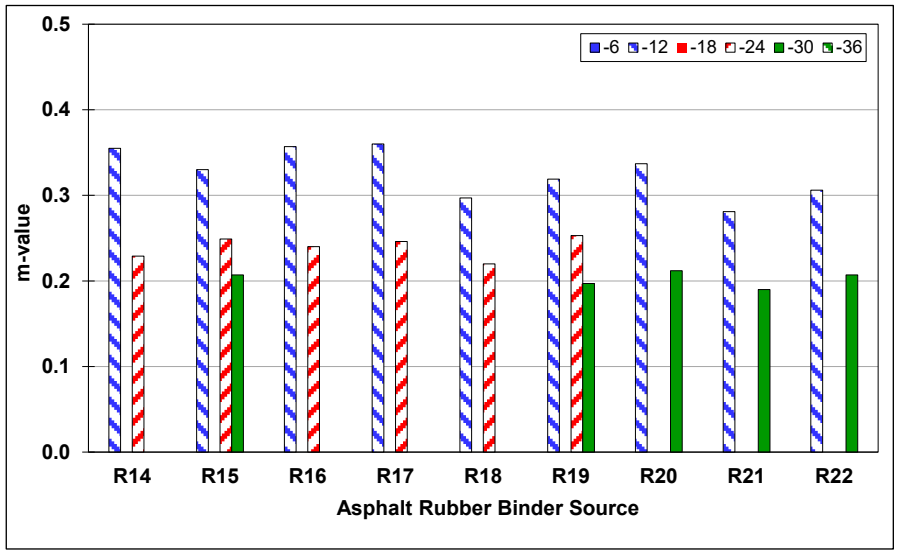

Figure 8.10: AR binder: Low-temperature m-value (R14-R22).

- Questions regarding other factors that may influence results, and specifically the variability between results, include:
  + Whether changes in the properties of the incompletely digested rubber particles occur at very low temperatures (i.e., in the range of glass transition).
  + Whether different rubber particles (e.g., synthetic versus natural rubber) have different coefficients of thermal expansion.
  + Whether the properties of the rubber particles are in any way effected by the type of temperature control medium used in the bending beam rheometer (i.e., ethanol for the testing discussed in this report).

Critical temperatures (Delta T_C) for the base and asphalt rubber binders are plotted in Figure 8.11. The generally recommended minimum Delta T_C for unmodified binders is -5.0°C *(8)*. No minimum Delta T_C has been recommended for asphalt rubber binders, but it is acknowledged that values determined for modified binders (polymer and rubber) may not be a true reflection of cracking performance. A review of the data led to the following observations:

- Delta T_C values for the base binders varied between +1.8°C and -6.8°C and between -4°C and -16.6°C for the asphalt rubber binders.
- All but two of the base binders met the minimum recommended -5.0°C value for unmodified binders, with one binder slightly lower at -5.4°C and the other at -6.8°C. Only four of the asphalt rubber binders met this criterion, suggesting that further studies relating Delta T_C to field-cracking performance of RHMA-G mixes are required before any conclusions can be drawn with regard to whether -5.0°C is an appropriate value for asphalt rubber binders.

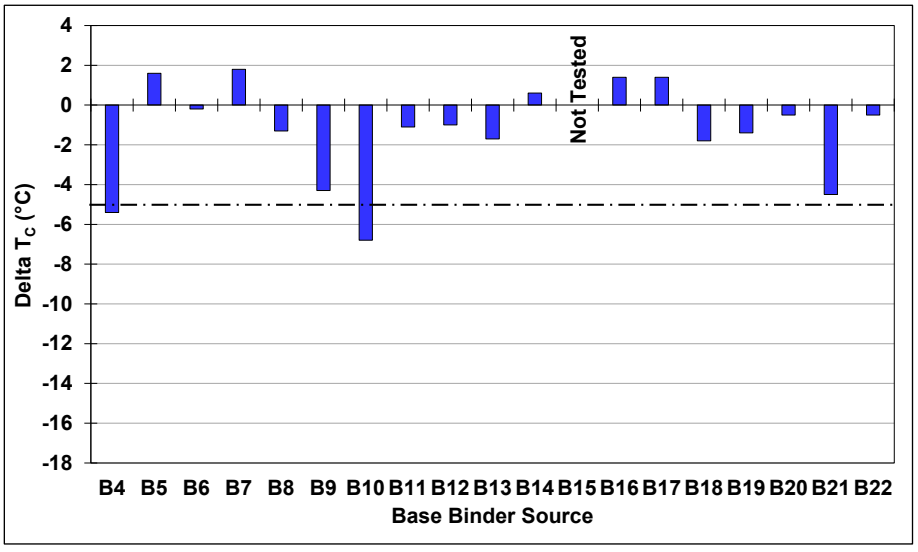

Figure 8.11: Delta T_C of base binders.

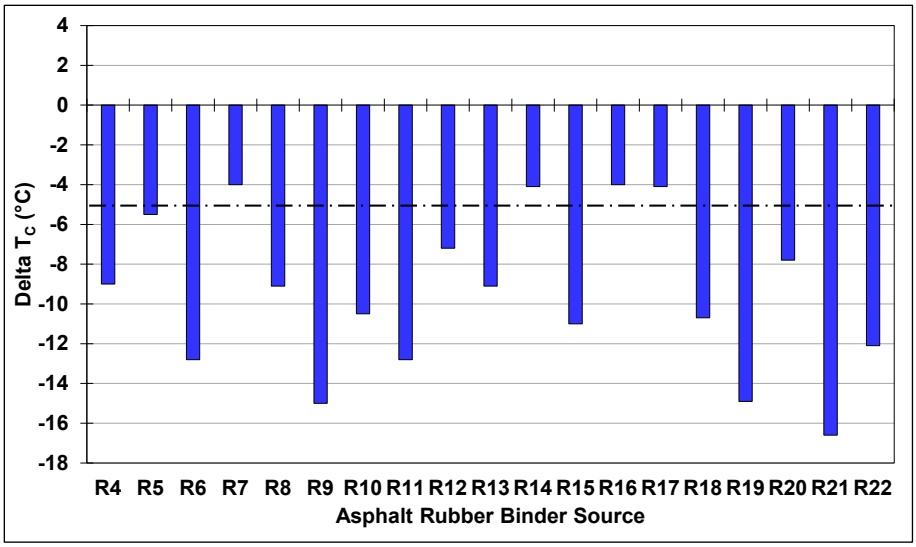

Figure 8.12: Delta T_C of asphalt rubber binders.

9. MIX TESTING

9.1 Introduction

This chapter covers preliminary mix testing to develop a database of stiffness, permanent deformation, and cracking test results against which binder test results can be compared. These comparisons will be used in Phase 3 of the study to determine whether the performance grades (PGs) determined from the binder testing are representative of actual expected performance or whether they need to be adjusted accordingly.

9.2 Specimen Air Void Contents

Air-void contents (based on saturated surface-dry bulk specific gravity) for the specimens compacted in a Superpave gyratory compactor (cylindrical AMPT and SCB specimens) and with a rolling wheel compactor (beam specimens) are listed in Table A.1, Table A.2, and Table A.3, respectively in Appendix A. Averages and standard deviations for the AMPT, SCB, and beam specimens are shown in Figure 9.1. Whiskers on the data show the lowest and highest air void contents of the replicate specimens.

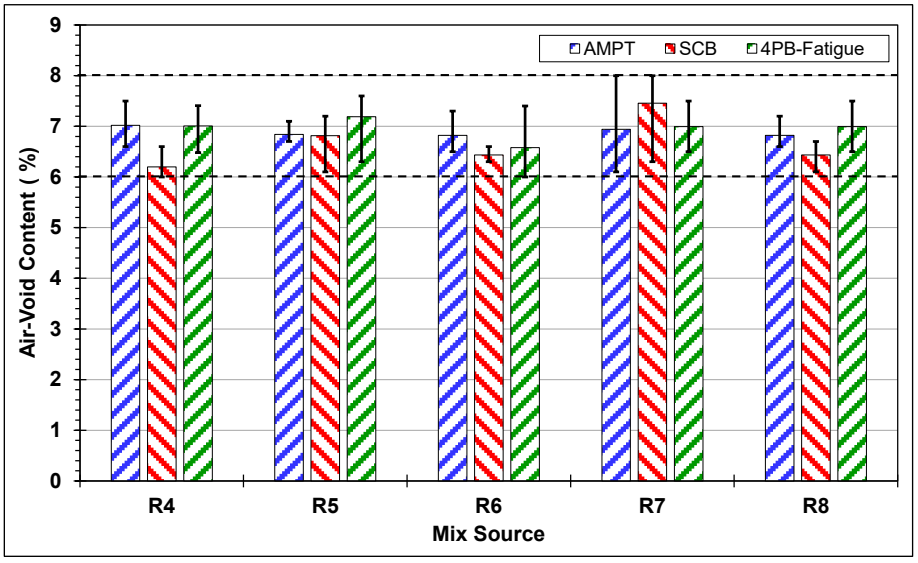

Figure 9.1: Specimen air-void contents.

All specimens were within the target limits (7.0±1.0%), indicating that consistent compaction was achieved. However, some specimens had air-void contents close to the limits. Any potential influences of air-void content were considered during analysis of the results.

9.3 Mix Stiffness: AMPT Dynamic Modulus

Dynamic modulus test results are listed in Table A.4 and Table A.5 in Appendix A. Table 9.1 lists the function parameters (Equation 3.1) used in the Arrhenius shift factor equation (Equation 3.3) to determine the master curves for the evaluated mixes, which are shown in Figure 9.2.

Table 9.1: Dynamic Modulus Master Curve Parameters

Mix	Master Curve Parameters			
	δ(MPa)	α	β	γ
R4	-2.00978	6.54885	-1.62476	-0.23620
R5	-2.98884	7.38279	-1.89871	-0.35582
R6	+0.37438	3.91528	-1.32789	-0.33064
R7	-1.30564	5.67048	-1.54182	-0.39657
R8	+0.38196	3.92519	-1.51476	-0.36474

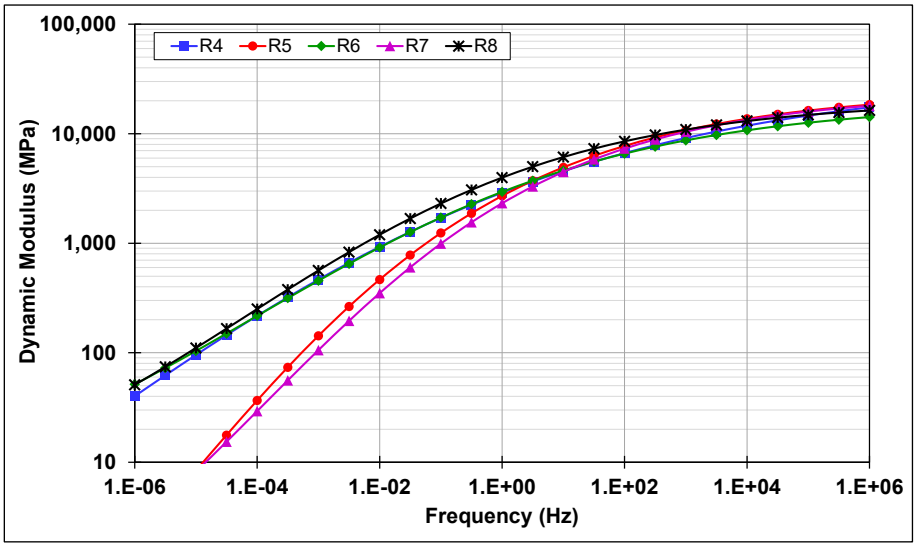

Figure 9.2: Dynamic shear modulus master curves.

The stiffness results for the R4, R6, and R8 mixes were similar to each other and were consistent with those measured on typical RHMA-G mixes. The R5 and R7 mixes had similar stiffnesses to the other three mixes at the medium to higher frequencies, but notably lower stiffnesses at the medium to lower frequencies. This implies that the R5 and R7 mixes could be susceptible to rutting at higher temperatures.

9.4 Mix Stiffness: Flexural Modulus

Table 9.2 lists the sigmoidal function parameters (Equation 3.3) to determine the master curves for the evaluated mixes.

Table 9.2: Flexural Modulus Master Curve Parameters

Mix	Master Curve Parameters			
	δ(kPa)	α	β	γ
R4	2.30103	1.62031	0.37267	0.69252
R5	2.30103	1.63938	0.40434	0.95376
R6	2.30103	1.57744	0.12049	0.70529
R7	2.30103	1.53835	0.99232	1.06779
R8	2.30103	1.60423	0.00868	0.69196

Flexural modulus test results are listed in Table A.6 through Table A.8 in Appendix A. Figure 9.3 shows the flexural modulus master curves for the different RHMA-G mixes. Results for four of the mixes were similar to each other and were consistent with those measured on typical RHMA-G mixes. The R7 mix had marginally lower stiffnesses in the mid to lower frequencies indicating the potential for mix sensitivity at intermediate temperatures.

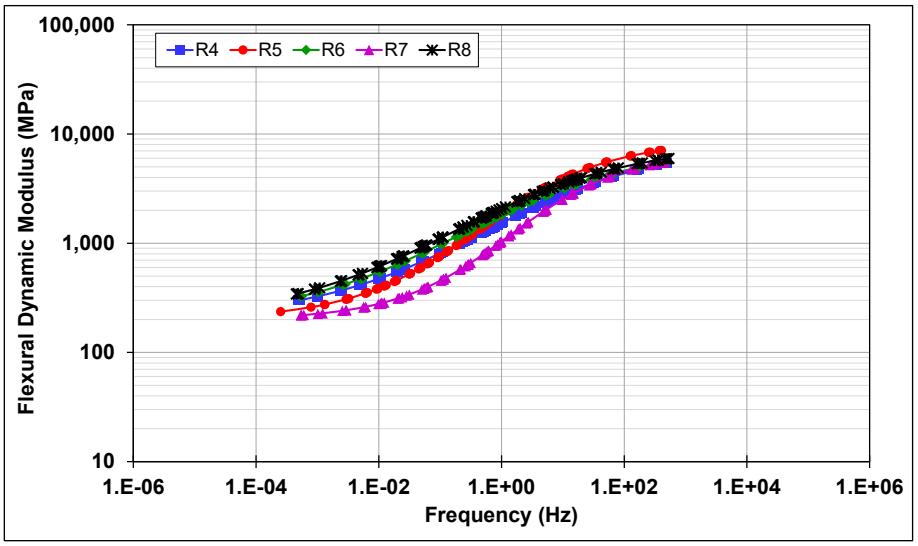

Figure 9.3: Flexural dynamic modulus master curves.

9.5 Rutting Performance: Unconfined Repeated Load Triaxial

Flow number test results are listed in Table A.7 in Appendix A. Figure 9.4 shows the relationship between cumulative permanent axial strains and the number of load cycles for all mixes evaluated. A review of the data led to the following observations:

- The repeatability of the test results met the single-operator precision specified in AASHTO T 378 for all mixes, but it showed some variability between the replicate specimens in each mix, which is consistent with repeated load testing.
- The evolution rate of cumulative permanent deformation with increasing loading cycles was initially similar for all mixes, but thereafter the R5 and R7 mixes appeared to be more

susceptible to rutting than the other three mixes, consistent with the dynamic modulus results.

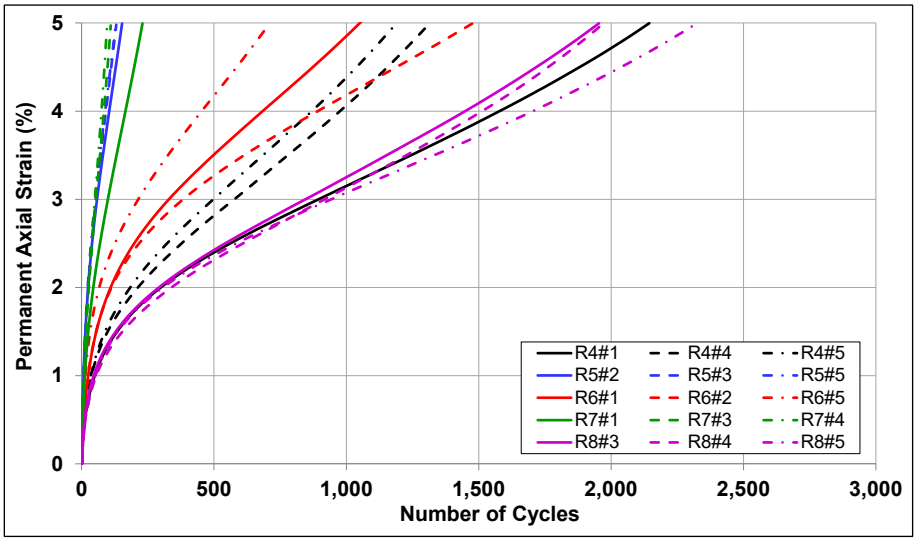

Figure 9.4: Cumulative permanent axial strain versus number of cycles (52°C).

Figure 9.5 shows the flow number values for the different mixes. Error bars on the data show the lowest and highest flow numbers of the three replicates in each mix. The R5 and R7 mixes had the lowest average flow numbers, considerably lower than the other three mixes and showing the same trends as the high-temperature PG results. Although there was considerable variability between the results of the three replicates in each mix, this ranking of average flow numbers was consistent with the true high-temperature grade results of the binders.

Figure 9.6 shows the number of cycles to 1%, 3%, and 5% permanent axial strain (note that the y-axis is on a log scale). Trends observed for the number of cycles to 3% and 5% permanent axial strain were similar to those observed for the flow number results. At lower strain levels, the difference in the number of cycles required to reach the selected strain level was much closer between the mixes (also clearly shown in Figure 9.4), with the rankings of some of the mixes different from those for the higher strain levels.

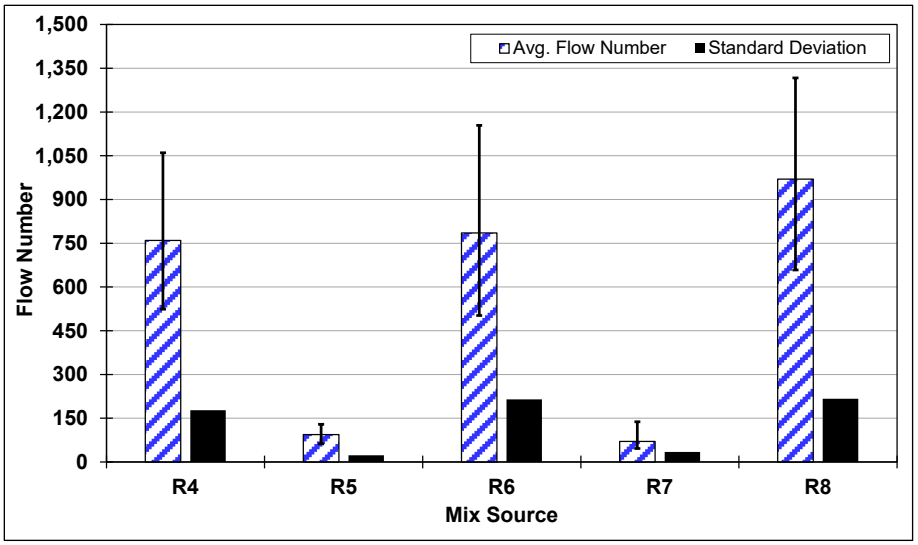

Figure 9.5: Average flow number (52°C).

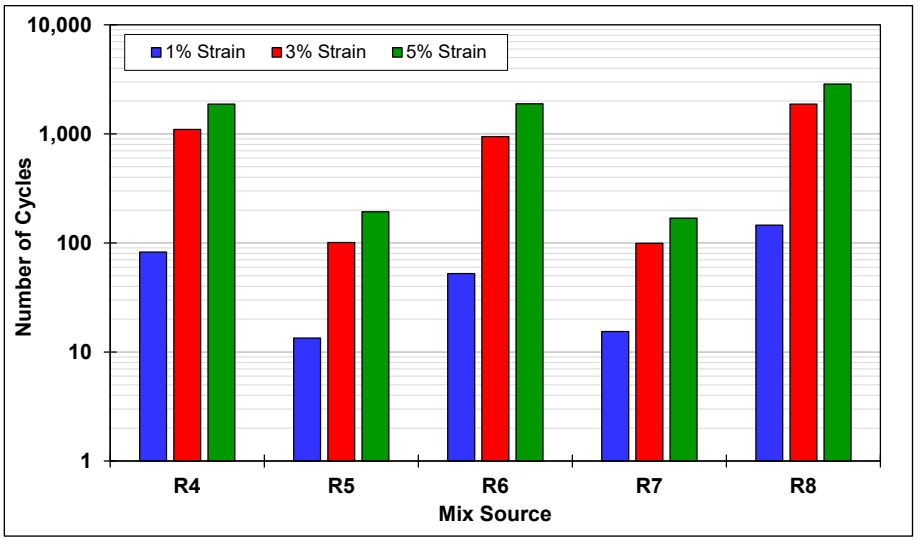

Figure 9.6: Number of cycles to 1%, 3%, and 5% permanent axial strain.

9.6 Cracking Performance: Four-Point Bending Beam Fatigue

Plots of the fatigue models for each mix are shown in Figure 9.7. The models were considered to be generally appropriate based on the reasonably high R-squared values of the model fitting and the repeatability of the test results at each strain level. The R5 mix beams had less variability than the other four mixes at low and high strains. Calculated fatigue lives at 200, 300, 400, and 600 µstrain of the five mixes are compared in Figure 9.8. Note that no mixes were tested at 200 µstrain and that fatigue life at this strain level was extrapolated.

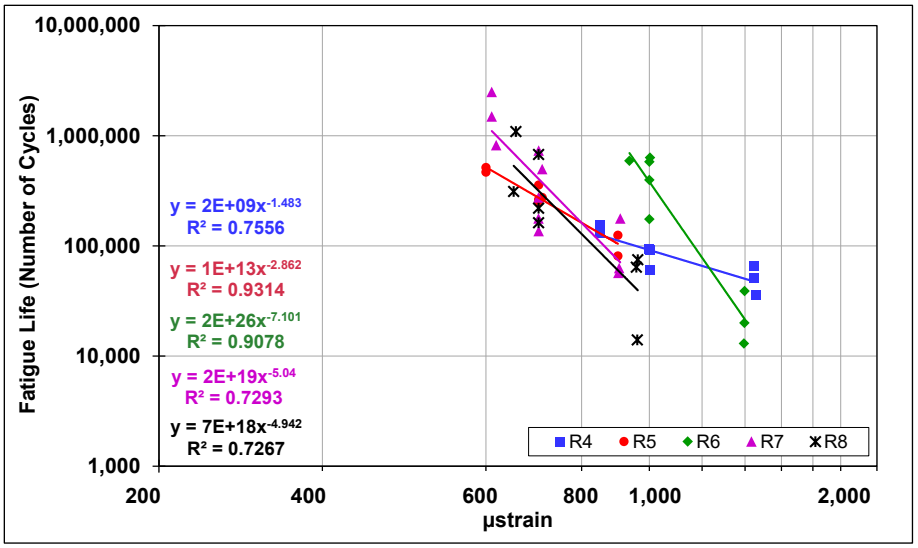

Figure 9.7: Fatigue regression models.

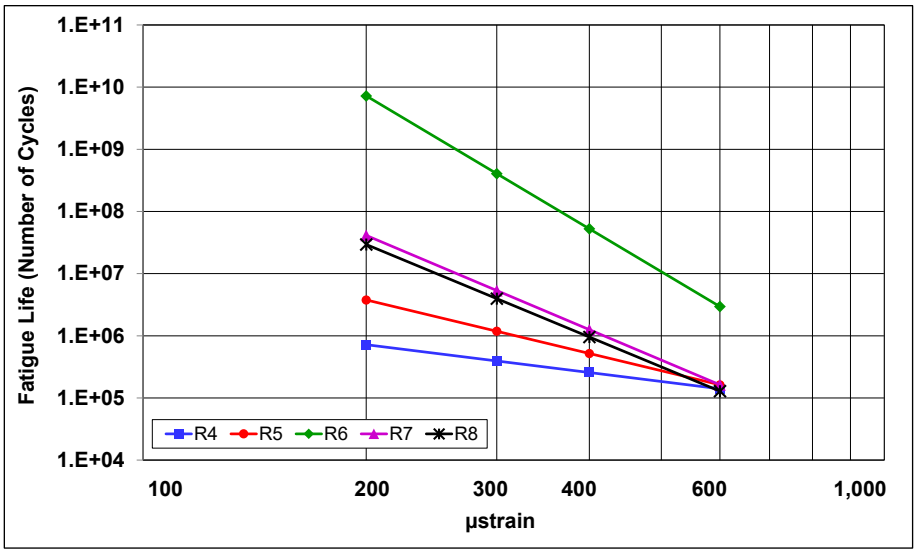

Figure 9.8: Calculated fatigue life at 200, 300, 400, and 600 µstrain.

A review of the data led to the following observations:

- Fatigue life decreased with increasing strain level, as expected.
- The R6 mix indicated notably better fatigue performance than the other mixes at all strains. This mix also indicated similar fatigue performance to other RHMA-G mixes previously tested at the UCPRC. The other four mixes had lower fatigue performance than the R6 mix and compared to mixes tested in other recent studies.
- There was considerable variation in fatigue performance among the mixes at low strain levels, with less variability with increasing strain. Fatigue life at 600 µstrain was essentially the same for all mixes except the R6 mix.

- The results were not consistent with the flexural modulus test results, the intermediate-temperature binder test results, or the Delta T_C results. However, if the R6 binder is excluded from the rankings, the fatigue life and binder m-value rankings were the same for the other four binders.

9.7 Cracking Performance: Semicircular Bend

Semicircular bend test results are listed in Table A.10 in Appendix A. Average fracture energies and flexibility indices for the five mixes are shown in Figure 9.9 and Figure 9.10. Error bars on the data show the lowest and highest fracture energies and flexibility indices for the replicates tested.

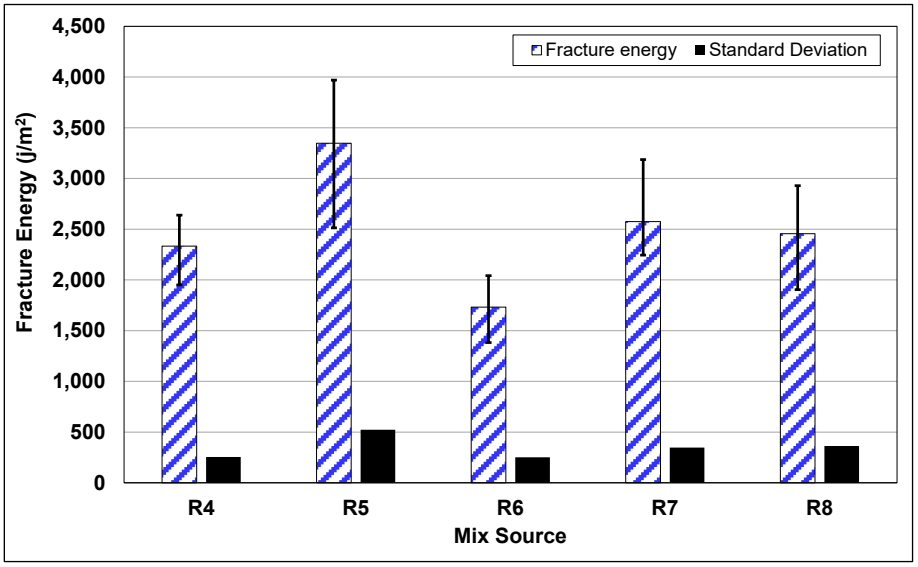

Figure 9.9: Semicircular bend fracture energy.

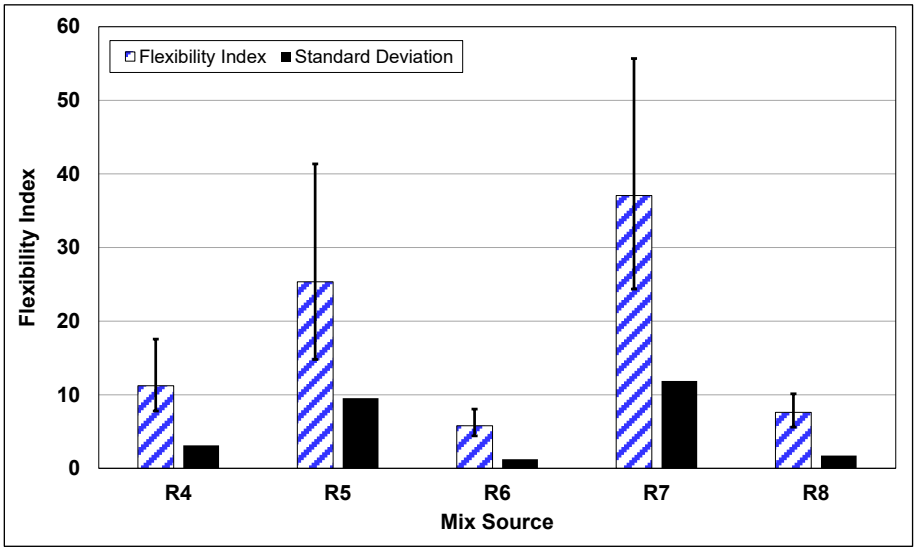

Figure 9.10: Semicircular bend flexibility index.

A review of the data led to the following observations:

- There was notable variability between mixes and between replicate specimens within each mix for both the fracture energy and flexibility index.
- The R6 mix had the lowest fracture energy and flexibility index but the highest fatigue life. Rankings of the three sets of cracking test results (calculated fatigue life, fracture energy, and flexibility index) are provided in Table 9.3 and do not indicate consistency across all mixes, although two mixes had similar rankings for the three tests (i.e., R7 and R8).

Table 9.3: Ranking of Cracking Test Results

Rank	Ranking		
	Fatigue Life	Fracture Energy	Flexibility Index
1	R6	R5	R7
2	R7	R7	R5
3	R8	R8	R4
4	R5	R4	R8
5	R4	R6	R6

- The flexibility index of the R7 mix was notably higher than the other mixes, indicating that this mix would likely have better cracking resistance than the others. However, this mix also had the highest variability between replicate specimens.
- Flexibility index results showed the same trends and rankings to the Delta T_C results (i.e., the R5 and R7 binders had the highest flexibility indices and lowest Delta T_C values).
- Flexibility index results showed the same trends and similar rankings to the non-recoverable creep compliance results.

9.8 Discussion

A comparison of binder and mix test results did not show any consistent trends across all five binders (Table 9.4). However, the following trends between some results were observed:

- Rutting test result rankings (flow number and cycles to 5% permanent axial strain) were consistent with the binder high-temperature PG result rankings.
- Flexibility index rankings (highest to lowest) were consistent with Delta T_C (lowest to highest) and non-recoverable creep compliance (highest to lowest). Flexibility index results (highest to lowest) also corresponded with mix rutting results (lowest to highest) as expected (i.e., cracking and rutting results are opposite).
- Beam fatigue rankings did not match any binder testing rankings, however, if the R6 binder and mix results are excluded, the mix fatigue life and binder m-value rankings are the same for the other four binders.

Table 9.4: Rankings of Select Binder and Mix Testing Results

Rank	High Cont. Grade	Int. Cont. Grade	m-Value at -12°C	Delta T_C	Jnr at 3.2 kPa	Flow Number	Cycles to 5% PAS	Fatigue Life	Fracture Energy	Flexibility Index
1	R6	R5	R7	R7	R7	R8	R8	R6	R5	R7
2	R4	R8	R8	R5	R5	R6	R6	R7	R7	R5
3	R8	R7	R6	R8	R8	R4	R4	R8	R8	R4
4	R5	R6	R5	R4	R6	R5	R5	R5	R4	R8
5	R7	R4	R4	R6	R4	R7	R7	R4	R6	R6

10. DETERMINATION OF RUBBER CONTENT IN ASPHALT RUBBER BINDERS

10.1 Introduction

This chapter covers a preliminary study to explore ways to determine the rubber content in asphalt rubber binder and potentially in recycled asphalt pavement (RAP) materials. Limited exploratory testing was initiated using Fourier-transform infrared (FTIR) spectroscopy.

10.2 Methodology

One base binder (BUT-162 [B4]) with eight different crumb rubber modifier (CRM) contents were tested in unaged and PAV-aged condition. Extender oil alone and base binder modified with extender oil only were also tested to determine the potential influence of extender oil on the results. A known styrene-butadiene rubber (SBR, 75% butadiene and 25% styrene) signature was used to identify the presence of CRM. The area under the curve in the SBR zone (965.1 cm^{-1} to 909.9 cm^{-1} [Figure 10.1]) was calculated to determine the quantity of rubber in the binder *(8,9)*. The area calculated under the curve of the SBR signatures of the base binder and base binder with modifier was subtracted from those of the asphalt rubber binders to focus the results on the CRM only.

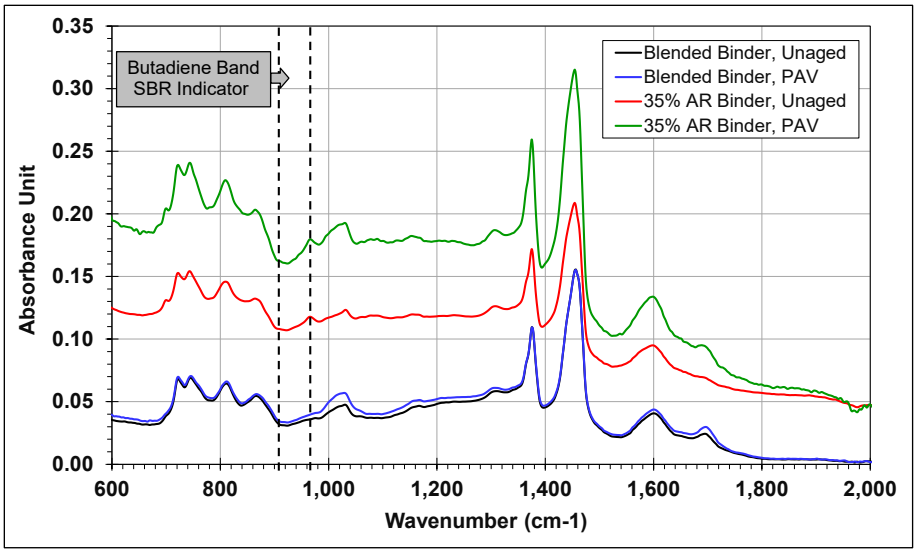

Figure 10.1: Typical wave form of FTIR data and butadiene band location.

The following were considered when identifying SBR as a baseline signature:

- SBR is a chemical compound present in synthetic rubber, it is a common blend elastomer used in approximately 40% of all synthetic rubber worldwide *(8)*, and it is widely used in tires.
- Since synthetic rubber and asphalt are both derived from crude oil, an SBR signature may be present in some unmodified binders and in petroleum-based binder modifiers.

Figure 10.2 shows the area under-the-curve calculations of the SBR signatures of the seven CRM dosages (2.5% to 35% by weight of the binder) in both unaged and PAV-aged conditions. In both conditions, the SBR signature values increased with increasing rubber dosage. Values for the PAV-aged binders were notably higher than those for the unaged binders, indicating that aging will influence values over time. These results indicate that FTIR is a potentially valid method for quantifying rubber content in rubber-modified binders.

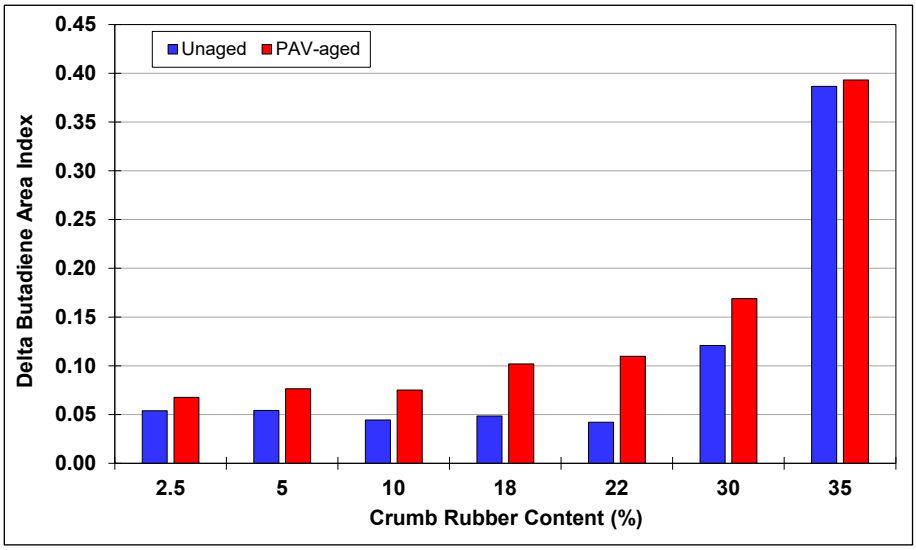

Figure 10.2: Area under the curve calculation for the butadiene signature of AR binders.

Mastics from an RHMA mix and from an HMA mix containing rubberized RAP were also tested. However, the results were inconclusive, which was attributed primarily to the size of the sample being larger than the measurement zone on the equipment used and to the potential influence of the fine aggregate in the mastic.

11. CONCLUSIONS AND RECOMMENDATIONS

11.1 Introduction

The work discussed in this interim report is part of a larger study, funded by the California Department of Transportation (Caltrans). The objective of the study focuses on developing and recommending testing procedures and criteria for performance-based specifications of asphalt rubber binders used in gap- and open-graded mixes using current Superpave performance grading equipment. Work in this phase covered the testing of 19 plant-produced binders and five of the gap-graded rubberized hot mix asphalt mixes produced with them.

11.2 Testing Summary

11.2.1 Rheology Testing

Rheology testing to determine the high-, intermediate-, and low-temperature performance grades and multiple stress creep recovery (MSCR) using the procedures developed in Phase 2 of the study, was undertaken to test the procedures. The following important observations from the results were made:

- Testing in this phase of the study provided results that were consistent with those obtained during preliminary testing in Phase 2e of the larger study.
- Although the low-temperature performance grades appeared to be reasonable, the high-temperature grades appeared to be unrealistically high, while the intermediate-temperature grades appeared to be potentially lower than anticipated, when compared to the base binders. Fourteen of the binders tested with concentric cylinder geometry and 13 tested with parallel plate geometry had performance grades higher than the maximum grade of 82°C listed in the AASHTO M 320 standard. Grades higher than 82 are considered to be unrealistically high and probably not a true indication of likely high-temperature performance (i.e., rut resistance under heavy loads on hot days).
- A comparison of the concentric cylinder and parallel plate (3 mm gap) geometries indicated that the results between the two geometries are different, with differences likely to be higher than the precision and bias of the individual procedures. Precision and bias statements for these procedures had not been developed at the time of preparing this report. These results indicate that the two geometries cannot be used interchangeably.
- No consistent trends in results were observed between any of the parameters tested.
- Observations in Phase 2e and during this phase of the study indicated that incompletely digested rubber particles appeared to have a dominant influence on results and caused

variability between results, regardless of the testing geometry used. Considering these incompletely digested particles as part of a homogenous binder may therefore not be appropriate when determining performance grades. This observation has prompted further study (Phase 3) to investigate the extent to which these incompletely digested particles might affect performance grading results along with testing procedures to overcome the problems. The study will focus on removal of larger incompletely digested particles from the binder by sieving or centrifuging and then testing the binders following standard performance grading procedures using parallel plate geometry with either 1 mm or 2 mm gaps. Results after removal of particles larger than 250, 500, and 850 µm will be compared with unprocessed binders. The 19 asphalt rubber binders tested in this phase of the study are being retested in Phase 3 to assess the removal of larger incompletely digested rubber particles on performance grades.

11.2.2 Mix Testing

Mix testing was undertaken to assess rutting and cracking performance in relation to binder performance grading to determine whether the rheology testing approaches provide properties that are representative of likely field performance. A comparison of binder and mix test results did not show any consistent trends. However, the following trends between some results were observed:

- Rutting test result rankings (flow number and cycles to 5% permanent axial strain) were consistent with the binder high-temperature performance result rankings.
- Flexibility index rankings (highest to lowest) were consistent with Delta T_C (lowest to highest) and non-recoverable creep compliance (highest to lowest). Flexibility index results (highest to lowest) also corresponded with mix rutting results (lowest to highest) as expected (i.e., cracking and rutting results are opposite).
- Beam fatigue rankings did not match any binder testing rankings. However, excluding the binder and mix results from one "outlier," the mix fatigue life and binder m-value rankings were the same for the other four binders/mixes.

11.2.3 Rubber Content Determination

Limited exploratory testing was conducted to assess the use of Fourier-transform infrared (FTIR) spectroscopy to determine rubber content in rubber-modified binders. One base binder with eight different crumb rubber modifier (CRM) contents, ranging from 2.5% to 35% by weight of the base binder, were tested in unaged and PAV-aged condition. Extender oil alone and base binder modified with extender oil only were also tested to determine the potential influence of

extender oil on the results. A known styrene-butadiene rubber (SBR, 75% butadiene and 25% styrene) signature was used to identify the presence of CRM.

In both aging conditions, the SBR signature values increased with increasing rubber dosage. Values for the PAV-aged binders were notably higher than those for the unaged binders, indicating that aging will influence values over time. The results indicate that FTIR is a potentially valid method for quantifying rubber content in rubber-modified binders.

11.3 Conclusions

Incompletely digested rubber particles—which have different sensitivities to temperature, aging, and applied stress and strain than the base asphalt binder—appear to dominate the binder rheology test results, leading to what appears to be unrealistic high- and intermediate-temperature performance grades. Work is continuing in Phase 3 of this study to adjust testing procedures to account for the influence that these incompletely digested particles have on results.

The proposed modifications to short- and long-term aging procedures (i.e., rolling thin-film oven and pressure aging vessel) and to the bending beam rheometer specimen preparation procedures developed in Phase 2 are considered to be more aligned with the original intent of the tests and will likely reduce the variability between replicate specimens during testing.

11.4 Recommendations

No recommendations for implementation are warranted at this stage of the study.

REFERENCES

1. California Integrated Waste Management Board. 2005. *California Waste Tire Generation, Markets, and Disposal: 2003 Staff Report*. Sacramento, CA: California Integrated Waste Management Board.
2. Federal Highway Administration. 2006. *Status of the Nation's Highways, Bridges, and Transit: Conditions and Performance*. Washington, DC: Federal Highway Administration.
3. Jones, D., Rizvi, H., Liang, Y., Hung, S., Buscheck, J., Alavi, Z. and Hofko, B. 2017. *Development of Performance-Based Specifications for Asphalt Rubber Binder: Interim Report on Phase 1 and Phase 2 Testing* (Research Report: UCPRC-RR-2017-01). Davis and Berkeley, CA: University of California Pavement Research Center. doi.org/10.7922/G2T72FQQ.
4. Harvey, J. and Bejarano, M. 2001. "Performance of Two Overlay Strategies under Heavy Vehicle Simulator Trafficking." *Transportation Research Record* 1769: 123–133.
5. Jones, D., Tsai, B.W., Ullidtz, P., Wu, R., Harvey, J. and Monismith, C. 2008. *Reflective Cracking Study: Second-Level Analysis Report* (Research Report: UCPRC-RR-2007-09). Davis and Berkeley, CA: University of California Pavement Research Center. escholarship.org /uc/item/1rc624m9.
6. Jones, D. and Harvey, J. 2009. "Accelerated Pavement Testing Experiment to Assess the Use of Modified Binders to Limit Reflective Cracking in Thin Asphalt Concrete Overlays." In *Transportation Research Circular E-C139: Use of Accelerated Pavement Testing to Evaluate Maintenance and Pavement Preservation Treatments*, 11–31. Washington, DC: Transportation Research Board. onlinepubs.trb.org/onlinepubs/circulars/ec139.pdf.
7. Jiao, L., Harvey, J., Wu, R., Elkashef, M., Jones, D. and Liang, Y. 2023. Preliminary Study on Developing a Surrogate Performance-Related Test for Fatigue Cracking of Asphalt Pavements (Research Report UCPRC-RR-2021-02). Davis and Berkeley, CA: University of California Pavement Research Center. escholarship.org/uc/item/52d1d1q5.
8. Asphalt Institute. 2019. *Use of the Delta TC Parameter to Characterize Asphalt Binder Behavior* (IS-240). Lexington KY: Asphalt Institute. asphaltinstitute.org/download/1305/.
9. Azevedo, J.B., Murakami, L.M.S., Ferriera, A.C., Diniz, M.F., Silva, L.M. and Dutra, R.L. 2018. "Quantification by FT-IR (UATR/NIRA) of NBR/SBR Blends." *Polímeros* 28, no. 5.
10. Araujo, E.M., Siqueira, D.D., Morais, D.D.S., Filho, E.A.S., Filho, E.A. and Fook, M.V.L. 2019. "Incorporation of a Recycled Rubber Compound from the Shoe Industry in Polystyrene: Effect of SBS Compatibilizer Content." *Journal of Elastomers and Plastics* 52, no. 1: 1–26.

APPENDIX A: MIX TEST RESULTS

Mix test results are summarized in the following tables:

- Table A.1: Air-Void Contents of Gyratory-Compacted AMPT Specimens
- Table A.2: Air-Void Contents of Gyratory-Compacted SCB Specimens
- Table A.3: Air-Void Contents of Rolling Wheel-Compacted Beam Specimens
- Table A.4: Dynamic Modulus Test Results
- Table A.5: Phase Angle Test Results for Dynamic Modulus
- Table A.6: Flexural Modulus Test Results at 10°C
- Table A.7: Flexural Modulus Test Results at 20°C
- Table A.8: Flexural Modulus Test Results at 30°C
- Table A.9: Repeated Load Triaxial Test Results
- Table A.10: Semicircular Bend Test Results

Table A.1: Air Void Contents of Gyratory-Compacted AMPT Specimens

Specimen Number	Air-Void Content (%)				
	R4	R5	R6	R7	R8
1	6.8	6.7	7.3	8.0	6.7
2	7.2	6.7	6.6	6.1	6.6
3	7.0	7.1	6.5	6.4	7.2
4	7.5	6.9	7.1	6.6	6.9
5	6.6	6.8	6.6	7.6	6.7
Mean	7.0	6.8	6.8	6.9	6.8
Std. Deviation	0.31	0.15	0.32	0.73	0.21
Std. Error	0.14	0.07	0.14	0.33	0.10

Table A.2: Air Void Contents of Gyratory-Compacted SCB Specimens

Specimen Number	Air-Void Content (%)				
	R4	R5	R6	R7	R8
1	6.6	7.0	6.4	8	6.7
2	6.6	7.0	6.4	8	6.7
3	6.0	6.6	6.3	8	6.1
4	6.0	6.6	6.3	6.3	6.3
5	6.0	7.2	6.6	7.8	6.1
6	6.0	7.2	6.6	7.8	6.7
Mean	6.2	6.9	6.4	7.7	6.4
Std. Deviation	0.28	0.25	0.12	0.61	0.27
Std. Error	0.11	0.09	0.05	0.23	0.11

Table A.3: Air Void Contents of Rolling Wheel Compacted Beam Specimens

Specimen Number	Air-Void Content (%)				
	R4	R5	R6	R7	R8
1	6.8	7.2	6.0	6.8	6.6
2	7.4	6.7	7.4	6.9	7.3
3	7.0	7.6	6.4	7.3	6.6
4	6.9	6.3	6.8	6.8	6.6
5	7.2	7.5	6.4	7.1	7.0
6	6.7	7.4	6.2	6.8	7.3
7	7.2	7.6	6.3	6.7	7.4
8	7.1	7.3	6.3	7.2	6.5
9	6.7	7.1	6.7	7.0	6.9
10	7.4	7.4	7.0	7.3	7.5
11	7.4	7.0	7.0	7.0	6.7
12	7.1	7.2	6.5	7.2	7.5
Mean	7.1	7.2	6.6	7.0	7.0
Std. Deviation	0.23	0.37	0.38	0.21	0.38
Std. Error	0.06	0.11	0.11	0.05	0.10

Table A.4: Dynamic Modulus Test Results

Mix	Specimen ID	Dynamic Modulus (MPa)								
		Temperature (°C)								
		4			20			45		
		Frequency (Hz)								
		0.1	1	10	0.1	1	10	0.1	1	10
R4	21	5,257	7,261	9,469	1,758	2,906	4,544	215	437	911
	25	3,821	5,388	7,251	1,472	2,472	3,881	214	457	948
	28	4,767	6,732	8,987	1,714	2,892	4,583	283	600	1,207
	32	4,175	5,848	7,850	1,546	2,577	4,057	253	503	1,009
	36	5,095	7,259	9,784	1,845	3,148	5,005	261	561	1,182
Mean		4,623	6,498	8,668	1,667	2,799	4,414	245	512	1,051
Std. Dev		546	758	966	138	244	402	27	61	121
Std. Err		315	437	558	80	141	232	16	35	70
R5	04	5,376	7,605	9,843	1,320	2,730	4,780	75	269	840
	08	4,561	6,816	9,152	952	2,113	3,965	87	320	952
	12	4,865	6,995	9,100	1,097	2,341	4,247	49	206	703
	17	5,417	7,866	10,344	1,250	2,688	4,928	90	312	931
	18	4,665	6,719	8,868	1,093	2,286	4,087	106	371	1,050
Mean		4,977	7,200	9,461	1,142	2,432	4,401	81	296	895
Std. Dev		357	454	548	130	239	383	19	55	117
Std. Err		206	262	317	75	138	221	11	32	68
R6	06	4,139	5,598	7,172	1,465	2,462	3,808	269	594	1,206
	07	4,670	6,376	8,294	1,802	2,946	4,516	383	827	1,617
	13	4,910	6,617	8,471	2,192	3,539	5,358	525	1,046	1,949
	16	4,469	6,161	7,992	1,492	2,554	4,055	270	589	1,210
	17	3,716	5,242	6,967	1,373	2,390	3,878	257	568	1,150
Mean		4,381	5,999	7,779	1,665	2,778	4,323	341	725	1,426
Std. Dev		418	507	603	301	426	573	103	186	310
Std. Err		241	293	348	174	246	331	59	108	179
R7	07	6,300	8,843	11,500	1,629	3,175	5,365	130	361	985
	16	4,460	6,754	9,247	932	2,133	4,038	42	138	472
	25	4,066	6,516	9,359	928	2,180	4,245	42	158	538
	30	3,438	5,542	8,017	561	1,433	2,975	29	122	454
Mean		4,566	6,914	9,531	1,013	2,230	4,155	61	195	612
Std. Dev		1,065	1,203	1,253	387	620	848	40	97	217
Std. Err		615	695	723	223	358	490	23	56	125
R8	11	6,559	8,559	10,582	2,261	3,730	5,650	241	594	1,349
	19	5,828	7,733	9,711	2,060	3,463	5,290	279	681	1,470
	22	6,231	8,190	10,222	2,409	3,865	5,752	346	799	1,645
	23	6,577	8,596	10,713	2,433	3,891	5,785	394	869	1,749
	27	6,351	8,331	10,353	2,211	3,638	5,518	314	752	1,607
Mean		6,309	8,282	10,316	2,275	3,717	5,599	315	739	1,564
Std. Dev		273	312	348	137	157	180	53	95	140
Std. Err		158	180	201	79	91	104	30	55	81

Table A.5: Phase Angle Test Results for Dynamic Modulus

Mix	Specimen ID	Phase Angle (δ) (Degrees)								
		Temperature (°C)								
		4			20			45		
		Frequency (Hz)								
		0.1	1	10	0.1	1	10	0.1	1	10
R4	21	14.4	11.9	9.9	23.1	20.4	17.3	30.5	30.9	30.1
	25	15.7	13.1	23.3	20.2	17.5	30.1	30.9	30.6	29.0
	28	16.4	13.3	10.9	24.4	21.4	18.4	30.9	30.8	29.4
	32	16.4	13.6	11.3	23.8	21.0	18.2	29.3	29.8	29.0
	36	16.9	13.8	11.2	24.9	21.7	18.5	31.0	31.2	30.0
Mean		16.0	13.1	13.3	23.3	20.4	20.5	30.5	30.7	29.5
Std. Dev		0.9	0.7	5.0	1.7	1.5	4.8	0.6	0.5	0.5
Std. Err		0.5	0.4	2.9	1.0	0.9	2.8	0.4	0.3	0.3
R5	04	16.9	12.2	9.1	34.6	27.1	20.0	41.4	41.2	40.0
	08	19.5	14.0	10.3	37.8	30.3	22.5	40.5	39.9	38.0
	12	18.0	12.9	9.5	35.5	28.6	21.4	45.2	44.9	42.6
	17	18.4	13.0	9.5	35.9	28.6	21.5	40.6	41.9	39.3
	18	18.0	13.0	9.6	35.0	28.1	21.2	39.0	39.0	36.5
Mean		18.2	13.0	9.6	35.8	28.5	21.3	41.3	41.4	39.3
Std. Dev		0.8	0.6	0.4	1.1	1.0	0.8	2.1	2.0	2.0
Std. Err		0.5	0.3	0.2	0.6	0.6	0.5	1.2	1.2	1.2
R6	06	14.3	11.4	9.2	24.4	20.4	16.6	33.1	31.6	28.5
	07	15.0	12.1	9.9	24.7	20.5	16.7	33.1	30.6	27.1
	13	13.9	11.2	9.2	23.2	19.8	16.5	30.1	28.5	26.2
	16	15.5	12.2	9.9	25.3	21.7	17.9	32.9	31.7	29.1
	17	16.4	13.1	10.6	25.9	22.4	18.9	31.6	30.3	28.4
Mean		15.0	12.0	9.7	24.7	21.0	17.3	32.2	30.6	27.9
Std. Dev		0.9	0.7	0.5	0.9	1.0	0.9	1.2	1.2	1.1
Std. Err		0.5	0.4	0.3	0.5	0.5	0.5	0.7	0.7	0.6
R7	07	16.2	12.2	9.3	31.3	25.2	19.5	38.0	40.1	38.4
	16	20.6	15.1	11.2	36.6	30.3	23.4	41.3	43.0	43.0
	25	23.3	17.0	12.4	38.3	31.0	23.6	45.6	44.2	43.1
	30	23.8	17.5	12.7	42.0	35.1	26.9	48.2	46.4	45.3
Mean		21.0	15.5	11.4	37.1	30.4	23.3	43.3	43.4	42.4
Std. Dev		3.0	2.1	1.3	3.9	3.5	2.6	3.9	2.3	2.5
Std. Err		1.7	1.2	0.8	2.2	2.0	1.5	2.3	1.3	1.5
R8	11	13.1	10.5	8.4	24.8	20.1	15.9	36.4	35.2	31.7
	19	13.8	10.7	8.5	25.3	20.4	16.1	35.2	33.4	29.9
	22	13.0	10.3	8.3	23.3	18.9	15.1	31.9	30.4	27.7
	23	12.8	10.1	8.1	23.3	19.0	15.0	32.6	31.5	28.3
	27	13.0	10.1	8.1	24.3	19.7	15.6	35.0	33.3	29.5
Mean		13.1	10.3	8.3	24.2	19.6	15.5	34.2	32.7	29.4
Std. Dev		0.3	0.2	0.2	0.8	0.6	0.4	1.7	1.7	1.4
Std. Err		0.2	0.1	0.1	0.5	0.3	0.2	1.0	1.0	0.8

Table A.6: Flexural Modulus Test Results at 10°C

Mix	Specimen ID	Flexural Modulus (E*) (MPa) at 10°C										
		Frequency (Hz)										
		0.01	0.02	0.05	0.1	0.2	0.5	1	2	5	10	15
R4	1	1,102	1,293	1,584	1,877	2,270	2,775	3,209	3,653	4,309	4,829	5,105
	2	1,230	1,447	1,803	2,123	2,625	3,203	3,679	4,200	4,936	5,515	5,832
	3	1,340	1,564	1,898	2,287	2,665	3,198	3,620	4,138	4,790	5,338	5,615
Mean		1,224	1,435	1,762	2,096	2,520	3,058	3,502	3,997	4,678	5,227	5,518
Std. Dev		97	111	131	169	177	201	209	245	268	291	305
Std. Err		56	64	76	97	102	116	121	141	155	168	176
R5	1	1,020	1,318	1,812	2,267	2,888	3,656	4,272	4,927	5,795	6,413	6,791
	2	1,324	1,674	2,255	2,787	3,524	4,377	5,070	5,769	6,678	7,358	7,693
	3	1,162	1,523	2,063	2,553	3,252	4,061	4,689	5,365	6,231	6,791	7,164
Mean		1,169	1,505	2,044	2,535	3,221	4,031	4,677	5,354	6,235	6,854	7,216
Std. Dev		124	146	182	213	261	295	326	344	360	388	370
Std. Err		72	84	105	123	151	170	188	199	208	224	213
R6	1	1,384	1,614	1,949	2,236	2,719	3,227	3,623	4,088	4,667	5,131	5,371
	2	1,320	1,580	1,892	2,204	2,625	3,136	3,544	3,994	4,588	5,014	5,275
	3	1,623	1,878	2,281	2,623	3,095	3,681	4,127	4,621	5,317	5,823	6,117
Mean		1,442	1,691	2,041	2,354	2,813	3,348	3,765	4,234	4,857	5,323	5,587
Std. Dev		130	133	171	190	203	239	258	276	327	357	376
Std. Err		75	77	99	110	117	138	149	160	189	206	217
R7	1	682	912	1,306	1,762	2,215	2,900	3,464	4,072	4,873	5,484	5,851
	2	607	796	1,148	1,483	2,012	2,660	3,186	3,771	4,577	5,183	5,498
	3	643	844	1,224	1,572	2,127	2,764	3,311	3,865	4,647	5,200	5,534
Mean		644	851	1,226	1,606	2,118	2,775	3,320	3,903	4,699	5,289	5,628
Std. Dev		31	48	64	117	83	98	114	126	126	138	159
Std. Err		18	28	37	67	48	57	66	73	73	79	92
R8	1	1,721	2,000	2,408	2,790	3,283	3,857	4,300	4,777	5,407	5,910	6,148
	2	1,496	1,743	2,105	2,430	2,862	3,371	3,775	4,203	4,749	5,155	5,396
	3	1,841	2,155	2,625	3,048	3,569	4,181	4,680	5,179	5,842	6,344	6,601
Mean		1,686	1,966	2,379	2,756	3,238	3,803	4,251	4,720	5,333	5,803	6,048
Std. Dev		143	170	213	253	290	333	371	400	449	491	497
Std. Err		83	98	123	146	168	192	214	231	259	284	287

Table A.6: Flexural Modulus Test Results at 20°C

Mix	Specimen ID	Flexural Modulus (E*) (MPa) at 20°C										
		Frequency (Hz)										
		0.01	0.02	0.05	0.1	0.2	0.5	1	2	5	10	15
R4	1	398	473	612	762	958	1,234	1,491	1,786	2,224	2,597	2,804
	2	417	518	671	836	1,085	1,401	1,693	2,042	2,576	3,003	3,273
	3	471	577	716	896	1,124	1,440	1,720	2,052	2,539	2,930	3,162
Mean		429	523	666	832	1,056	1,358	1,635	1,960	2,446	2,844	3,079
Std. Dev		31	43	42	55	71	90	102	123	158	177	200
Std. Err		18	25	25	32	41	52	59	71	91	102	116
R5	1	227	319	505	683	969	1,394	1,798	2,274	3,004	3,600	3,908
	2	294	402	613	834	1,197	1,719	2,206	2,767	3,580	4,193	4,609
	3	253	340	548	744	1,073	1,568	2,022	2,546	3,344	3,917	4,325
Mean		258	354	555	754	1,080	1,560	2,009	2,529	3,309	3,903	4,281
Std. Dev		28	35	44	62	93	133	167	202	237	242	288
Std. Err		16	20	26	36	54	77	96	116	137	140	166
R6	1	517	631	812	988	1,230	1,572	1,862	2,194	2,673	3,089	3,284
	2	548	571	714	1,011	1,019	1,526	1,691	1,953	2,566	3,185	3,089
	3	632	749	957	1,157	1,474	1,858	2,194	2,582	3,153	3,554	3,844
Mean		566	650	828	1,052	1,241	1,652	1,916	2,243	2,797	3,276	3,406
Std. Dev		49	74	100	75	186	147	209	259	255	200	320
Std. Err		28	43	58	43	107	85	121	150	147	116	185
R7	1	137	185	303	407	610	915	1,224	1,597	2,190	2,693	2,984
	2	107	172	275	366	535	806	1,112	1,460	2,025	2,523	2,797
	3	114	162	264	363	558	837	1,127	1,464	2,003	2,448	2,728
Mean		120	173	281	379	568	853	1,154	1,507	2,073	2,555	2,836
Std. Dev		13	9	16	20	31	46	50	64	83	103	108
Std. Err		7	5	9	11	18	26	29	37	48	59	63
R8	1	570	714	943	1,227	1,478	1,890	2,232	2,642	3,183	3,619	3,851
	2	501	619	822	1,024	1,298	1,670	1,968	2,322	2,801	3,162	3,401
	3	632	789	1,031	1,332	1,621	2,050	2,432	2,830	3,432	3,877	4,108
Mean		568	707	932	1,195	1,466	1,870	2,211	2,598	3,139	3,553	3,787
Std. Dev		54	69	86	128	132	156	190	209	259	296	292
Std. Err		31	40	50	74	76	90	110	121	150	171	169

Table A.6: Flexural Modulus Test Results at 30°C

Mix	Specimen ID	Flexural Modulus (E*) (MPa) at 30°C										
		Frequency (Hz)										
		0.01	0.02	0.05	0.1	0.2	0.5	1	2	5	10	15
R4	1	131	155	214	255	338	458	580	714	951	1,144	1,242
	2	135	175	247	284	381	522	664	820	1,083	1,324	1,454
	3	147	180	264	313	405	540	674	829	1,102	1,313	1,427
Mean		138	170	242	284	375	507	639	788	1,045	1,261	1,374
Std. Dev		7	11	21	24	28	35	42	52	67	82	94
Std. Err		4	6	12	14	16	20	24	30	39	48	55
R5	1	-	-	107	147	215	340	480	667	1,000	1,298	1,525
	2	45	86	128	179	265	413	582	809	1,214	1,570	1,831
	3	26	52	102	138	204	347	496	710	1,091	1,404	1,663
Mean		35	69	112	155	228	367	519	729	1,102	1,424	1,673
Std. Dev		10	17	11	18	27	33	45	59	88	112	125
Std. Err		6	10	6	10	15	19	26	34	51	65	72
R6	1	156	202	277	354	458	612	757	937	1,213	1,456	1,587
	2	147	189	260	335	441	589	731	904	1,181	1,408	1,540
	3	176	222	308	385	501	667	823	1,025	1,323	1,601	1,750
Mean		160	204	282	358	467	622	770	955	1,239	1,488	1,626
Std. Dev		12	13	20	21	26	33	39	51	61	82	90
Std. Err		7	8	11	12	15	19	22	29	35	47	52
R7	1	80	40	71	86	122	196	277	401	636	851	994
	2	38	96	67	82	118	189	268	386	601	805	950
	3	27	33	47	69	94	150	218	320	513	672	789
Mean		48	56	61	79	112	178	255	369	583	776	911
Std. Dev		23	28	11	7	12	20	26	35	52	76	88
Std. Err		13	16	6	4	7	12	15	20	30	44	51
R8	1	145	187	259	364	487	675	864	1,080	1,420	1,692	1,862
	2	137	181	250	333	429	587	750	936	1,226	1,455	1,582
	3	148	209	314	390	533	754	955	1,208	1,589	1,914	2,095
Mean		143	192	274	363	483	672	856	1,075	1,412	1,687	1,846
Std. Dev		5	12	28	23	43	68	84	111	149	188	210
Std. Err		3	7	16	13	25	39	48	64	86	108	121

Table A.7: Repeated Load Triaxial

Mix	Specimen ID	Flow Number (Cycles)	µstrain at Flow Point	Cycles at 1% PAS	Cycles at 3% PAS	Cycles at 5% PAS
R4	21	1,060	21,627	135	1,879	2,963
	25	718	29,200	46	766	1,681
	28	680	30,988	41	641	1,288
	32	817	23,943	100	1,160	1,822
	36	524	20,403	90	1,047	1,628
Mean		760	25,232	82	1,099	1,876
Std. Dev		177	4,168	35	433	571
Std. Err		102	2,406	20	250	330
R5	4	77	28,561	12	87	155
	8	129	30,313	15	130	253
	12	98	27,938	16	114	216
	17	62	30,685	10	63	123
	18	102	29,127	14	111	219
Mean		94	29,325	13	101	193
Std. Dev		23	1,037	2	23	47
Std. Err		13	598	1	14	27
R6	6	720	27,282	56	878	1,654
	7	1,154	29,387	57	1,212	2,528
	13	843	25,233	85	1,366	2,648
	16	706	30,395	32	689	1,468
	17	502	28,166	32	578	1,135
Mean		785	28,093	52	945	1,887
Std. Dev		215	1,779	20	301	598
Std. Err		124	1,027	11	174	345
R7	7	138	24,614	25	195	349
	16	48	31,257	8	48	92
	25	66	23,296	17	98	156
	29	54	22,008	16	86	133
	30	46	23,713	11	69	113
Mean		70	24,978	15	99	169
Std. Dev		35	3,250	6	51	93
Std. Err		20	1,876	3	29	53
R8	11	1,030	16,737	239	2,904	4,143
	19	658	24,707	63	940	1,647
	22	855	20,139	130	1,717	2,708
	23	989	20,728	156	1,770	2,627
	27	1,317	23,144	139	2,049	3,201
Mean		970	21,091	145	1,876	2,865
Std. Dev		217	2,731	56	632	814
Std. Err		125	1,577	33	365	470

Table A.8: Semicircular Bend Test Results

Mix	Specimen ID	Strength (psi)	Slope	Fracture Energy (J/m^2)	Flexibility Index
R4	5T-1	53.7	-1.82	2,202	12.11
	5T-2	56.7	-1.50	2,635	17.57
	6T-1	60.1	-2.33	2,149	9.22
	6T-2	57.5	-2.50	1,951	7.80
	8T-1	61.2	-2.59	2,639	10.19
	8T-2	62.9	-2.33	2,425	10.41
R5	1-B2	82.0	-2.95	3,780	12.81
	2-B1	70.4	-2.42	2,830	11.69
	3T-1	58.5	-0.96	3,971	41.36
	3T-2	64.8	-1.77	3,394	19.17
	4B-1	70.8	-1.69	3,789	22.42
	4B-2	58.2	-1.03	3,610	35.05
	5B-1	70.7	-1.90	2,807	14.78
	5B-2	50.0	-1.30	2,513	19.33
R6	3-B1	58.7	-3.12	1,811	5.80
	3-B2	53.9	-2.52	2,032	8.06
	3-T1	61.2	-3.10	2,042	6.59
	3-T2	53.7	-3.05	1,486	4.87
	2-T1	53.2	-3.14	1,384	4.41
	2-T2	60.2	-3.28	1,641	5.00
R7	12B-1	44.8	-0.63	3,187	50.58
	12B-2	44.3	-0.98	2,783	28.39
	3B-1	45.3	-0.93	2,264	24.35
	11-B1	33.5	-0.43	2,694	62.66
	11-B2	31.3	-0.41	2,283	55.68
	15-B1	41.4	-0.77	2,693	34.98
	15-B2	37.6	-0.79	2,245	28.41
R8	1-T1	72.2	-3.19	2,930	9.18
	1-T2	65.6	-2.36	2,394	10.14
	2-B1	73.5	-3.19	2,653	8.32
	2-T1	75.3	-3.71	2,099	5.66
	2-T2	66.8	-3.40	1,903	5.60
	3-B1	80.3	-4.12	2,759	6.70